

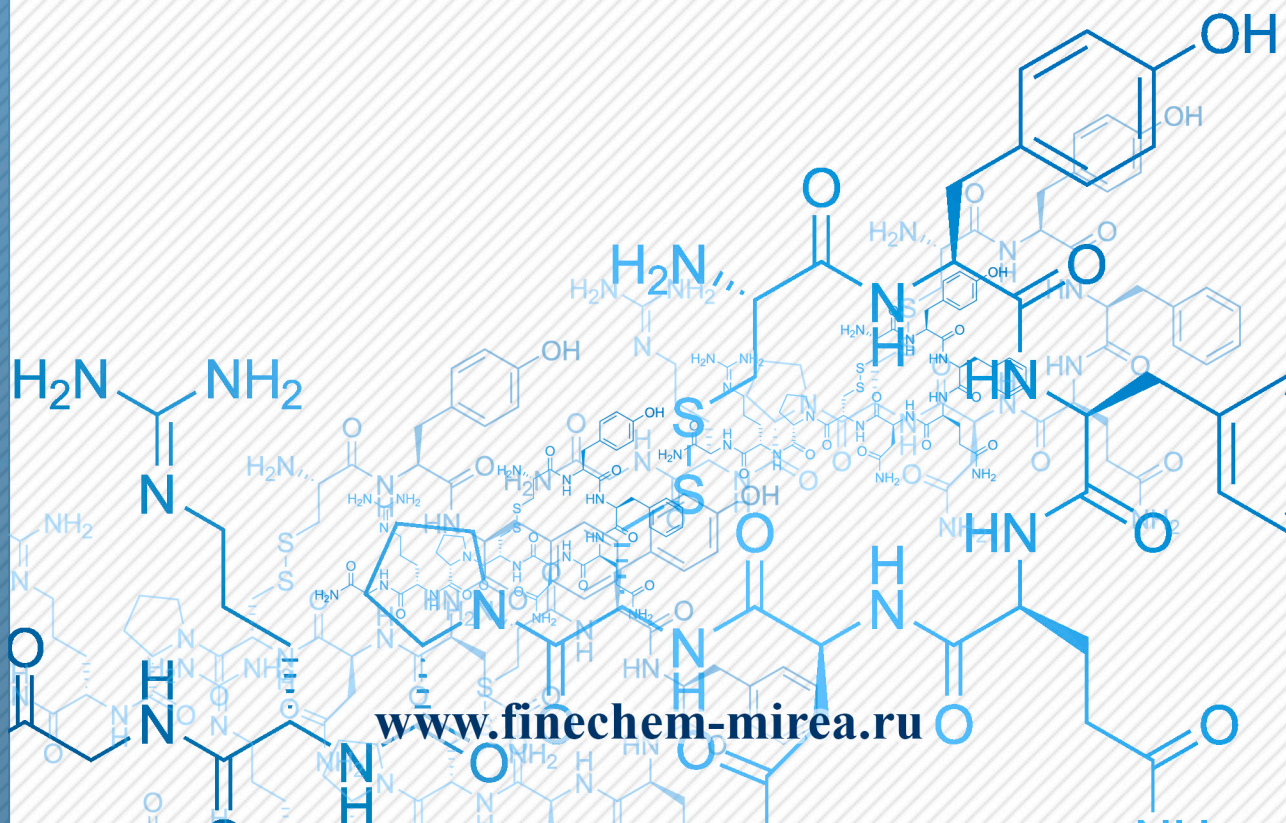


ISSN 2686-7575 (Online)

ТОНКИЕ ХИМИЧЕСКИЕ ТЕХНОЛОГИИ

Fine Chemical Technologies

- | Theoretical Bases of Chemical Technology
- | Chemistry and Technology of Organic Substances
- | Chemistry and Technology of Medicinal Compounds and Biologically Active Substances
- | Biochemistry and Biotechnology
- | Synthesis and Processing of Polymers and Polymeric Composites
- | Chemistry and Technology of Inorganic Materials
- | Analytical Methods in Chemistry and Chemical Technology
- | Mathematical Methods and Information Systems in Chemical Technology



17(6)

2022

www.finechem-mirea.ru



ISSN 2686-7575 (Online)

ТОНКИЕ ХИМИЧЕСКИЕ ТЕХНОЛОГИИ

Fine
Chemical
Technologies

- | Theoretical Bases of Chemical Technology
- | Chemistry and Technology of Organic Substances
- | Chemistry and Technology of Medicinal Compounds and Biologically Active Substances
- | Biochemistry and Biotechnology
- | Synthesis and Processing of Polymers and Polymeric Composites
- | Chemistry and Technology of Inorganic Materials
- | Analytical Methods in Chemistry and Chemical Technology
- | Mathematical Methods and Information Systems in Chemical Technology

Tonkie Khimicheskie Tekhnologii =
Fine Chemical Technologies
Vol. 17, No. 6, 2022

Тонкие химические технологии =
Fine Chemical Technologies
Том 17, № 6, 2022

<https://doi.org/10.32362/2410-6593-2022-17-6>
www.finechem-mirea.ru

The peer-reviewed scientific and technical journal Fine Chemical Technologies highlights the modern achievements of fundamental and applied research in the field of fine chemical technologies, including theoretical bases of chemical technology, chemistry and technology of medicinal compounds and biologically active substances, organic substances and inorganic materials, biochemistry and biotechnology, synthesis and processing of polymers and polymeric composites, analytical and mathematical methods and information systems in chemistry and chemical technology.

Founder and Publisher

Federal State Budget
Educational Institution of Higher Education
“MIREA – Russian Technological University”

78, Vernadskogo pr., Moscow, 119454, Russian Federation.

Publication frequency: bimonthly.

The journal was founded in 2006. The name was Vestnik MITHT until 2015 (ISSN 1819-1487).

The journal is included into the List of peer-reviewed science press of the State Commission for Academic Degrees and Titles of the Russian Federation.

The journal is indexed:

SCOPUS, DOAJ, Chemical Abstracts, Science Index, RSCI, Ulrich’s International Periodicals Directory

Editor-in-Chief:

Andrey V. Timoshenko – Dr. Sci. (Eng.), Cand. Sci. (Chem.), Professor, MIREA – Russian Technological University, Moscow, Russian Federation. Scopus Author ID 56576076700, ResearcherID Y-8709-2018, <https://orcid.org/0000-0002-6511-7440>, timoshenko@mirea.ru

Deputy Editor-in-Chief:

Valery V. Fomichev – Dr. Sci. (Chem.), Professor, MIREA – Russian Technological University, Moscow, Russian Federation. Scopus Author ID 57196028937, <http://orcid.org/0000-0003-4840-0655>, fomichev@mirea.ru

Executive Editor:

Sergey A. Durakov – Cand. Sci. (Chem.), Associate Professor, MIREA – Russian Technological University, Moscow, Russian Federation, Scopus Author ID 57194217518, ResearcherID AAS-6578-2020, <http://orcid.org/0000-0003-4842-3283>, durakov@mirea.ru

Editorial staff:

Managing Editor Cand. Sci. (Eng.) Galina D. Seredina
Science editors Dr. Sci. (Chem.), Prof. Tatyana M. Buslaeva
Dr. Sci. (Chem.), Prof. Anatolii A. Ischenko
Dr. Sci. (Eng.), Prof. Valery F. Kornushko
Dr. Sci. (Eng.), Prof. Anatolii V. Markov
Dr. Sci. (Chem.), Prof. Yuri P. Mirosnikov
Dr. Sci. (Chem.), Prof. Vladimir A. Tverskoy
Desktop publishing Larisa G. Semernya

86, Vernadskogo pr., Moscow, 119571, Russian Federation.
Phone: +7(495) 246-05-55 (#2-88)
E-mail: seredina@mirea.ru

The registration number ПИ № ФС 77–74580 was issued in December 14, 2018 by the Federal Service for Supervision of Communications, Information Technology, and Mass Media of Russia.

The subscription index of *Pressa Rossii*: **36924**

Научно-технический рецензируемый журнал «Тонкие химические технологии» освещает современные достижения фундаментальных и прикладных исследований в области тонких химических технологий, включая теоретические основы химической технологии, химию и технологию лекарственных препаратов и биологически активных соединений, органических веществ и неорганических материалов, биохимию и биотехнологию, синтез и переработку полимеров и композитов на их основе, аналитические и математические методы и информационные системы в химии и химической технологии.

Учредитель и издатель

федеральное государственное бюджетное образовательное учреждение высшего образования «МИРЭА – Российский технологический университет»

119454, РФ, Москва, пр-т Вернадского, д. 78.

Периодичность: один раз в два месяца.

Журнал основан в 2006 году. До 2015 года издавался под названием «Вестник МИТХТ» (ISSN 1819-1487).

Журнал входит в Перечень ведущих рецензируемых научных журналов ВАК РФ.

Индексируется:

SCOPUS, DOAJ, Chemical Abstracts, РИНЦ (Science Index), RSCI, Ulrich’s International Periodicals Directory

Главный редактор:

Тимошенко Андрей Всеволодович – д.т.н., к.х.н., профессор, МИРЭА – Российский технологический университет, Москва, Российская Федерация. Scopus Author ID 56576076700, ResearcherID Y-8709-2018, <https://orcid.org/0000-0002-6511-7440>, timoshenko@mirea.ru

Заместитель главного редактора:

Фомичёв Валерий Вячеславович – д.х.н., профессор, МИРЭА – Российский технологический университет, Москва, Российская Федерация. Scopus Author ID 57196028937, <http://orcid.org/0000-0003-4840-0655>, fomichev@mirea.ru

Выпускающий редактор:

Дураков Сергей Алексеевич – к.х.н., доцент, МИРЭА – Российский технологический университет, Москва, Российская Федерация, Scopus Author ID 57194217518, ResearcherID AAS-6578-2020, <http://orcid.org/0000-0003-4842-3283>, durakov@mirea.ru

Редакция:

Зав. редакцией к.т.н. Г.Д. Середина
Научные редакторы д.х.н., проф. Т.М. Буслаева
д.х.н., проф. А.А. Ищенко
д.т.н., проф. В.Ф. Корнюшко
д.т.н., проф. А.В. Марков
д.х.н., проф. Ю.П. Миросников
д.х.н., проф. В.А. Тверской
Компьютерная верстка Л.Г. Семерня

119571, Москва, пр. Вернадского, 86, оф. Л-119.
Тел.: +7(495) 246-05-55 (#2-88)
E-mail: seredina@mirea.ru

Регистрационный номер и дата принятия решения о регистрации СМИ: ПИ № ФС 77-74580 от 14.12.2018 г. СМИ зарегистрировано Федеральной службой по надзору в сфере связи, информационных технологий и массовых коммуникаций (Роскомнадзор).

Индекс по Объединенному каталогу «Пресса России»: **36924**

Editorial Board

Andrey V. Blokhin – Dr. Sci. (Chem.), Professor, Belarusian State University, Minsk, Belarus. Scopus Author ID 7101971167, ResearcherID AAF-8122-2019 <https://orcid.org/0000-0003-4778-5872>
blokhin@bsu.by.

Sergey P. Verevkin – Dr. Sci. (Eng.), Professor, University of Rostock, Rostock, Germany. Scopus Author ID 7006607848, ResearcherID G-3243-2011, <https://orcid.org/0000-0002-0957-5594>,
sergey.verevkin@uni-rostock.de.

Konstantin Yu. Zhizhin – Corresponding Member of the Russian Academy of Sciences (RAS), Dr. Sci. (Chem.), Professor, N.S. Kurnakov Institute of General and Inorganic Chemistry of the RAS, Moscow, Russian Federation. Scopus Author ID 6701495620, ResearcherID C-5681-2013, <http://orcid.org/0000-0002-4475-124X>,
kyuzhizhin@igic.ras.ru.

Igor V. Ivanov – Dr. Sci. (Chem.), Professor, MIREA – Russian Technological University, Moscow, Russian Federation. Scopus Author ID 34770109800, ResearcherID I-5606-2016, <http://orcid.org/0000-0003-0543-2067>,
ivanov_i@mirea.ru.

Carlos A. Cardona – PhD (Eng.), Professor, National University of Columbia, Manizales, Colombia. Scopus Author ID 7004278560, <http://orcid.org/0000-0002-0237-2313>,
ccardonaal@unal.edu.co.

Oskar I. Koifman – Academician at the RAS, Dr. Sci. (Chem.), Professor, President of the Ivanovo State University of Chemistry and Technology, Ivanovo, Russian Federation. Scopus Author ID 6602070468, ResearcherID R-1020-2016, <http://orcid.org/0000-0002-1764-0819>,
president@isuct.ru.

Elvira T. Krut'ko – Dr. Sci. (Eng.), Professor, Belarusian State Technological University, Minsk, Belarus. Scopus Author ID 6602297257,
ela_krutko@mail.ru.

Anatolii I. Miroshnikov – Academician at the RAS, Dr. Sci. (Chem.), Professor, M.M. Shemyakin and Yu.A. Ovchinnikov Institute of Bioorganic Chemistry of the RAS, Member of the Presidium of the RAS, Chairman of the Presidium of the RAS Pushchino Research Center, Moscow, Russian Federation. Scopus Author ID 7006592304, ResearcherID G-5017-2017,
aiv@ibch.ru.

Aziz M. Muzafarov – Academician at the RAS, Dr. Sci. (Chem.), Professor, A.N. Nesmeyanov Institute of Organoelement Compounds of the RAS, Moscow, Russian Federation. Scopus Author ID 7004472780, ResearcherID G-1644-2011, <https://orcid.org/0000-0002-3050-3253>,
aziz@ineos.ac.ru.

Редакционная коллегия

Блохин Андрей Викторович – д.х.н., профессор Белорусского государственного университета, Минск, Беларусь. Scopus Author ID 7101971167, ResearcherID AAF-8122-2019 <https://orcid.org/0000-0003-4778-5872>
blokhin@bsu.by.

Верёвкин Сергей Петрович – д.т.н., профессор Университета г. Росток, Росток, Германия. Scopus Author ID 7006607848, ResearcherID G-3243-2011, <https://orcid.org/0000-0002-0957-5594>,
sergey.verevkin@uni-rostock.de.

Жижин Константин Юрьевич – член-корр. Российской академии наук (РАН), д.х.н., профессор, Институт общей и неорганической химии им. Н.С. Курнакова РАН, Москва, Российская Федерация. Scopus Author ID 6701495620, ResearcherID C-5681-2013, <http://orcid.org/0000-0002-4475-124X>,
kyuzhizhin@igic.ras.ru.

Иванов Игорь Владимирович – д.х.н., профессор, МИРЭА – Российский технологический университет, Москва, Российская Федерация. Scopus Author ID 34770109800, ResearcherID I-5606-2016, <http://orcid.org/0000-0003-0543-2067>,
ivanov_i@mirea.ru.

Кардона Карлос Ариэль – PhD, профессор Национального университета Колумбии, Манизалес, Колумбия. Scopus Author ID 7004278560, <http://orcid.org/0000-0002-0237-2313>,
ccardonaal@unal.edu.co.

Койфман Оскар Иосифович – академик РАН, д.х.н., профессор, президент Ивановского государственного химико-технологического университета, Иваново, Российская Федерация. Scopus Author ID 6602070468, ResearcherID R-1020-2016, <http://orcid.org/0000-0002-1764-0819>,
president@isuct.ru.

Крутько Эльвира Тихоновна – д.т.н., профессор Белорусского государственного технологического университета, Минск, Беларусь. Scopus Author ID 6602297257,
ela_krutko@mail.ru.

Мирошников Анатолий Иванович – академик РАН, д.х.н., профессор, Институт биоорганической химии им. академиков М.М. Шемякина и Ю.А. Овчинникова РАН, член Президиума РАН, председатель Президиума Пушкинского научного центра РАН, Москва, Российская Федерация. Scopus Author ID 7006592304, ResearcherID G-5017-2017,
aiv@ibch.ru.

Музафаров Азиз Мансурович – академик РАН, д.х.н., профессор, Институт элементоорганических соединений им. А.Н. Несмеянова РАН, Москва, Российская Федерация. Scopus Author ID 7004472780, ResearcherID G-1644-2011, <https://orcid.org/0000-0002-3050-3253>,
aziz@ineos.ac.ru.

Ivan A. Novakov – Academician at the RAS, Dr. Sci. (Chem.), Professor, President of the Volgograd State Technical University, Volgograd, Russian Federation. Scopus Author ID 7003436556, ResearcherID I-4668-2015, <http://orcid.org/0000-0002-0980-6591>, president@vstu.ru.

Alexander N. Ozerin – Corresponding Member of the RAS, Dr. Sci. (Chem.), Professor, Enikolopov Institute of Synthetic Polymeric Materials of the RAS, Moscow, Russian Federation. Scopus Author ID 7006188944, ResearcherID J-1866-2018, <https://orcid.org/0000-0001-7505-6090>, ozerin@ispm.ru.

Tapani A. Pakkanen – PhD, Professor, Department of Chemistry, University of Eastern Finland, Joensuu, Finland. Scopus Author ID 7102310323, tapani.pakkanen@uef.fi.

Armando J.L. Pombeiro – Academician at the Academy of Sciences of Lisbon, PhD, Professor, President of the Center for Structural Chemistry of the Higher Technical Institute of the University of Lisbon, Lisbon, Portugal. Scopus Author ID 7006067269, ResearcherID I-5945-2012, <https://orcid.org/0000-0001-8323-888X>, pombeiro@ist.utl.pt.

Dmitrii V. Pyshnyi – Corresponding Member of the RAS, Dr. Sci. (Chem.), Professor, Institute of Chemical Biology and Fundamental Medicine, Siberian Branch of the RAS, Novosibirsk, Russian Federation. Scopus Author ID 7006677629, ResearcherID F-4729-2013, <https://orcid.org/0000-0002-2587-3719>, pyshnyi@niboch.nsc.ru.

Alexander S. Sigov – Academician at the RAS, Dr. Sci. (Phys. and Math.), Professor, President of MIREA – Russian Technological University, Moscow, Russian Federation. Scopus Author ID 35557510600, ResearcherID L-4103-2017, sigov@mirea.ru.

Alexander M. Toikka – Dr. Sci. (Chem.), Professor, Institute of Chemistry, Saint Petersburg State University, St. Petersburg, Russian Federation. Scopus Author ID 6603464176, ResearcherID A-5698-2010, <http://orcid.org/0000-0002-1863-5528>, a.toikka@spbu.ru.

Andrzej W. Trochimczuk – Dr. Sci. (Chem.), Professor, Faculty of Chemistry, Wrocław University of Science and Technology, Wrocław, Poland. Scopus Author ID 7003604847, andrzej.trochimczuk@pwr.edu.pl.

Aslan Yu. Tsvadze – Academician at the RAS, Dr. Sci. (Chem.), Professor, A.N. Frumkin Institute of Physical Chemistry and Electrochemistry of the RAS, Moscow, Russian Federation. Scopus Author ID 7004245066, ResearcherID G-7422-2014, tsiv@phyche.ac.ru.

Новаков Иван Александрович – академик РАН, д.х.н., профессор, президент Волгоградского государственного технического университета, Волгоград, Российская Федерация. Scopus Author ID 7003436556, ResearcherID I-4668-2015, <http://orcid.org/0000-0002-0980-6591>, president@vstu.ru.

Озерин Александр Никифорович – член-корр. РАН, д.х.н., профессор, Институт синтетических полимерных материалов им. Н.С. Ениколопова РАН, Москва, Российская Федерация. Scopus Author ID 7006188944, ResearcherID J-1866-2018, <https://orcid.org/0000-0001-7505-6090>, ozerin@ispm.ru.

Пакканен Тапани – PhD, профессор, Департамент химии, Университет Восточной Финляндии, Йоенсуу, Финляндия. Scopus Author ID 7102310323, tapani.pakkanen@uef.fi.

Помбейро Армандо – академик Академии наук Лиссабона, PhD, профессор, президент Центра структурной химии Высшего технического института Университета Лиссабона, Португалия. Scopus Author ID 7006067269, ResearcherID I-5945-2012, <https://orcid.org/0000-0001-8323-888X>, pombeiro@ist.utl.pt.

Пышный Дмитрий Владимирович – член-корр. РАН, д.х.н., профессор, Институт химической биологии и фундаментальной медицины Сибирского отделения РАН, Новосибирск, Российская Федерация. Scopus Author ID 7006677629, ResearcherID F-4729-2013, <https://orcid.org/0000-0002-2587-3719>, pyshnyi@niboch.nsc.ru.

Сигов Александр Сергеевич – академик РАН, д.ф.-м.н., профессор, президент МИРЭА – Российского технологического университета, Москва, Российская Федерация. Scopus Author ID 35557510600, ResearcherID L-4103-2017, sigov@mirea.ru.

Тойкка Александр Матвеевич – д.х.н., профессор, Институт химии, Санкт-Петербургский государственный университет, Санкт-Петербург, Российская Федерация. Scopus Author ID 6603464176, ResearcherID A-5698-2010, <http://orcid.org/0000-0002-1863-5528>, a.toikka@spbu.ru.

Трохимчук Анджей – д.х.н., профессор, Химический факультет Вроцлавского политехнического университета, Вроцлав, Польша. Scopus Author ID 7003604847, andrzej.trochimczuk@pwr.edu.pl.

Тсвадзе Аслан Юсупович – академик РАН, д.х.н., профессор, Институт физической химии и электрохимии им. А.Н. Фрумкина РАН, Москва, Российская Федерация. Scopus Author ID 7004245066, ResearcherID G-7422-2014, tsiv@phyche.ac.ru.

CONTENTS

СОДЕРЖАНИЕ

**Theoretical Bases
of Chemical Technology**

Korotkova T.G.

Parameters of the UNIQUAC model for describing the vapor–liquid phase equilibrium of D₂–T₂, D₂–DT, DT–T₂ hydrogen isotope mixtures

459

Peshnev B.V., Burlyayeva E.V., Terenteva V.B., Nikishin D.V., Nikolaev A.I., Andronov K.S.
Evaluation of the influence of hydrodynamic cavitation treatment of dark petroleum products on the yield of fractions with boiling points up to 400°C

473

**Chemistry and Technology
of Organic Substances**

Shiryayeva A.D., Moiseeva S.V., Levanova S.V., Glazko I.L.

Features of triamyl citrate synthesis

483

**Теоретические основы
химической технологии**

Короткова Т.Г.

Параметры модели UNIQUAC для описания фазового равновесия пар – жидкость изотопных смесей водорода D₂–T₂, D₂–DT, DT–T₂

Пешнев Б.В., Бурляева Е.В., Терентьева В.Б., Никишин Д.В., Николаев А.И., Андронов К.С.

Оценка влияния гидродинамической кавитационной обработки темных нефтепродуктов на выход фракций, выкипающих до 400 °С

**Химия и технология
органических веществ**

Ширяева А.Д., Моисеева С.В., Леванова С.В., Глазко И.Л.

Особенности синтеза триамилцитрата

Biochemistry and Biotechnology

Loginova N.Yu., Chesovskikh Yu.S., Borodulin V.B.
Investigation of the biological activity
of the water-soluble
C₆₀/poly-*N*-vinylpyrrolidone complex

492

Synthesis and Processing of Polymers and Polymeric Composites

Kovalenko G.M., Bokova E.S., Evsyukova N.V.
Physicochemical fundamentals
of processing solutions of thermoplastic
poly(ether urethane)s to obtain
fibrous-porous polymer composite
materials

504

*Povernov P.A., Shibryaeva L.S., Lusova L.R.,
Popov A.A.*
Modern polymer composite
materials for bone surgery:
Problems and prospects

514

Биохимия и биотехнология

Логинава Н.Ю., Чесовских Ю.С., Бородулин В.Б.
Исследование биологической активности
водорастворимого комплекса
C₆₀/поли-*N*-винилпирролидон

Синтез и переработка полимеров и композитов на их основе

Коваленко Г.М., Бокова Е.С., Евсюкова Н.В.
Физико-химические основы переработки
растворов термопластичных полиэфируретанов
для прогнозирования возможности
их применения в производстве волокнисто-
пористых композиционных материалов

*Повернов П.А., Шибряева Л.С., Люсова
Л.Р., Попов А.А.*

Современные полимерные композиционные
материалы для костной хирургии:
проблемы и перспективы

THEORETICAL BASES OF CHEMICAL TECHNOLOGY

ТЕОРЕТИЧЕСКИЕ ОСНОВЫ ХИМИЧЕСКОЙ ТЕХНОЛОГИИ

ISSN 2686-7575 (Online)

<https://doi.org/10.32362/2410-6593-2022-17-6-459-472>

UDC 544.342



RESEARCH ARTICLE

Parameters of the UNIQUAC model for describing the vapor–liquid phase equilibrium of D_2 – T_2 , D_2 –DT, DT– T_2 hydrogen isotope mixtures

Tatyana G. Korotkova✉

Kuban State Technological University, Krasnodar, 350072 Russia

✉ Corresponding author, e-mail: korotkova.1964@mail.ru

Abstract

Objectives. Determination of the parameters of the binary energy interaction of the (UNIversal QUAsiChemical) UNIQUAC model on the basis of mathematical processing of experimental literature data on the phase equilibrium of hydrogen isotopic mixtures D_2 – T_2 , D_2 –DT, DT– T_2 to calculate the activity coefficients of the components D_2 , DT, and T_2 .

Methods. The method of successive approximations was used in junction with the “from stage to stage” method, which consists in calculating a single evaporation process on a theoretical plate.

Results. Equations were written for calculating the activity coefficients of hydrogen isotopes on the basis of the Sherwood theory as applied to binary D_2 – T_2 , D_2 –DT, DT– T_2 and ternary D_2 –DT– T_2 hydrogen isotope mixtures. The graphical dependences of the activity coefficients and separation coefficients of mixtures D_2 – T_2 , D_2 –DT, and DT– T_2 are compared in the range of the concentration of a highly volatile component from 0 to 100 mol % at atmospheric pressure for three options: ideal mixtures; non-ideal mixtures using the Sherwood theory; non-ideal mixtures on the basis of the UNIQUAC model. The dependences of the separation coefficients α were found to be similar for all binary isotopic mixtures. However, when considering mixtures as ideal, α increases. According to Sherwood’s theory, α remains a practically constant value, which is independent of the composition of the mixture. The UNIQUAC model predicts a decrease in α with an increase in the concentration of a less volatile component in the mixture. The profile of the distribution of hydrogen isotopes D_2 , DT, and T_2 of a three-component mixture D_2 –DT– T_2 along the

height of a distillation column operating in a closed mode was calculated for three variants. It was accepted that: pressure along the height of the column is constant and equal to atmospheric 760 mm Hg. Art.; number of theoretical plates 21; concentration of components in the liquid phase on the first plate (stage), in mol %: $x_{D_2} = 65$; $x_{DT} = 10$; $x_{T_2} = 25$; the accuracy of calculating the composition of the vapor phase is 10^{-10} .

Conclusions. The parameters of the binary energy interaction of the UNIQUAC model of hydrogen isotopic mixtures D_2-T_2 , D_2-DT , and $DT-T_2$ are determined. The UNIQUAC model is adequate in relation to experimental data on the coefficient of separation. Due to systematic deviations in the theoretical Sherwood and ideal models, they are not suitable for further calculations of phase equilibrium of isotopic mixtures of hydrogen D_2-T_2 , D_2-DT , $DT-T_2$, and D_2-DT-T_2 .

Keywords: UNIQUAC model, hydrogen isotopic mixtures D_2-T_2 , D_2-DT , $DT-T_2$, D_2-DT-T_2 , vapor–liquid phase equilibrium


For citation: Korotkova T.G. Parameters of the UNIQUAC model for describing the vapor–liquid phase equilibrium of D_2-T_2 , D_2-DT , $DT-T_2$ hydrogen isotope mixtures. *Tonk. Khim. Tekhnol. = Fine Chem. Technol.* 2022;17(6):459–472 (Russ., Eng.). <https://doi.org/10.32362/2410-6593-2022-17-6-459-472>

НАУЧНАЯ СТАТЬЯ

Параметры модели UNIQUAC для описания фазового равновесия пар – жидкость изотопных смесей водорода D_2-T_2 , D_2-DT , $DT-T_2$

Т.Г. Короткова 

Кубанский государственный технологический университет, Краснодар, 350072 Россия

 Автор для переписки, e-mail: korotkova1964@mail.ru

Аннотация

Цели. Определение параметров бинарного энергетического взаимодействия модели UNiVersal QUASiChemical (UNIQUAC) на основе математической обработки литературных экспериментальных данных по фазовому равновесию изотопных смесей водорода D_2-T_2 , D_2-DT , $DT-T_2$ для расчета коэффициентов активности компонентов D_2 , DT и T_2 .

Методы. Применены метод последовательных приближений и метод «от ступени к ступени», заключающийся в расчете процесса однократного испарения на теоретической тарелке.

Результаты. Записаны уравнения для расчета коэффициентов активности изотопов водорода на основе теории Шервуда применительно к бинарным D_2-T_2 , D_2-DT , $DT-T_2$ и тройной D_2-DT-T_2 изотопным смесям водорода. Приведено сравнение графических зависимостей коэффициентов активности и коэффициентов разделения смесей D_2-T_2 , D_2-DT , $DT-T_2$ в диапазоне изменения концентрации легколетучего компонента от 0 до 100 мол. % при атмосферном давлении для трех вариантов: идеальных смесей; неидеальных с использованием теории Шервуда и неидеальных на основе модели UNIQUAC. Выявлено, что характер поведения зависимостей коэффициентов разделения α аналогичен для всех бинарных изотопных смесей. При рассмотрении смесей в качестве идеальных α возрастает. По теории Шервуда α остается

практически постоянной величиной, не зависящей от состава смеси. Модель UNIQUAC прогнозирует снижение α с ростом концентрации легколетучего компонента в смеси. Для трех вариантов вычислен профиль распределения изотопов водорода D_2 , DT и T_2 трехкомпонентной смеси D_2 -DT- T_2 по высоте ректификационной колонны, работающей в замкнутом режиме. Принято: давление по высоте колонны постоянно и равно атмосферному 760 мм рт. ст.; число теоретических тарелок 21; концентрации компонентов в жидкой фазе на первой тарелке (ступени), в мол. %: $x_{D_2} = 65$; $x_{DT} = 10$; $x_{T_2} = 25$; точность расчета состава паровой фазы 10^{-10} .

Выводы. Определены параметры бинарного энергетического взаимодействия модели UNIQUAC изотопных смесей водорода D_2 - T_2 , D_2 -DT, DT- T_2 . Модель UNIQUAC адекватна по отношению к экспериментальным данным по коэффициентам разделения. Теоретическая модель Шервуда и идеальная модель дают систематические отклонения и не пригодны для дальнейших расчетов фазового равновесия изотопных смесей водорода D_2 - T_2 , D_2 -DT, DT- T_2 и D_2 -DT- T_2 .

Ключевые слова: модель UNIQUAC, изотопные смеси водорода D_2 - T_2 , D_2 -DT, DT- T_2 , D_2 -DT- T_2 , фазовое равновесие пар – жидкость

Для цитирования: Короткова Т.Г. Параметры модели UNIQUAC для описания фазового равновесия пар – жидкость изотопных смесей водорода D_2 - T_2 , D_2 -DT, DT- T_2 . *Тонкие химические технологии*. 2022;17(6):459–472. <https://doi.org/10.32362/2410-6593-2022-17-6-459-472>

INTRODUCTION

When calculating the low-temperature distillation of liquid mixtures of hydrogen isotopes, the separation factor α^o is determined as the ratio of the vapor pressures of the pure components of the highly volatile P_1^o to the hardly volatile P_2^o , calculated at a certain temperature [1], while the phase equilibrium constant of the i th component K_i is given as the ratio of the vapor pressure of the pure component to the total pressure P [2]. This approach involves classifying isotopic mixtures of hydrogen as ideal, obeying Raoult's law.

$$\alpha_{\text{ideal}} = \alpha^o = \frac{P_1^o}{P_2^o}, \quad (1)$$

$$K_i = \frac{P_i^o}{P}. \quad (2)$$

It is known from experimental studies that mixtures D_2 - T_2 , D_2 -DT, and DT- T_2 deviate from ideal ones [3, 4]. Note that isotopic mixtures of hydrogen are not azeotropic. In such binary mixtures, the low-boiling component is highly volatile, while the high-boiling component is hardly volatile. The non-ideality of the mixture in the liquid phase is taken into account by the activity coefficient of the component, the calculation of which presents a

certain difficulty, since the identification of empirical or thermodynamically justified equations should be based on experimental data on vapor–liquid equilibrium.

The theory of multicomponent liquid hydrogen solutions presented in Sherwood and Souers in 1984 takes into account non-ideal vapor–liquid equilibrium [5]. Activity coefficient of the i th component γ_i is related to the molar excess Gibbs free energy of mixing $\Delta\bar{G}_i^E$ according to the following expression:

$$\gamma_i = \exp\left(\frac{\Delta\bar{G}_i^E}{RT}\right), \quad (3)$$

$$\Delta\bar{G}_i^E = \sum_j x_j A_{i,j} - G^E, \quad (4)$$

$$G^E = \frac{1}{2} \sum_i \sum_j x_i x_j A_{i,j} \quad (A_{i,j} = 0, i = j), \quad (5)$$

where T is temperature, K; R is the universal gas constant, $R = 8.314$ J/(mol K); x is the mole fraction of the component in the liquid; $A_{i,j}$ is the parameter of the binary interaction of hydrogen isotopes, J/mol; indices i and j are component numbers.

Based on the virial equation of state, an equation was obtained for calculating the total pressure P (Pa)

as the sum of the partial pressures of the components in which the second virial coefficient of the gas mixture B_i (m^3/mol) takes into account the imperfection of the gas phase, while the binary interaction parameter $A_{i,j}$ (J/mol) represents the imperfection of the liquid phase. In the case of a binary mixture, the equation is represented as:

$$P = x_1 P_1^{\circ} \exp\left(\frac{B_1 P_1^{\circ} - B_1 P + x_2^2 A_{12}}{RT}\right) + x_2 P_2^{\circ} \exp\left(\frac{B_2 P_2^{\circ} - B_2 P + x_1^2 A_{12}}{RT}\right), \quad (6)$$

where

$$B = B_0 \left(\frac{T}{20}\right)^{-b}, \quad (7)$$

$$A_{12} = 12.1(\lambda_1^2 - \lambda_2^2)^{1.6} \exp\left[\left(\frac{14.74}{T}\right)^6\right]. \quad (8)$$

Here, P_1° and P_2° are vapor pressure values of pure components, Pa; x_1 and x_2 are mole fractions of components in the liquid, mole fractions; index 1 denotes the highly volatile component, while index 2 is the hardly volatile component.

Coefficients for calculating partial pressures of hydrogen isotopes D_2 , DT , and T_2 are presented in Table 1 [5].

For a ternary mixture, Eq. (5) is given as:

$$G^E = x_1 x_2 A_{12} + x_1 x_3 A_{13} + x_2 x_3 A_{23}. \quad (9)$$

For the first component of the ternary mixture

$$\Delta \bar{G}_1^E = (1 - x_1) x_2 A_{12} + (1 - x_1) x_3 A_{13} - x_2 x_3 A_{23}. \quad (10)$$

In the present article, the parameters of the binary energy interaction of the UNIQUAC model for calculating the activity coefficients γ of components D_2 , DT , and T_2 for isotopic mixtures of hydrogen are obtained by analyzing the known experimental data [3, 4]. We compared the calculated data obtained for ideal mixtures and non-ideal mixtures for binary D_2 – T_2 , D_2 – DT , DT – T_2 and ternary mixtures D_2 – DT – T_2 according to the UNIQUAC method and informed by the theory of multicomponent liquid hydrogen solutions [5] presented above and referred to as the Sherwood theory in further presentation.

Based on the calculation of the vapor–liquid phase equilibrium, the separation coefficients α are calculated for mixtures D_2 – T_2 , D_2 – DT , DT – T_2 at different boiling temperatures depending on pressure and composition. The calculations were performed in the Pascal programming language. To calculate the separation factor α , the Raoult–Dalton law is applied for non-ideal mixtures

$$\alpha = \frac{P_1^{\circ} \gamma_1}{P_2^{\circ} \gamma_2}. \quad (11)$$

METHODS

To determine the energy binary interaction parameters Δu_{12} and Δu_{21} of the UNIQUAC model, the method of successive approximations was used until the minimum deviation of the calculated values of the separation coefficients from the experimental ones was reached.

For the calculation of closed rectification, the “stage to stage” method was used, which consists in calculating the process of single evaporation on a theoretical plate. When calculating from bottom to top for a steady process on each overlying tray, the composition of the liquid is equal to the composition of the vapor rising from the underlying tray.

Table 1. Coefficients for calculating partial pressures of hydrogen isotopes

Isotope	B_0 ($10^6 \text{ m}^3/\text{mol}$)	b	λ
D_2	–184	1.64	1.224
DT	–190	1.70	1.111
T_2	–197	1.77	1.000

RESULTS AND DISCUSSION

Vapor pressure of pure components D₂, DT, T₂

The value of the separation factor α depends to a great extent on the vapor pressure of pure components, whose calculation is carried out according to empirical equations.

Vapor pressure D₂. The results of measurements on the vapor pressure $P_{D_2}^{\circ}$ of normal deuterium D₂ are given in [6–10]. Equations have been proposed by a number of authors [7, 10–13]. In this work, the following equation was used [7]:

$$\lg P_{D_2}^{\circ} = 8.58549 - \frac{74.2894}{T} - 0.029345 \cdot T + 0.00047507 \cdot T^2, \quad (12)$$

where $P_{D_2}^{\circ}$ is the vapor pressure of deuterium, Pa; T is the temperature, K.

Vapor pressure DT. Equations [14, 15] were proposed to calculate the deuterotritium vapor pressure DT P_{DT}° . The Sherwood equation is adopted [15]:

$$\ln P_{DT}^{\circ} = 11.3802 - \frac{167.989}{T} + 4.5193 \cdot 10^{-3} \cdot T + 7.6369 \cdot 10^{-5} \cdot T^2, \quad (13)$$

where P_{DT}° is the vapor pressure of deuterotritium, kPa; T is the temperature, K.

Vapor pressure T₂. The vapor pressure $P_{T_2}^{\circ}$ of normal tritium T₂ was measured by Grilly. The measurement results and the calculation equation $P_{T_2}^{\circ}$ are given in [10]. There is also data of $P_{T_2}^{\circ}$ in the work [9]. Other equations [14, 16] were proposed to calculate $P_{T_2}^{\circ}$. In this work, the Grilly equation is adopted.

$$\lg P_{T_2}^{\circ} = 6.0334 - \frac{78.925}{T} + 2 \cdot 10^{-4} (T - 25)^2, \quad (14)$$

where $P_{T_2}^{\circ}$ is the vapor pressure, mm Hg; T is the temperature, K.

Equations (12)–(14) used in this work are selected based on a comparison of calculated and experimental data. It is of note that, on the whole, the analyzed equations adequately describe the experimental data.

There is no experimental data on the vapor pressure of DT in the literature. Preference is given to the

Sherwood equation [15] rather than the Frost–Kalkwarf equation [14] due to the fact that Sherwood performed an analysis of the available P – T – x – y data in dilute solutions, where the heteronuclear isotope is present as stable trace particles. Here, the vapor pressure of trace components was calculated on the basis of a phase equilibrium model using the Chueh–Prausnitz modification of the Redlich–Kwong equation. This model better describes the parameter A_{ij} to take into account the imperfection of hydrogen isotopic mixtures.

A small deviation between the calculated vapor pressure curves, which are constructed according to the Sherwood and Frost–Kalkwarf equations, increases with increasing temperature. In the Frost–Kalkwarf equation, the deuterotritium vapor pressure P_{DT}° is defined as the geometric mean, i.e., as the square root of the product of the vapor pressures of the pure components D₂ and T₂: $P_{DT}^{\circ} = \sqrt{P_{D_2}^{\circ} P_{T_2}^{\circ}}$.

Equations for calculating the activity coefficients of hydrogen isotopes based on the theory of multicomponent liquid hydrogen solutions for isotopic mixtures D₂–T₂, D₂–DT, DT–T₂ and D₂–DT–T₂

Based on the Sherwood theory [5], the activity coefficients of the components in binary mixtures γ_{D_2} and γ_{T_2} ; γ_{D_2} and γ_{DT} ; γ_{DT} and γ_{T_2} can be determined from Eq. (6), writing it in the form of

$$P - x_1 P_1^{\circ} \gamma_1 \exp\left(\frac{B_1 P_1^{\circ} - B_1 P}{RT}\right) - x_2 P_2^{\circ} \gamma_2 \exp\left(\frac{B_2 P_2^{\circ} - B_2 P}{RT}\right) = 0, \quad (15)$$

where

$$\gamma_1 = \exp\left(\frac{x_2^2 A_{12}}{RT}\right), \quad (16)$$

$$\gamma_2 = \exp\left(\frac{x_1^2 A_{12}}{RT}\right). \quad (17)$$

Here, index 1 is the highly volatile component, while index 2 is the hardly volatile component.

The temperature T of the vapor–liquid phase equilibrium for a given mixture composition and external pressure P is the root of the function of Eq. (15), which can be obtained with some accuracy

using one of the well-known numerical methods, for example, the method of successive approximations. Here, the values of B_1 , B_2 , γ_1 , γ_2 , and A_{12} are recalculated during the iterative search for temperature.

Let us apply Sherwood's theory to a three-component mixture D_2 –DT– T_2 . We introduce the notation: $D_2 - 1$; DT – 2; $T_2 - 3$, where the numbers indicate the number of the component in accordance with their volatility. The highly volatile component is D_2 , the hardly volatile component is T_2 , and DT is an intermediate component, which behaves as a hardly volatile component with respect to D_2 , and as a highly volatile component with respect to T_2 over the entire range of concentrations. Then Eq. (15) takes the form of

$$\begin{aligned} P - x_1 P_1^0 \gamma_1 \exp\left(\frac{B_1 P_1^0 - B_1 P}{RT}\right) - \\ - x_2 P_2^0 \gamma_2 \exp\left(\frac{B_2 P_2^0 - B_2 P}{RT}\right) - \\ - x_3 P_3^0 \gamma_3 \exp\left(\frac{B_3 P_3^0 - B_3 P}{RT}\right) = 0, \end{aligned} \quad (18)$$

where by expanding Eqs. (3)–(5), we have

$$\begin{aligned} \gamma_1 &= \exp\left(\frac{\Delta \bar{G}_1^E}{RT}\right) = \\ &= \exp\left(\frac{(1-x_1)x_2 A_{12} + (1-x_1)x_3 A_{13} - x_2 x_3 A_{23}}{RT}\right), \end{aligned} \quad (19)$$

$$\begin{aligned} \gamma_2 &= \exp\left(\frac{\Delta \bar{G}_2^E}{RT}\right) = \\ &= \exp\left(\frac{(1-x_2)x_1 A_{12} + (1-x_2)x_3 A_{23} - x_1 x_3 A_{13}}{RT}\right), \end{aligned} \quad (20)$$

$$\begin{aligned} \gamma_3 &= \exp\left(\frac{\Delta \bar{G}_3^E}{RT}\right) = \\ &= \exp\left(\frac{(1-x_3)x_1 A_{13} + (1-x_3)x_2 A_{23} - x_1 x_2 A_{12}}{RT}\right). \end{aligned} \quad (21)$$

The above equations are subsequently used in the calculation of the phase equilibrium of the single evaporation process in the vapor–liquid system.

Separation factor of D_2 – T_2

The results of an experimental study of the separation factor α of the D_2 – T_2 isotope mixture were obtained by Sherman *et al.* [3] for three temperatures at a D_2 : T_2 molar ratio of 0.991:0.009. The experimental value of the separation factor was calculated from the expression, where the index 1 is the highly volatile component, index 2 is the hardly volatile component

$$\alpha = \frac{y_1 x_2}{y_2 x_1} \quad (22)$$

The averaged experimental values of the separation coefficient of the D_2 – T_2 isotope mixture are given in Table 2.

Analyzing the obtained α values for the D_2 – T_2 binary mixture and those obtained for other molar ratios of the D_2 –DT– T_2 ternary mixture [3], Sherman noted that the values of the separation factor $\alpha_{D_2-T_2}$ are approximately 5–6% lower than the ideal α^0 values.

In this work, the mathematical processing of experimental data [3] is carried out as follows. Molar ratio 0.991:0.009 converted to mole fractions: $x_{D_2} = 0.994$; $x_{T_2} = 0.006$. Molar mass $D_2 = 4.028204$ g/mol; $T_2 = 6.032100$ g/mol [17]. For the obtained molar composition of the liquid isotope mixture D_2 – T_2 , the phase equilibrium y – x was calculated in the temperature range from 20 to 30 K. The activity coefficients γ_{D_2} and γ_{T_2} were calculated using the UNIQUAC equation [18]. The volume parameters r and area q are taken to be the same as for the hydrogen isotope H_2 , which are given in the Hysys modeling software (*Aspen Technology*, USA): $r = 0.4092$; $q = 0.47549$ and are taken here and below to be the same for all hydrogen isotopes. This assumption is acceptable, since the approximately

Table 2. Experimental values of the separation factor of the D_2 – T_2 isotopic mixture

Temperature, K	Separation factor α
23	1.455 ± 0.048
25	1.382 ± 0.056
27	1.318 ± 0.077

similar radius of hydrogen isotopes is: $r_{\text{H}_2} = 0.7414 \cdot 10^{-10}$ m, $r_{\text{D}_2} = 0.7417 \cdot 10^{-10}$ m, $r_{\text{T}_2} = 0.7414 \cdot 10^{-10}$ m, $r_{\text{DT}} = 0.7417 \cdot 10^{-10}$ m [17].

The identification of the parameters of the binary energy interaction Δu_{12} and Δu_{21} between the molecules of the D_2 and T_2 components of the UNIQUAC group composition model was carried out according to the experimental data (Table 2) in the following sequence. Arbitrarily set parameters Δu_{12} , Δu_{21} , whose values are in the range from $-\infty$ to $+\infty$. For a given molar composition of the mixture ($x_{\text{D}_2} = 0.994$ mol fract.; $x_{\text{T}_2} = 0.006$ mol fract.) the activity coefficients were calculated according to the UNIQUAC equation, and the pressure was iteratively determined by the method of successive approximations for each given boiling point of the mixture in the range from 20 to 30 K until the sum of the molar concentrations of the components in the vapor phase was equal to unity.

$$\sum_i y_i = \sum_i \frac{P_i^0}{P} x_i \gamma_i = 1. \quad (23)$$

The calculation accuracy was 10^{-10} . The separation factor was calculated according to Eq. (11). Based on the obtained values (α , t), a graph was built and the deviation of the calculated values of α from the experimental values for three temperatures was determined (Table 2). Restriction: the $y-x$ phase equilibrium curve with the found parameters Δu_{12} and Δu_{21} should not have an azeotrope point. The discovered parameters Δu_{12} and Δu_{21} are presented in Table 3.

A similar calculation was carried out with the activity coefficients calculated according to Eqs. (16) and (17) based on the Sherwood theory, where the separation coefficient was calculated according to Eq. (22).

Table 3. UNIQUAC model parameters Δu_{12} и Δu_{21} for mixtures $\text{D}_2\text{-T}_2$, $\text{D}_2\text{-DT}$, DT-T_2

Mixture	Δu_{12} , cal/mol	Δu_{21} , cal/mol
$\text{D}_2(1) - \text{T}_2(2)$	11.23	-2.21
$\text{D}_2(1) - \text{DT}(2)$	31.2	-21.43
$\text{DT}(1) - \text{T}_2(2)$	2.91	-1.93

Note: The energy binary interaction parameters Δu_{12} и Δu_{21} are given at the universal gas constant $R = 1.98721$ cal/(mol·K); $r = 0.4092$; $q = 0.47549$.

Figure 1 shows the experimental values of the separation factor [3] along with the calculated curves constructed when considering the mixture as ideal ($\alpha^0(1)$), based on the theory of multicomponent liquid hydrogen solutions ($\alpha(2)$), as well as when calculating the activity coefficients according to the UNIQUAC equation ($\alpha(3)$), where the relative the deviation between the experimental and calculated data according to the UNIQUAC equation does not exceed 0.5%.

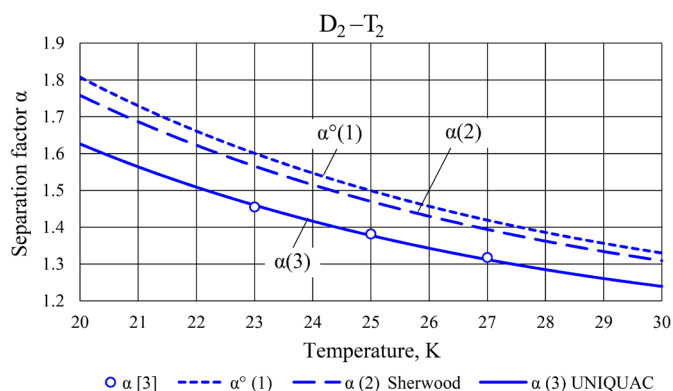


Fig. 1. $\text{D}_2\text{-T}_2$ separation factor dependence from temperature with liquid phase composition $x_{\text{D}_2} = 0.994$ mol fract.; $x_{\text{T}_2} = 0.006$ mol fract.

The discovered parameters Δu_{12} and Δu_{21} are used to calculate the phase equilibrium $y-x$ at a pressure of 760 mm Hg and concentration change x_{D_2} from 0 to 100 mol %. The boiling point was calculated according to the algorithm described and presented in the form of a block diagram in [19].

Figure 2 shows the calculated curves of the dependence of activity coefficients γ_{D_2} and γ_{T_2} on concentration x_{D_2} in the liquid phase, both as obtained according to the Sherwood theory and using the UNIQUAC model.

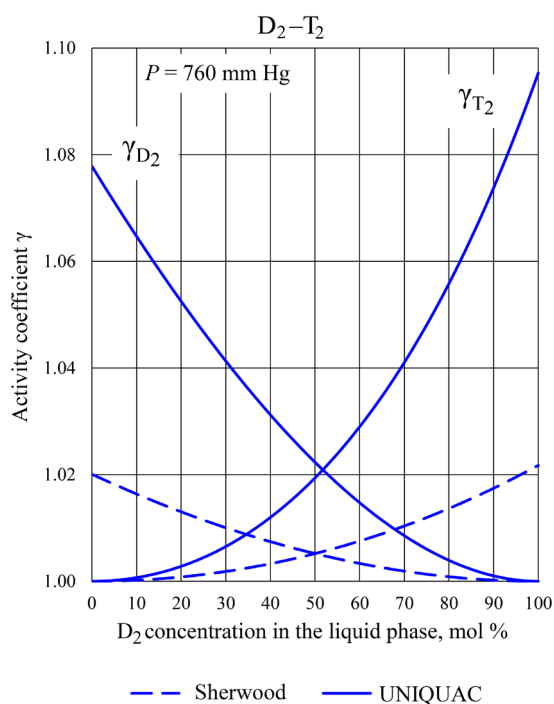


Fig. 2. Calculated curves of activity coefficients γ_{D_2} and γ_{T_2} of D_2 – T_2 mixture components versus D_2 concentration in the liquid phase at atmospheric pressure.

Figure 3 shows the calculated dependences of the separation coefficient α of the D_2 – T_2 mixture on the concentration x_{D_2} in the liquid phase at a pressure of 760 mm Hg. An analysis of the curves shows that, with increasing concentration x_{D_2} , the separation factor $\alpha^{\circ}(1)$ calculated from Eq. (1) increases; meanwhile, $\alpha(2)$ calculated according to the Sherwood theory changes insignificantly, and $\alpha(3)$ calculated according to the UNIQUAC equation decreases. Moreover, for smaller values of x_{D_2} , the value of $\alpha(3)$ is greater than $\alpha^{\circ}(1)$ and $\alpha(2)$, while for larger values of x_{D_2} the value of $\alpha(3)$ is smaller. This means that the UNIQUAC calculation predicts that the separation between D_2 and T_2 will deteriorate as the concentration x_{D_2} in the mixture increases.

Note that the separation factor $\alpha(2)$ calculated using the Sherwood theory is practically independent of the concentrations of the components in the mixture. As will be shown below for D_2 –DT and DT– T_2 mixtures, this is a feature of the theory of multicomponent liquid hydrogen solutions.

Vapor–liquid phase equilibrium and separation factor D_2 –DT

Experimental studies of the separation factor α of the D_2 –DT isotope mixture at various temperatures were carried out by Bigeleisen and Kerr in [4]. The

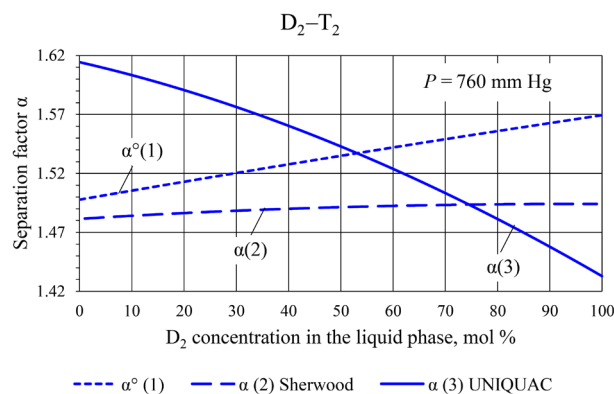


Fig. 3. Dependence of the separation factor α of the D_2 – T_2 mixture on the concentration of D_2 in the liquid phase at atmospheric pressure.

concentration x_{DT} was $1 \cdot 10^{-8}$ mole fractions. Here the separation factor is defined as the ratio of the concentration of DT in the liquid phase x_{DT} to the concentration of DT in the vapor phase y_{DT} .

$$\alpha_{D_2-DT} = \frac{x_{DT}}{y_{DT}}. \quad (24)$$

Such a calculation of the separation factor is legitimate, since, at a concentration of $x_{DT} = 1 \cdot 10^{-8}$ mole fractions the concentrations D_2 both in the liquid and vapor phases tend to 1, and, being in the numerator and denominator of Eq. (24), are reduced. From Eq. (24), one can determine the value of the concentration DT in the vapor phase y_{DT} .

Binary energy interaction parameters Δu_{12} and Δu_{21} between the molecules of the D_2 and DT components of the UNIQUAC group composition model were identified as with the D_2 – T_2 mixture. The results are shown in Table 3 and in Fig. 4.

The maximum relative deviation of the experimental value of the separation factor from the calculated one according to UNIQUAC is 1.6%. Figure 4 demonstrated plotted in the form of squares the separation factors α_{D_2-DT} , obtained by Sherman in [3] in the study of the phase equilibrium of a three-component mixture D_2 –DT– T_2 at molar ratios $D_2 : DT : T_2$ in the liquid phase of 0.931 : 0.062 : 0.0011 and 0.879 : 0.117 : 0.0041.

At the next stage, taking γ_{D_2} equal to 1 from Eq. (11), the experimental values of the activity coefficient γ_{DT} were calculated. Vapor pressures were calculated from experimental temperatures using Eqs. (12) and (13). The calculation results are given in Table 4.

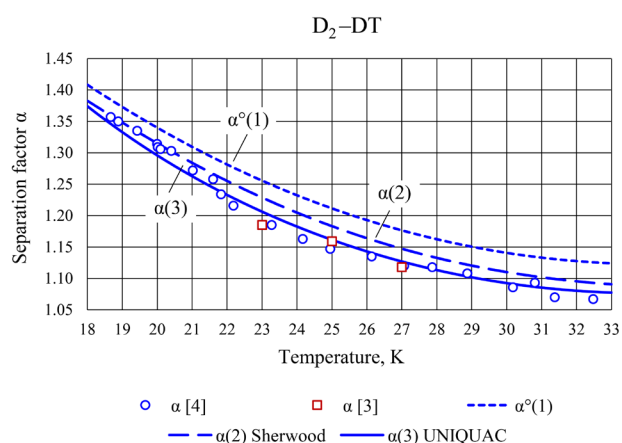


Fig. 4. Temperature dependence of the D_2 -DT separation factor at concentration $x_{DT} = 10^{-8}$ mol fract.

The values of the activity coefficient γ_{DT} given in Table 4 are in the range from 1.017 to 1.057 demonstrating their slight deviation from unity. Nevertheless, the application of the Sherwood theory is widely practiced in the calculation of columns for the separation of nonideal mixtures of hydrogen isotopes [1].

Figure 5 compares the behavior of the deuterotritium activity coefficient DT with temperature. The data of Table 4 are plotted as experimental points. The calculated curves were obtained from the Sherwood and UNIQUAC models. The position of the experimental points shows an increase in the activity coefficient γ_{DT} with increasing temperature; thus, according to the Sherwood model γ_{DT} , it decreases. The application of the discovered parameters of the

Table 4. Experimental and calculated data D_2 -DT

Experimental data [4]			Calculated data			
x_{DT} , mol fract.	T , K	α_{D_2-DT}	y_{DT} , mol fract.	$P_{D_2}^o$, kPa	P_{DT}^o , kPa	γ_{DT}
$1 \cdot 10^{-8}$	18.669	1.357	$7.369 \cdot 10^{-9}$	16.746	12.096	1.02018
$1 \cdot 10^{-8}$	18.882	1.350	$7.407 \cdot 10^{-9}$	18.465	13.410	1.01998
$1 \cdot 10^{-8}$	19.428	1.335	$7.491 \cdot 10^{-9}$	23.487	17.289	1.01760
$1 \cdot 10^{-8}$	19.997	1.314	$7.610 \cdot 10^{-9}$	29.757	22.207	1.01979
$1 \cdot 10^{-8}$	20.015	1.309	$7.639 \cdot 10^{-9}$	29.974	22.378	1.02325
$1 \cdot 10^{-8}$	20.093	1.306	$7.657 \cdot 10^{-9}$	30.928	23.133	1.02371
$1 \cdot 10^{-8}$	20.402	1.303	$7.675 \cdot 10^{-9}$	34.932	26.318	1.01867
$1 \cdot 10^{-8}$	21.015	1.272	$7.862 \cdot 10^{-9}$	44.006	33.620	1.02902
$1 \cdot 10^{-8}$	21.601	1.258	$7.949 \cdot 10^{-9}$	54.210	41.953	1.02716
$1 \cdot 10^{-8}$	21.828	1.234	$8.104 \cdot 10^{-9}$	58.596	45.568	1.04206
$1 \cdot 10^{-8}$	22.181	1.216	$8.224 \cdot 10^{-9}$	65.925	51.649	1.04969
$1 \cdot 10^{-8}$	23.272	1.185	$8.439 \cdot 10^{-9}$	92.812	74.309	1.05401
$1 \cdot 10^{-8}$	24.163	1.163	$8.598 \cdot 10^{-9}$	120.018	97.677	1.05651
$1 \cdot 10^{-8}$	24.952	1.147	$8.718 \cdot 10^{-9}$	148.497	122.490	1.05695
$1 \cdot 10^{-8}$	26.137	1.135	$8.811 \cdot 10^{-9}$	199.841	167.879	1.04880
$1 \cdot 10^{-8}$	27.069	1.120	$8.929 \cdot 10^{-9}$	248.171	211.143	1.04944
$1 \cdot 10^{-8}$	27.872	1.118	$8.945 \cdot 10^{-9}$	295.945	254.253	1.04113
$1 \cdot 10^{-8}$	28.871	1.108	$9.025 \cdot 10^{-9}$	363.957	315.995	1.03951
$1 \cdot 10^{-8}$	30.177	1.086	$9.208 \cdot 10^{-9}$	468.507	411.305	1.04887
$1 \cdot 10^{-8}$	30.807	1.093	$9.149 \cdot 10^{-9}$	525.802	463.570	1.03774
$1 \cdot 10^{-8}$	31.378	1.070	$9.346 \cdot 10^{-9}$	581.854	514.646	1.05663
$1 \cdot 10^{-8}$	32.479	1.067	$9.372 \cdot 10^{-9}$	701.712	623.475	1.05481

binary energy interaction of the UNIQUAC model (Table 3) of the D_2 –DT mixture to calculate the activity coefficient γ_{DT} demonstrated qualitative agreement. The scatter of the experimental points indicates the complexity of carrying out experimental studies on the phase equilibrium of hydrogen isotope mixtures.

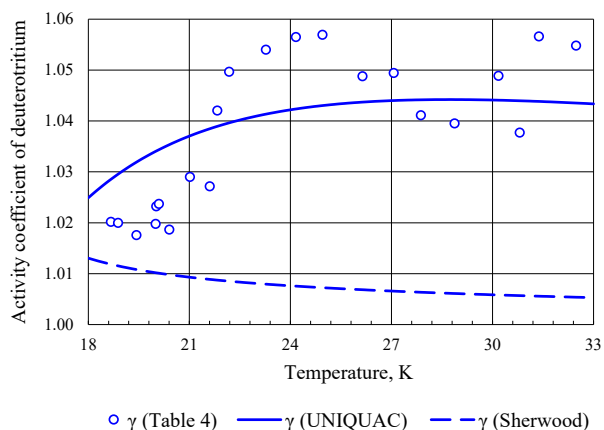


Fig. 5. Temperature dependence of activity coefficient DT.

Figure 6 shows the calculated curves of dependence of activity coefficients γ_{D_2} and γ_{DT} on concentration x_{D_2} in the liquid phase; these were obtained according to the Sherwood theory and using the UNIQUAC method. The behavior of the curve γ_{D_2} is non-standard. If we take into account a small deviation of values from unity, we can conclude that this will not greatly affect the separation of isotopes in a distillation column or cascades of columns.

Figure 7 shows the calculated dependences of the separation factor α_{D_2-DT} on the D_2 concentration in the liquid phase at atmospheric pressure. The character of the curves is similar to that of the D_2 – T_2 mixture. The difference here is that the curve constructed according to Sherwood's theory decreases slightly with growth x_{D_2} , and does not increase.

Vapor–liquid phase equilibrium and separation factor DT– T_2

While Sherman [3] does not provide experimental data on the separation factor $\alpha_{D_2-T_2}$ in his experimental study of the separation factor α_{DT-T_2} , he reports that α_{DT-T_2} is below $\alpha_{DT-T_2}^{\circ}$, as obtained for ideal mixtures by approximately 1%. Taking into account the experience of the experimenter, a temperature dependence curve $\alpha_{DT-T_2}^{\circ}$ was constructed and the parameters of the binary energy interaction Δu_{12} and Δu_{21} of the UNIQUAC model for the DT– T_2 mixture were selected (Table 3), which made it

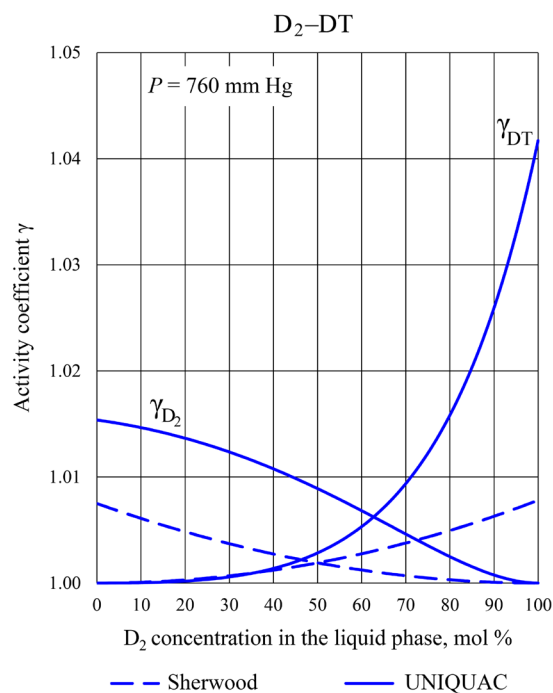


Fig. 6. Calculated curves of the activity coefficients γ_{D_2} and γ_{DT} of the components of the D_2 –DT mixture versus the concentration D_2 in the liquid phase at atmospheric pressure.

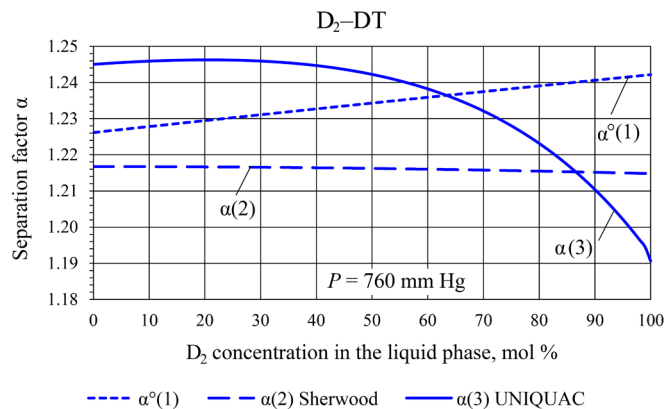


Fig. 7. Dependence of the separation coefficient α of a D_2 –DT mixture on the D_2 concentration in the liquid phase at atmospheric pressure.

possible to reduce α_{DT-T_2} by about 1%. Restriction: the y – x phase equilibrium curve with the found parameters Δu_{12} and Δu_{21} should not have an azeotrope point. A comparison of the curves of the dependence of the separation factor $\alpha_{D_2-T_2}$, α_{D_2-DT} , α_{DT-T_2} , and $\alpha_{DT-T_2}^{\circ}$ on the temperature is shown in Fig. 8. As consistent with the data of other researchers, the curve of dependence of the separation factor of the DT– T_2 mixture is located between the curves $\alpha_{D_2-T_2}$ and α_{DT-T_2} .

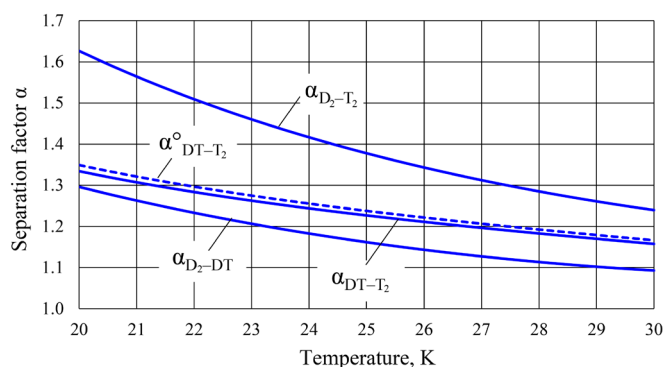


Fig. 8. Dependence of separation factor $\alpha_{D_2-T_2}$, α_{D_2-DT} , α_{DT-T_2} , and $\alpha^o_{DT-T_2}$ on temperature.

Figure 9 shows the dependence of the activity coefficients γ_{DT} и γ_{T_2} of the $DT-T_2$ mixture components on the concentration of DT in the liquid phase at atmospheric pressure. The curves calculated by the UNIQUAC equation are located above the curves obtained by the Sherwood theory. This is typical for all three considered binary mixtures D_2-T_2 , D_2-DT , $DT-T_2$.

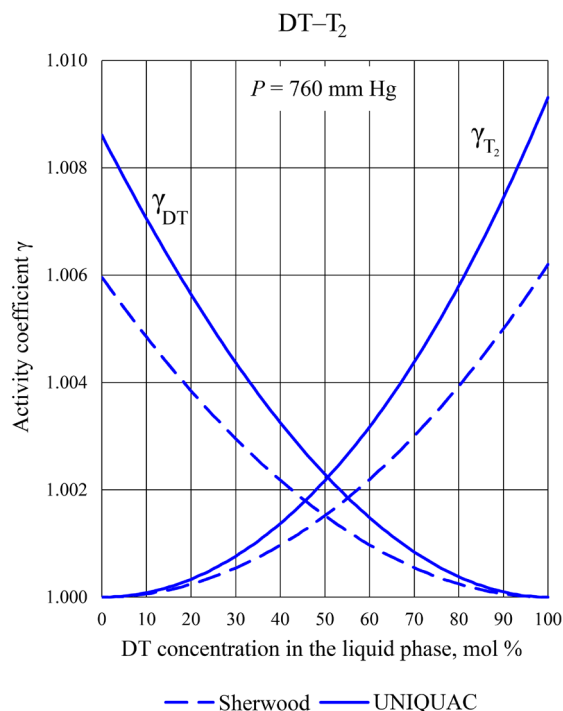


Fig. 9. Curves of the activity coefficients γ_{DT} and γ_{T_2} of the components of the $DT-T_2$ mixture versus the concentration of DT in the liquid phase at atmospheric pressure.

Figure 10 shows the dependence of the separation factor α of a $DT-T_2$ mixture on the concentration of DT in the liquid phase at atmospheric pressure. The behavior of the curves is similar to those

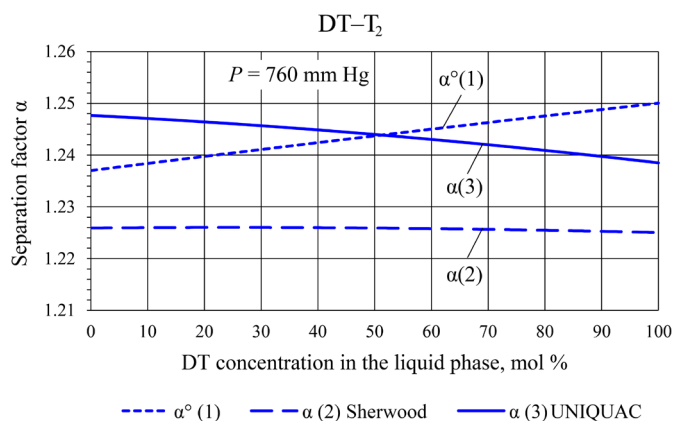


Fig. 10. Dependence of the separation factor α of a $DT-T_2$ mixture on the concentration of DT in the liquid phase at atmospheric pressure.

shown in Figs. 3 and 7 for mixtures D_2-T_2 and D_2-DT : $\alpha^o(1)$ increases, $\alpha(2)$ remains practically constant, while $\alpha(3)$ decreases with increasing concentration of the volatile component in the mixture.

Analyzing graphic dependences in Figs. 3, 7, and 10, it can be concluded that, based on Sherwood's theory, the separation factor is not affected by the composition of the liquid phase.

Distribution profile of components D_2 , DT , and T_2 along the height of the distillation column of a three-component mixture D_2-DT-T_2 with closed rectification

Under actual production conditions, the pressure, boiling point, and composition of the liquid on the plate changes along the height of the distillation column. Consequently, the vapor pressures of pure components and the separation factor change. Due to the small deviation from ideality of hydrogen isotope mixtures, obtaining a reliable description of the boiling points of pure components at various pressures, which correspond to the vapor pressures of pure components, is of great importance. Table 5 shows the values of the boiling points D_2 , DT , T_2 at various pressures calculated from Eqs. (12), (13) and (14) alongside literature data at atmospheric pressure [7, 20].

Let us consider the distribution profile of hydrogen isotopes of a three-component mixture D_2-DT-T_2 along the height of a distillation column operating in a closed mode for three options: for an ideal mixture at $\gamma_i = 1$, both when calculating the activity coefficients according to the Sherwood theory using Eqs. (19)–(21) and according to the UNIQUAC equation using the parameters of the binary energy interaction (Table 3). Let us use the “stage to stage” method. Let us assume that the

Tabl 5. Boiling point of hydrogen isotope at various pressures

Isotope	Isotope boiling point, K							
	Pressure, mm Hg							
	600	700	760		800	900	1000	1100
D ₂	22.785	23.290	23.569	23.56 [7]	23.746	24.162	24.546	24.904
DT	23.506	24.010	24.288	24.38 [20]	24.464	24.878	25.260	25.616
T ₂	24.245	24.754	25.035	25.04 [20]	25.213	25.631	26.017	26.375

pressure along the height of the column is constant and equal to atmospheric 760 mm Hg Art.; number of theoretical plates 21; concentration of components in the liquid phase on the first plate (stage), in mol %: $x_{D_2} = 65$; $x_{DT} = 10$; $x_{T_2} = 25$; the accuracy of vapor phase composition calculation is 10^{-10} .

Figure 11 shows the distribution profile of the concentrations of the components D₂, DT, and T₂ in the liquid phase on the plates of the column from the 11th to the 21st. Along the abscissa, the concentration of the component varies from 0 to 2 mol % for DT and T₂ isotopes (Fig. 11a) and from 97 to 100 mol % for D₂ (Fig. 11b) in order to better represent the profile of the curves. The calculation according to the UNIQUAC model showed that the separation of the three-component mixture

D₂–DT–T₂ proceeds somewhat worse than according to the Sherwood theory and when the mixture is considered as ideal.

In future studies, it will be of interest to calculate the cascades of continuous distillation columns when feeding is introduced into the middle part of the column using modern simulation environments. Such calculations for the separation of the H₂–HD–HT–D₂–DT–T₂ isotope mixture, which includes six hydrogen isotopes, are currently being carried out in the Aspen Hysys medium [21, 22]. In [21], researchers use the Peng–Robinson equation of state. However, the authors note that, in order to improve the description of the vapor–liquid equilibrium using the Peng–Robinson equation of state, it is necessary to tune the parameters of the binary interaction.

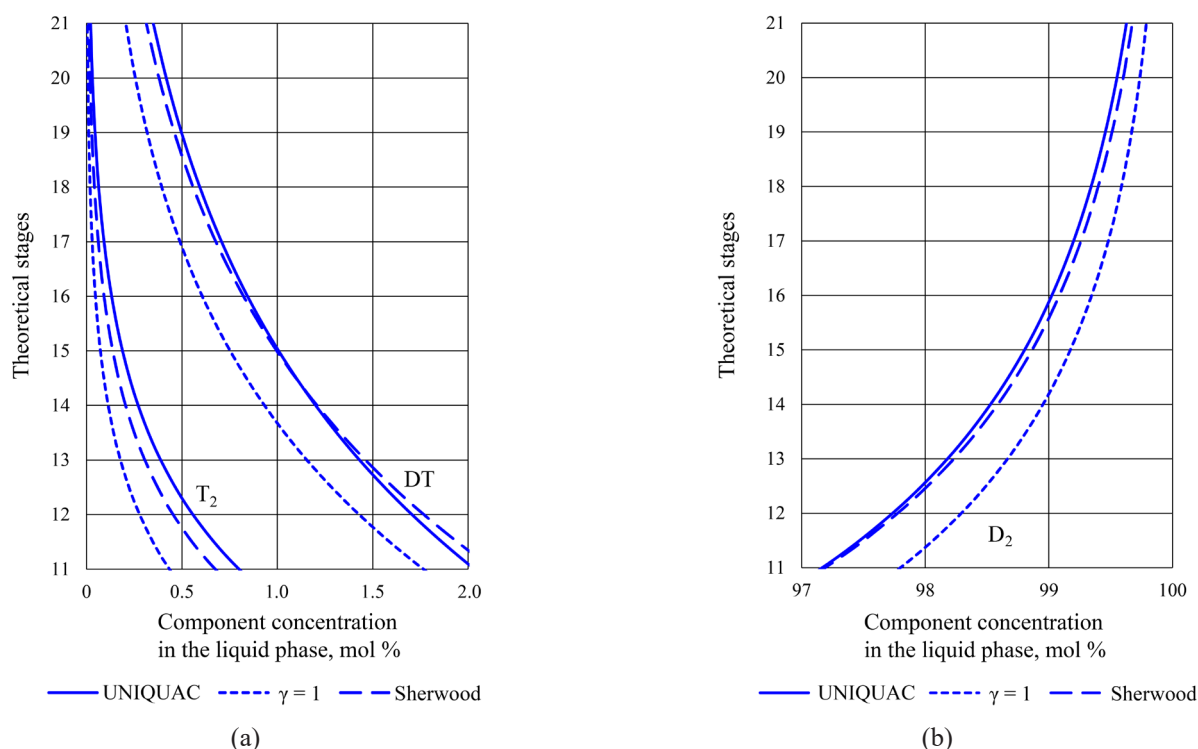


Fig. 11. The distribution profile of the concentrations of the components D₂, DT, and T₂ along the height of the column with closed distillation for a pressure of 760 mm Hg: (a) DT and T₂; (b) D₂.

CONCLUSIONS

The parameters of the binary energy interaction of the UNIQUAC model are determined on the basis of mathematical processing of literary experimental data on the phase equilibrium of hydrogen isotopic mixtures D_2-T_2 , D_2-DT , $DT-T_2$.

Equations are given for calculating the activity coefficients of hydrogen isotopes based on the Sherwood theory as applied to binary D_2-T_2 , D_2-DT , $DT-T_2$, as well as ternary D_2-DT-T_2 hydrogen isotope mixtures.

A comparison is made of the graphical dependences of the activity coefficients and mixture separation coefficients of D_2-T_2 , D_2-DT , $DT-T_2$ in the range of the concentration of a highly volatile component from 0 to 100 mol % at atmospheric pressure for three options: ideal mixtures; non-ideal using the Sherwood theory and non-ideal based on the UNIQUAC model. It was found that the behavior of the curves of separation coefficients α is similar for all binary isotopic mixtures. However, when considering mixtures as ideal, α increases. Sherwood's theory showed that at $P = \text{const}$ α remains practically constant, independent of the composition of the mixture. The UNIQUAC model predicts a decrease in α with an increase in the concentration of a highly volatile component in the mixture.

The profile of distribution of hydrogen isotopes of a three-component mixture D_2-DT-T_2 along the height of a distillation column operating in a closed mode is calculated for three variants. The "stage to stage" method was applied, which consists in calculating the process of single evaporation on a theoretical plate. The pressure along the height of the column is assumed constant at atmospheric 760 mm Hg Art.; number of theoretical plates is 21; concentration of components in the liquid phase on the first plate (stage), in mol %: $x_{D_2} = 65$; $x_{DT} = 10$; $x_{T_2} = 25$; accuracy of vapor phase composition calculation is 10^{-10} . The calculation according to the UNIQUAC model showed that the separation of a three-component mixture D_2-DT-T_2 proceeds somewhat less optimally than according to the Sherwood theory and when considering the mixture as ideal.

On the basis of the conducted studies, the UNIQUAC model is shown to adequately reflect experimental data on separation factors. However, due to the presence of systematic deviations, the theoretical Sherwood and ideal models are not suitable for further calculations of the phase equilibrium of hydrogen isotopic mixtures D_2-T_2 , D_2-DT , $DT-T_2$, and D_2-DT-T_2 .

The author declares no conflicts of interest.

REFERENCES

1. Alekseev I., Arkhipov E., Bondarenko S., Fedorchenko O., Ganzha V., Ivshin K., Kammel P., Kravtsov P., Petitjean C., Trofimov V., Vasilyev A., Vasyanina T., Vorobyov A., Vznuzdaev M. Cryogenic distillation facility for isotopic purification of protium and deuterium. *Rev. Sci. Instrum.* 2015;86(12):125102. <https://doi.org/10.1063/1.4936413>
2. Kinoshita M., Naruse Yu. Parameter Setting Method for Control System of Cryogenic Distillation Column. *J. Nucl. Sci. Technol.* 1981;18(8):595–607. <https://doi.org/10.1080/18811248.1981.9733295>
3. Sherman R.H., Bartlit J.R., Briesmeister R.A. Relative volatilities for the isotopic system deuterium – deuterium tritide – tritium. *Cryogenics.* 1976;16(10):611–613. [https://doi.org/10.1016/0011-2275\(76\)90198-3](https://doi.org/10.1016/0011-2275(76)90198-3)
4. Bigeleisen J., Kerr E.C. Vapor – Liquid Equilibria of Dilute Solutions of HT in $e-H_2$ and DT in $e-D_2$ from the Triple Points to the Critical Temperatures of the Solutions. *J. Chem. Phys.* 1963;39(3):763–768. <https://doi.org/10.1063/1.1734321>
5. Sherwood A.E., Souers P.C. Thermodynamics of Liquid Hydrogen Solutions. *Nuclear Technology/Fusion.* 1984;5(3):350–355. <https://doi.org/10.13182/FST84-A23110>
6. Hoge H.J., Arnold R.D. Vapor Pressures of Hydrogen, Deuterium, and Hydrogen Deuteride and Dew-Point Pressures of Their Mixtures. *J. Res. Natl Bureau Stand.* 1951;47(2):63–74. URL: https://nvlpubs.nist.gov/nistpubs/jres/47/jresv47n2p63_a1b.pdf
7. Gamburg D.Yu., Semenov V.P., Dubovkin N.F., Smirnova L.N. *Vodorod. Svoistva, poluchenie, khranenie, transportirovanie, primenenie (Properties, receipt, storage, transportation, application)*. Gamburg D.Yu., Dubovkin N.F. (Eds.). Moscow: Khimiya; 1989. 672 p. (in Russ.). ISBN 5-7245-0034-5
8. Farkas L. Heavy isotope of hydrogen. *Uspekhi fizicheskikh nauk (UFN)* 1935;15(1):13–51 (in Russ.). <https://doi.org/10.3367/UFNr.0015.193501b.0013>
[Farkas L. Das schwere Wasserstoffisotop. *Naturwissenschaften.* 1934;22:658–662. <https://doi.org/10.1007/BF01498704>]

9. Hammel E.F. Some Calculated Properties of Tritium. *J. Chem. Phys.* 1950;18(2):228–229. <https://doi.org/10.1063/1.1747597>
10. Grilly E.R. The Vapor Pressures of Hydrogen, Deuterium and Tritium up to Three Atmospheres. *J. Amer. Chem. Soc.* 1951;73(2):843–846. <https://doi.org/10.1021/ja01146a103>
11. Malkov M.P., Zel'dovich A.G., Fradkov A.B., Danilov I.B. *Vydelenie deiteriya iz vodoroda metodom glubokogo okhlazhdeniya (Separation of Deuterium from Hydrogen by Deep Cooling)*. Malkov M.P. (Ed.). Moscow: Gosatomizdat; 1961. 151 p. (in Russ.).
12. Scott R.B., Brickwedde F.G., Urey H.C., Wahl M.H. The Vapor Pressures and Derived Thermal Properties of Hydrogen and Deuterium. *J. Chem. Phys.* 1934;2(8):454. <https://doi.org/10.1063/1.1749509>
13. Shtekher M.S. *Topliva i rabochie tela raketnykh dvigatelei (Fuels and working bodies of rocket engines)*. Moscow: Mashinostroenie; 1976. 304 p. (in Russ.).
14. Mittelhauser H.M., Thodos G. Vapour pressure relationships up to the critical point of hydrogen, deuterium, and tritium, and their diatomic combinations. *Cryogenics*. 1964;4(6):368–373. [https://doi.org/10.1016/0011-2275\(64\)90078-5](https://doi.org/10.1016/0011-2275(64)90078-5)
15. Sherwood A.E. Vapor Pressure of HD, HT, and DT. *Fluid Phase Equilibria*. 1989;51:327–338. [https://doi.org/10.1016/0378-3812\(89\)80374-7](https://doi.org/10.1016/0378-3812(89)80374-7)
16. Souers P.C., Briggs C.K., Pyper J.W., Tsugawa R.T. *Hydrogen Vapor Pressures from 4 to 30 K: A Review*. Lawrence Livermore National Laboratory. 1977 UCRL-52226. 35 p. URL: https://inis.iaea.org/collection/NCLCollectionStore/_Public/08/334/8334372.pdf
17. Aldehani M. *Hydrogen-Water Isotope Exchange in a Trickle Bed Column by Process Simulation and 3D Computational Fluid Dynamics Modelling*. PhD Thesis. Lancaster University; 2016. 208 p. URL: https://eprints.lancs.ac.uk/id/eprint/82667/1/2016_Mohammed_PhD.pdf
18. Walas S. *Fazovyie ravnovesiya v khimicheskoi tekhnologii (Phase Equilibria in Chemical Engineering)*: in 2 v.: transl. from Eng. Moscow: Mir; 1989. V. 1. 304 p. V. 2. 354 p. (in Russ.).
[Walas S.M. *Phase Equilibria in Chemical Engineering*. Boston, London, Sydney: Butterworth-Heinemann; 1985. 671 p. ISBN-13/978-075069313.]
19. Korotkova T.G., Kas'yanov G.I. Calculating a Rectification Column for Separating Mixtures of Light and Heavy Water. *Russ. J. Phys. Chem.* 2021;95(5):1051–1060. <https://doi.org/10.1134/S0036024421050186>
[Original Russian Text: Korotkova T.G., Kas'yanov G.I. Calculating a Rectification Column for Separating Mixtures of Light and Heavy Water. *Zhurnal fizicheskoi khimii*. 2021;95(5):800–809 (in Russ.). <https://doi.org/10.31857/S0044453721050186>]
20. Zefirov N.S. (Ed.). *Khimicheskaya entsiklopediya: v 5 t.: T. 5. Triptofan-Yatrokhimiya (Chemical Encyclopedia: in 5 v. V. 5. Tryptophan-Iatrochemistry)*. Moscow: Bol'shaya Rossiiskaya entsiklopediya; 1998. 782 p. (in Russ.).
21. Iraola E., Nougues J. M., Sedano L., Feliu J. A., Batet L. Dynamic simulation tools for isotopic separation system modeling and design. *Fusion Eng. Des.* 2021;169: 112452. <https://doi.org/10.1016/j.fusengdes.2021.112452>
22. Nougues J. M., Feliu J. A., Campanyà G., Iraola E., Batet L., Sedano L. Advanced Tools for ITER Tritium Plant System Modeling and Design. *Fusion Sci. Technol.* 2020;76(5):649–652. <https://doi.org/10.1080/15361055.2020.1741278>

About the author:

Tatyana G. Korotkova, Dr. Sci. (Eng.), Professor, Department of Life Safety, Kuban State Technological University (2, Moskovskaya ul., Krasnodar, 350072, Russia). E-mail: korotkova1964@mail.ru. Scopus Author ID 56195415000, ResearcherID AAQ-3126-2021, RSCI SPIN-code 3212-7120, <https://orcid.org/0000-0001-9278-871X>

Об авторе:

Короткова Татьяна Германовна, д.т.н. доцент, профессор кафедры безопасности жизнедеятельности ФГБОУ ВО «Кубанский государственный технологический университет» (350072, Россия, г. Краснодар, ул. Московская, д. 2). E-mail: korotkova1964@mail.ru. Scopus Author ID 56195415000, ResearcherID AAQ-3126-2021, SPIN-код РИНЦ 3212-7120, <https://orcid.org/0000-0001-9278-871X>

The article was submitted: September 15, 2022; approved after reviewing: September 27, 2022; accepted for publication: November 28, 2022.

*Translated from Russian into English by H. Moshkov
Edited for English language and spelling by Thomas Beavitt*

THEORETICAL BASES OF CHEMICAL TECHNOLOGY
ТЕОРЕТИЧЕСКИЕ ОСНОВЫ ХИМИЧЕСКОЙ ТЕХНОЛОГИИ

ISSN 2686-7575 (Online)

<https://doi.org/10.32362/2410-6593-2022-17-6-473-482>



UDC 66-963;620.93

RESEARCH ARTICLE

Evaluation of the influence of hydrodynamic cavitation treatment of dark petroleum products on the yield of fractions with boiling points up to 400°C

Boris V. Peshnev¹, Elena V. Burlyayeva¹, Vera B. Terenteva², Denis V. Nikishin^{1,✉}, Alexander I. Nikolaev¹, Konstantin S. Andronov¹

¹MIREA – Russian Technological University (M.V. Lomonosov Institute of Fine Chemical Technologies), Moscow, 119571 Russia

²The 25th State Research Institute of Himmotology, Ministry of Defence of the Russian Federation, Moscow, 121467 Russia

✉ Corresponding author, e-mail: nikishin@mirea.ru

Abstract

Objectives. The reduction of the anthropogenic burden on the environment is generally associated with the transition to alternative energy sources. However, some of these have only regional significance, while the effectiveness of others remains doubtful. On this point, innovative processes aimed at increasing the depth of oil refining may be equally important for reducing the carbon footprint. Wave-based technologies such as cavitation may also be included in these processes. Among the various methods for inducing such cavitation phenomena in oil refining, hydrodynamic approaches are especially promising. It has been shown that the treatment effectiveness increases with greater pressure or when augmenting the number of cavitation processing cycles. The aim of this work is to identify the factor (i.e., pressure gradient or number of treatment cycles) having the greatest influence on the change of the characteristics of the oil product.

Methods. Cavitation phenomena were created by pumping dark oil products through a diffuser. The pressure gradient ranged from 20 to 50 MPa, while the number of cavitation processing cycles varied from 1 to 10. The influence of cavitation conditions on the change of fractional composition of petroleum products was analyzed. Target fractions are those having a boiling point up to 400°C.

Results. It is shown that increased pressure generated in the diffuser leads to a linear increase in the yield of desired cuts. The dependence of the yield of these fractions on the number of processing cycles is described by the growth model with saturation. A proposed equation describes the influence of pressure and number of cycles on the yield of the fractions from initial boiling point temperature (T_{IBP}) to 400°C following cavitation processing of dark oil products. Some of the coefficients of this equation have been associated with the physicochemical characteristics of the feedstock.

Conclusions. An equation for predicting the maximum possible yield of the $T_{\text{IBP}}-400^{\circ}\text{C}$ fraction as a result of cavitation processing under different conditions of the process is proposed according to the physicochemical characteristics of the feedstock. The prediction error did not exceed 12%. The equation analysis and comparison of energy consumption between different process regimes shows that a higher yield of the target product is achieved by increasing pressure gradient rather than the number of processing cycles.

Keywords: cavitation, petroleum products, oil refining, depth of oil refining, energy efficiency

For citation: Peshnev B.V., Burlyaeva E.V., Terenteva V.B., Nikishin D.V., Nikolaev A.I., Andronov K.S. Evaluation of the influence of hydrodynamic cavitation treatment of dark petroleum products on the yield of fractions with boiling points up to 400°C. *Tonk. Khim. Tekhnol. = Fine Chem. Technol.* 2022;17(6):473–482 (Russ., Eng.). <https://doi.org/10.32362/2410-6593-2022-17-6-473-482>

НАУЧНАЯ СТАТЬЯ

Оценка влияния гидродинамической кавитационной обработки темных нефтепродуктов на выход фракций, выкипающих до 400 °С

Б.В. Пешнев¹, Е.В. Бурляева¹, В.Б. Терентьева², Д.В. Никишин^{1,✉}, А.И. Николаев¹, К.С. Андронов¹

¹МИРЭА – Российский технологический университет (Институт тонких химических технологий им. М. В. Ломоносова), Москва, 119571 Россия

²25-й Государственный научно-исследовательский институт химмотологии Министерства обороны Российской Федерации, Москва, 121467 Россия

✉ Автор для переписки, e-mail: nikishin@mirea.ru

Аннотация

Цели. Снижение антропогенной нагрузки человечества на окружающую среду связывают с использованием альтернативных источников энергии. Однако часть из них имеет только региональное значение, а эффективность других дискуссионна. Для сокращения углеродного следа не меньший интерес представляют инновационные процессы, направленные на увеличение глубины переработки нефти. К числу таких процессов можно отнести и волновые технологии, частным случаем которых является кавитация. Кавитационные явления для нефтепереработки создают различными методами, наиболее перспективным из которых считаются гидродинамические. Установлено, что эффективность воздействия возрастает как при повышении давления при прокачке нефтепродукта, так и при увеличении количества актов воздействия. Цель данной работы – какой из двух факторов – градиент давлений или количество циклов воздействия – оказывает большее влияние на изменение характеристик нефтепродукта.

Методы. Явление кавитации создавали, прокачивая темные нефтепродукты через диффузор. Давление варьировалось от 20 до 50 МПа, а количество актов воздействия – от 1 до 10. Анализировалось влияние условий кавитации на изменение фракционного состава нефтепродуктов. В качестве целевых рассматривались фракции, выкипающие до 400 °С.

Результаты. Показано, что выход целевых фракций линейно увеличивается при повышении давления, возникающего в диффузоре. Зависимость выхода этих фракций от количества циклов обработки описывается моделью роста с насыщением. Предложено уравнение, описывающее влияние давления и количества циклов на выход фракции от температуры начала кипения ($T_{НК}$) до 400 °С после кавитационной обработки темных нефтепродуктов. Установлена связь некоторых из коэффициентов этого уравнения с физико-химическими характеристиками исходного сырья.

Выводы. Предложено уравнение, позволяющее по физико-химическим характеристикам исходного сырья предсказать максимально возможный выход фракции $T_{НК}-400$ °С в результате кавитационной обработки при различных условиях ведения процесса. Ошибка прогнозирования не превышает 12%. Анализ полученного уравнения и сопоставление энергозатрат при различных режимах ведения процесса показывают, что больший выход целевого продукта достигается в результате увеличения давления, а не числа циклов обработки.

Ключевые слова: кавитация, нефтепродукты, переработка нефти, глубина переработки, энергетическая эффективность

Для цитирования: Пешнев Б.В., Бурляева Е.В., Терентьева В.Б., Никишин Д.В., Николаев А.И., Андронов К.С. Оценка влияния гидродинамической кавитационной обработки темных нефтепродуктов на выход фракций, выкипающих до 400 °С. *Тонкие химические технологии.* 2022;17(6):473–482. <https://doi.org/10.32362/2410-6593-2022-17-6-473-482>

INTRODUCTION

Recently, there has been a pronounced tendency in the global energy sector to minimize emissions of carbon oxides (hydrocarbon combustion products) into the atmosphere. To achieve this, various alternatives are offered: wind power, hydrogen-based energy forms, solar energy, storage, etc. Each of the methods under consideration has advantages (which are typically considered in detail) and disadvantages (which advocates generally keep silent about). For example, wind and geothermal energy are only of regional importance. The use of solar energy is also complicated by the seasonal factor. Renewable sources of raw energy materials (biofuels) involve the use of significant areas of agricultural land. When using hydrogen as an energy vector, net zero carbon is achieved only when the gas is obtained by electrolyzing water using renewable energy sources. In other cases, the carbon footprint may be even greater than that of traditional energy carriers.

In this regard, in order to reduce the anthropogenic load of mankind on the environment, it may be more

effective to develop technologies aimed at increasing the depth of oil refining.

Oil refining depth is understood as the ratio of the volume of products obtained from oil (minus the cost of refining it) to that of the feedstock oil [1, 2]. As a rule, only refined products are taken into account. The overall oil refining depth in Russia is estimated at 84.4%, varying from 74.5% (enterprises of *Rosneft*) to 94.6% (*Omskii NPZ, Gazprom Neft*). For comparison, the oil refining depth at the enterprises of the European Union is estimated at 85%, while in the United States of America, the comparable figure reaches 96%.¹

An increase in oil refining depth is usually associated with the use of visbreaking, hydrocracking, and coking processes. In recent years, new plasma- and wave-based technologies for increasing the yield of light fractions in oil refining processes have been

¹ The territory of discoveries. PJSC Rosneft. Annual report. 2020. URL: https://www.rosneft.ru/upload/site1/document_file/a_report_2020.pdf (accessed September 21, 2021).

proposed [3–5]. The latter should be recognized as more promising, since they do not imply complete destruction of raw materials, but can be successfully combined with traditional processes [6, 7]. Such wave-based technologies include those relying on the phenomenon of cavitation.

Cavitation consists in the nucleation at the interface of phases (liquid–liquid, liquid–solid) of a gas bubble nucleus, including its growth and subsequent collapse. It is noted that at the stage of compression of a gas bubble, temperatures can reach 5000 K, while, following collapse, they can increase to 10000 K [8–10]. If this phenomenon occurs in a hydrocarbon environment, it can lead to cracking reactions. The validity of this assumption is confirmed by reports of a decrease in the boiling point of petroleum products, the distillation temperatures of 50% of fractions, as well as a decrease in viscosity [11–13]. A number of researchers recorded the appearance of unsaturated hydrocarbons and hydrocarbons of lower molecular weight following exposure to cavitation [14, 15].

Although a large number of publications have been devoted to the study of the effect of cavitation on the physicochemical characteristics of petroleum products, the overwhelming majority of them are descriptive. The authors mainly record the changes that are taking place, and there have been practically no attempts to generalize them, to propose a mathematical model that would allow predicting changes based on the characteristics of the raw materials. One more important point was left aside. The researchers noted that when processing raw materials in a hydrodynamic flow, the changes

depend not only on the pressure arising in the diffuser, but also on the number of exposure cycles, but which of these factors affects the result more significantly was not considered.

The present work is dedicated to identifying the factors that have the greatest impact on the change in the characteristics of petroleum products.

EXPERIMENTAL

Dark oil products of primary and secondary oil refining were selected as objects of research: fuel oil, catalytic gas oil (CGO), vacuum gas oil (VGO) and fuel oil provided by *Gazpromneft – MNPZ* (FOM), Russia, as well as fuel oil (FOK) provided by *Kirishinefteorgsintez*, Russia. The characteristics of the research objects are given in Table 1.

The studies were conducted in accordance with the methodology described in [6, 16]. Petroleum products were pumped through a diffuser, on which pressure was applied to actuate the phenomenon of cavitation. The pressure varied from 20 to 50 MPa, while the number of exposure cycles ranged from 1 to 10. The total yield of fractions boiling off in the temperature range from the initial boiling point (T_{IBP}) to 400°C was taken as the target indicator.

RESULTS AND DISCUSSION

The effect of the processing conditions of the FOM sample on the yield of the fraction T_{IBP} –400°C is shown in Fig. 1.

Table 1. Characteristic of research subjects

Indicator	Sample			
	CGO	VGO	FOM	FOK
Density, g/cm ³	1.1002	0.8998	0.9684	0.9478
Yield of T_{IBP} –350°C fraction, wt %	5.2	8.4	5.0	13.2
Yield of 350–400°C fraction, wt %	25.8	34.5	9.0	15.8
Yield of 400–480°C fraction, wt %	69.0	40.9	28.0	47.0
Yield of 480+°C fraction, wt %		16.2	58.0	24.0

Note: CGO – catalytic gas oil; VGO – vacuum gas oil; FOM – fuel oil provided by *Gazpromneft – MNPZ*; FOK – fuel oil provided by *Kirishinefteorgsintez*.

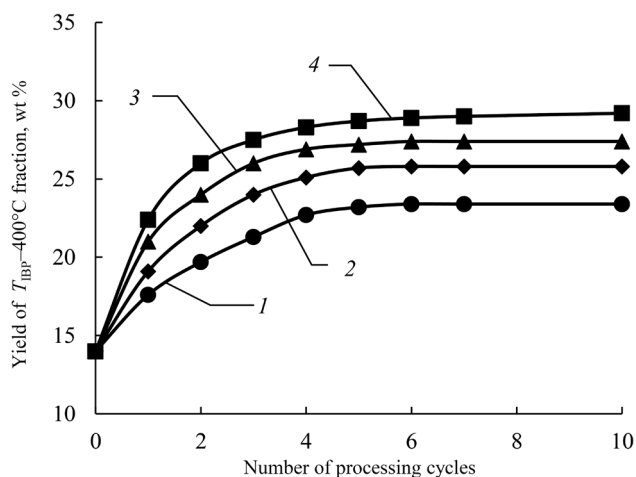


Fig. 1. Influence of the processing conditions on the yield of fractions $T_{\text{IBP}}-400^{\circ}\text{C}$ of a fuel oil (*Gazpromneft-NMPZ*) sample: 1 – treatment pressure 20 MPa; 2 – treatment pressure 30 MPa; 3 – treatment pressure 40 MPa; 4 – treatment pressure 50 MPa.

The presented results are consistent with those obtained earlier: an increase in pressure and the number of exposure cycles led to an increase in the yield of the fraction boiling up to 400°C . At the same time, the greatest increase in the yield of target fractions occurred during the first processing cycles. After 5 cycles of exposure, no significant increase in the yield of fractions was recorded, with the curve of their yield dependence on the number of treatment cycles reaching the saturation line. Similar results were obtained for other samples.

Such dependencies are well described by growth models with saturation. These models based on exponential dependence are often called linear growth functions, since the growth rate of the studied quantity is a decreasing linear function [17]. One such model proposed by L. Bertalanffy has been widely used to solve problems in chemistry and biology [18].

According to this model, the dependence of the yield of fractions R on the number of cycles t can be described by equation (1):

$$R(t) = A(1 - Be^{-kt}), \quad (1)$$

where A is the limit value of R (saturation value); B is the coefficient characterizing the difference between the initial and limit values of R ($R(0) = A(1-B)$); k is the growth rate coefficient. The greater the k , the faster saturation is achieved.

For all samples, the dependence of the yield of the target fractions on pressure, regardless of the number of processing cycles, is linear (Fig. 2), while the values of the correlation coefficient between the yield of the fraction $T_{\text{IBP}}-400^{\circ}\text{C}$ and pressure exceed 0.98.

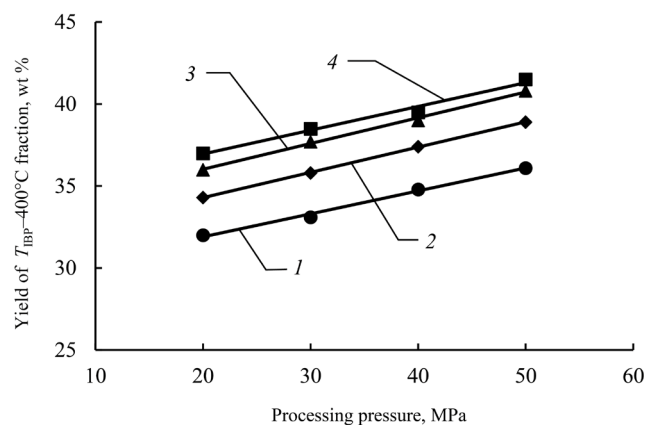


Fig. 2. Influence of the processing conditions on the yield of fractions $T_{\text{IBP}}-400^{\circ}\text{C}$ of a fuel oil (FOK) (*Kirishinefteorgsintez*) sample: 1 – 1 processing cycle; 2 – 3 processing cycles; 3 – 5 processing cycles; 4 – 10 processing cycles.

As a result, the relationship between the yield of the fraction $T_{\text{IBP}}-400^{\circ}\text{C}$, pressure and the number of sample processing cycles can be described by the following mathematical model (2):

$$R = (A_0 + A_1 \cdot p)(1 - (B_0 + B_1 \cdot p)e^{-(k_0 + k_1 \cdot p)t}) \quad (2)$$

For each sample, all coefficients of the model were calculated using the least squares method. The error of the calculated values of the fraction yield for each sample did not exceed 3% (Table 2). Thus, the proposed model describes the experimental data well.

Further analysis showed that there is a linear relationship between the yield of the fraction $T_{\text{IBP}}-400^{\circ}\text{C}$ of the initial sample (before its processing, R_0) and the values of the coefficients A_0 and B_0 , which is described by equations (3) and (4):

$$A_0 = 0.72 \cdot R_0 + 12.3 \quad (3)$$

$$B_0 = -0.012 \cdot R_0 + 0.53 \quad (4)$$

Table 2. Growth model coefficients and calculation error values

Sample	Coefficients						Error, %	Error at average values of k , %
	A_0	A_1	B_0	B_1	k_0	k_1		
CGO	33.4	0.45	0.16	0.005	0.38	0.005	1.7	2.0
VGO	42.8	0.21	0.025	0.003	0.4	0.002	2.7	4.0
FOM	21.8	0.14	0.37	0.003	0.01	0.015	1.3	2.9
FOK	34.4	0.13	0.16	0.002	0.15	0.011	2.7	2.9

The value of the correlation coefficient between A_0 and R_0 is 0.98, while the corresponding value between B_0 and R_0 is 0.99.

Since the use of average values of growth coefficients $k_0 = 0.26$ and $k_1 = 0.009$ for all samples leads to only an insignificant increase in error, no greater than 4%, these coefficients can be taken as constants. The error values for the selected values k_0 and k_1 are also given in Table 2.

The coefficients A_1 and B_1 characterize the relationship between the output of the target fraction, the pressure, and the number of cycles. However, it was not possible to establish the relationship between the values of these coefficients and the characteristics of the initial sample on the basis of the available data. It is possible that the values of these coefficients are influenced by the group composition of the raw material or its gas content. The paper [19] presents the results indicating the influence of gas content on the yield and characteristics of fractions of petroleum products during their cavitation treatment. These results also suggest the influence of group composition.

The analysis of the obtained results allowed us to assume that the value of the yield of the fraction $T_{IBP}-400^\circ\text{C}$ after 7 processing cycles (after the curve reaches saturation) at different pressure values can be predicted using only data on the initial sample (before processing). The coefficients of linear dependence (5) were determined using the least squares method:

$$R = 0.25 \cdot p + 0.85 \cdot R_0 + 7.4 \quad (5)$$

The constructed model is adequate according to the Fisher criterion. The value of the determination

coefficient R^2 for this model is 0.85, while the error is 12%.

Thus, before cavitation takes place, it is possible to estimate to what maximum value the yield of the target fraction will increase as a result of treatment at different pressures.

The presented results indicate that it is possible to predict the effectiveness of the impact (pressure created in the diffuser and the number of exposure cycles) on the yield of fractions boiling up to 400°C .

Analysis of equation (2) suggests that pressure has a greater effect on increasing the yield of the target fraction. For confirmation, the energy consumption levels for the creation of cavitation phenomena at different pressures and processing cycles, as well as target product output, were compared. To do this, equation (6), given in [20], was used to calculate the useful power of the pump:

$$N_p = \rho V g H, \quad (6)$$

where N_p is the pump power output; ρ is the density of the pumped liquid; V is the volumetric flow rate (capacity) of the pump; g is the acceleration of gravity; H is the head.

During the calculations, an assumption was made about the constancy of the mass of the sample during processing; for this purpose, it was necessary to take into account the change in the density of the sample after each exposure cycle. In all cases, the volumetric flow rate of the initial sample was assumed to be $0.1 \text{ m}^3/\text{s}$.

It follows from equation (6) that an increase in pressure (by 2, 3, etc. times) or an increase in the number of processing cycles (by the same number of times) leads

to the same increase in energy consumption. The relationship between the energy costs of creating cavitation under different conditions of the process is shown in Fig. 3 along with the yield of the fraction $T_{IBP}-400^{\circ}\text{C}$.

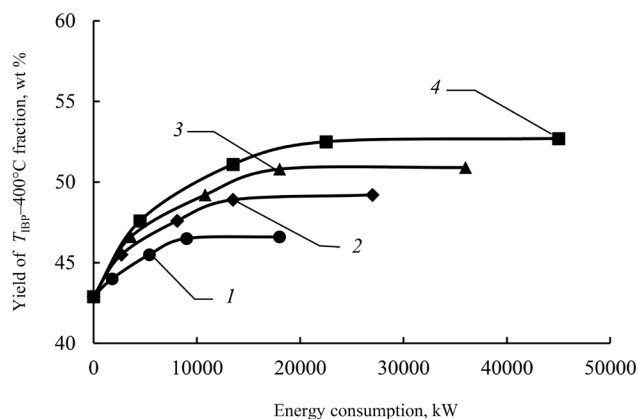


Fig. 3. Influence of energy consumptions and pressure on the yield of fractions $T_{IBP}-400^{\circ}\text{C}$ of a vacuum gasoil sample in cavitation processing: 1 – treatment pressure 20 MPa; 2 – treatment pressure 30 MPa; 3 – treatment pressure 40 MPa; 4 – treatment pressure 50 MPa.

Similar results were obtained for other samples. It can be seen that energy consumption increases comparably both with an increase in pressure and with an increase in the number of processing cycles. However, a greater effect (an increase in the yield of fractions of $T_{IBP}-400^{\circ}\text{C}$) is achieved with an increase in pressure.

CONCLUSIONS

As a result of the conducted research, an equation describing the effect of pressure and the number of cycles on the yield of the fraction $T_{IBP}-400^{\circ}\text{C}$ after cavitation treatment of dark oil products is proposed. The connection of some of the coefficients of this equation with the physicochemical characteristics of the feedstock is established. The equation can be used to predict the maximum possible yield of the fraction $T_{IBP}-400^{\circ}\text{C}$ as a result of cavitation treatment under various conditions of the process according to the physicochemical characteristics of the feedstock with a prediction error less than 12%. The analysis of the equation and the comparison of energy consumptions between different process regimes shows that a higher yield of the target product can be achieved by increasing pressure gradient rather than the number of processing cycles.

Authors' contribution

All authors equally contributed to the research work.

The authors declare no conflicts of interest.

REFERENCES

1. Kapustin V.M. *Tekhnologiya pererabotki nefii*. V 4 ch. Ch. 1. *Pervichnaya pererabotka nefii (Oil Refining Technology)*. In 4 v. V. 1. *Primary oil refining*. Moscow: KolosS; 2013. 334 p. (in Russ.). ISBN 978-5-9532-0825-3
2. Chebotova V.I., Ulanov V.V. Oil refining depth in Russia. *Delovoi zhurnal NEFTEGAZ.RU = Business magazine Neftegaz.RU*. 2021;(109):14–17 (in Russ.).

СПИСОК ЛИТЕРАТУРЫ

1. Капустин В.М. *Технология переработки нефти*. В 4-х частях. Часть первая. *Первичная переработка нефти*. М.: КолосС; 2013. 334 с. ISBN 978-5-9532-0825-3
2. Чеботова В.И., Уланов В.В. Глубина переработки нефти в России. *Деловой журнал NEFTEGAZ.RU*. 2021;(109):14–17.

3. Artemov A.V., Pereslavl'tsev A.V., Krutyakov Yu.A., Voshchinin S.A., Kudrinskii A.A., Bul'ba V.A., Ostryi I.I. Plasma technologies for processing hydrocarbon raw and waste materials. *Ekologiya i promyshlennost' Rossii = Ecology and Industry of Russia*. 2011;(10):18–23 (in Russ.).
4. Ganieva G.R., Timerkaev B.A. Plasmachemical method of exposure to heavy hydrocarbons. *Neftekhimiya*. 2016;56(6):651–654 (in Russ.). <https://doi.org/10.7868/S0028242116060046>
5. Pivovarova N.A. Use of wave effect in processing of the hydrocarbonic raw material (Review). *Pet. Chem.* 2019;59(6):559–569. <https://doi.org/10.1134/S0965544119060148>
[Original Russian Text: Pivovarova N.A. Use of wave effect in processing of the hydrocarbonic raw material (Review). *Neftekhimiya*. 2019;59(7):727–738 (in Russ.). <https://doi.org/10.1134/S002824211907013X>]
6. Ivanov S.V., Vorobyev S.I., Torhovskiy V.N., Gerzeliev I.M. The application of hydrodynamic cavitation to increase the efficiency of the catalytic cracking of vacuum gas oil. *Tonk. Khim. Tekhnol. = Fine Chem. Technol. (Vestnik MITHT)*. 2013;8(3):67–69 (in Russ.).
7. Balpanova N.Zh., Tusipkhan A., Gyl'maliev A.M., Ma F., Kyzkenova A.Zh., Aitbekova D.E., Khalikova Z.S., Baikenova G.G., Baikenov M.I. Kinetics of cavitation of an intermediate fraction of coal tar. *Solid Fuel Chem.* 2020;54(4):208–213. <https://doi.org/10.3103/S0361521920040023>
[Original Russian Text: Balpanova N.Zh., Tusipkhan A., Gulmaliev A.M., Ma F., Kyzkenova A.Zh., Aitbekova D.E., Khalikova Z.S., Baikenova G.G., Baikenov M.I. Kinetics of cavitation of an intermediate fraction of coal tar. *Khimiya Tverdogo Topлива*. 2020;(4):21–27 (in Russ.). <https://doi.org/10.31857/S0023117720040027>]
8. Ivanitskiy G.K. Numerical simulation of bubble cloud behavior in hydrodynamic cavitation. *Sovremennaya nauka: issledovaniya, idei, rezul'taty, tekhnologii = Modern science: Researches, Ideas, Results, Technologies*. 2011;(7):52–58 (in Russ.).
9. Bhangu S.K., Ashokkumar M. Theory of Sonochemistry. *Top. Curr. Chem.* 2016;374(4):56. <https://doi.org/10.1007/s41061-016-0054-y>
10. Avvaru B., Venkateswaran N., Uppara P., Iyengar S.B., Katti S.S. Current knowledge and potential applications of cavitation technologies for the petroleum industry. *Ultrason. Sonochem.* 2018;42:493–507. <https://doi.org/10.1016/j.ultsonch.2017.12.010>
11. Askarian M., Vatani A., Edalat M. Heavy oil upgrading via hydrodynamic cavitation in the presence of an appropriate hydrogen donor. *J. Petr. Sci. Eng.* 2017;151:55–61. <https://doi.org/10.1016/j.petrol.2017.01.037>
12. Promtov M.A. Change in fractional composition of oil in hydro-pulse cavitation processing. *Vestnik TGTU = Transactions TSTU*. 2017;23(3):412–419 (in Russ.). <https://doi.org/10.17277/vestnik.2017.03.pp.412-419>
13. Tao R., Xu. X. Reducing the viscosity of crude oil by pulsed electric or magnetic field. *Energy & Fuels*. 2006;20(5):2046–2051. <https://doi.org/10.1021/ef060072x>
14. Besov A.S., Koltunov K.Yu. Brulev S.O., Kirilenko V.N., Kuz'menkov S.I., Pal'chikov E.I. Destruction of hydrocarbons in the cavitation region activated by aqueous electrolyte solutions in the presence of electric field. *Tech. Phys. Lett.* 2003;29(3):207–209. <https://doi.org/10.1134/1.1565635>
[Original Russian Text: Besov A.S., Koltunov K.Yu., Brulev S.O., Kirilenko V.N., Kuz'menkov S.I., Pal'chikov E.I. Destruction of hydrocarbons in the cavitation region activated by aqueous electrolyte solutions in the presence of electric field. *Pis'ma v Zhurnal Tekhnicheskoi Fiziki*. 2003;29(5):71–77 (in Russ.).]
3. Артемов А.В., Переславцев А.В., Крутяков Ю.А., Вошинин С.А., Кудринский А.А., Бульба В.А., Острый И.И. Плазменные технологии переработки углеводородного сырья и отходов. *Экология и промышленность России*. 2011;(10):18–23.
4. Ганиева Г.Р., Тимеркаев Б.А. Плазмохимическое разложение тяжелых углеводородов. *Нефтехимия*. 2016;56(6):651–654. <https://doi.org/10.7868/S0028242116060046>
5. Пивоварова Н.А. Использование волновых воздействий в переработке углеводородного сырья (Обзор). *Нефтехимия*. 2019;59(7):727–738. <https://doi.org/10.1134/S002824211907013X>
6. Иванов С.В., Воробьев С.И., Торховский В.Н., Герзелев И.М. Применение гидродинамической кавитации для повышения эффективности каталитического крекинга вакуумного газойля. *Тонкие химические технологии (Вестник МИТХТ им. М.В. Ломоносова)*. 2013;8(3):67–69.
7. Балпанова Н.Ж., Тусипхан А., Гюльмалиев А.М., Ма Ф., Кызкенова А.Ж., Айтбекова Д.Е., Халикова З.С., Байкенова Г.Г., Байкенов М.И. Кинетика кавитации средней фракции каменноугольной смолы. *Химия твердого топлива*. 2020;(4):21–27. <https://doi.org/10.31857/S0023117720040027>
8. Иванитский Г.К. Численное моделирование динамики пузырькового кластера в процессах гидродинамической кавитации. *Современная наука: исследования, идеи, результаты, технологии*. 2011;(7):52–58.
9. Bhangu S.K., Ashokkumar M. Theory of Sonochemistry. *Top. Curr. Chem.* 2016;374(4):56. <https://doi.org/10.1007/s41061-016-0054-y>
10. Avvaru B., Venkateswaran N., Uppara P., Iyengar S.B., Katti S.S. Current knowledge and potential applications of cavitation technologies for the petroleum industry. *Ultrason. Sonochem.* 2018;42:493–507. <https://doi.org/10.1016/j.ultsonch.2017.12.010>
11. Askarian M., Vatani A., Edalat M. Heavy oil upgrading via hydrodynamic cavitation in the presence of an appropriate hydrogen donor. *J. Petr. Sci. Eng.* 2017;151:55–61. <https://doi.org/10.1016/j.petrol.2017.01.037>
12. Промтов М.А. Изменение фракционного состава нефти при гидроимпульсной кавитационной обработке. *Вестник Тамбовского государственного университета*. 2017;23(3):412–419. <https://doi.org/10.17277/vestnik.2017.03.pp.412-419>
13. Tao R., Xu. X. Reducing the viscosity of crude oil by pulsed electric or magnetic field. *Energy & Fuels*. 2006;20(5):2046–2051. <https://doi.org/10.1021/ef060072x>
14. Бесов А.С., Колтунов К.Ю., Брулев С.О., Кириленко В.Н., Кузьменков С.И., Пальчиков Е.И. Деструкция углеводородов в кавитационной области в присутствии электрического поля при активации водными растворами электролитов. *Письма в журнал технической физики (Письма в ЖТФ)*. 2003;29(5):71–77.
15. Торховский В.Н., Воробьев С.И., Егорова Е.В., Иванов С.В., Антонюк С.Н., Городский С.Н. Превращение алканов под действием единичного импульса гидродинамической кавитации. Поведение среднецепных алканов C₂₁-C₃₈. *Тонкие химические технологии (Вестник МИТХТ им. М.В. Ломоносова)*. 2014;9(4):59–69.
16. Торховский В.Н., Воробьев С.И., Антонюк С.Н., Егорова Е.В., Иванов С.В., Кравченко В.В., Городский С.Н. Использование многоциклового кавитации для интенсификации переработки нефтяного сырья. *Технологии нефти и газа*. 2015;97(2):9–17.

15. Torhovskiy V.N., Vorobyev S.I., Egorova E.V., Antonyuk S.N., Gorodskiy S.N., Ivanov S.V. Transformation of alkanes under treatment of single impulse of hydrodynamic cavitation. Behaviour of medium-chain alkanes C_{21} – C_{38} . *Tonk. Khim. Tekhnol. = Fine Chem. Technol. (Vestnik MITHT)*. 2014;9(4):59–69 (in Russ.).
16. Torhovskij V.N., Vorob'ev S.I., Antonjuk S.N., Egorova E.V., Ivanov S.V., Kravchenko V.V., Gorodskij S.N. Intensification of petroleum feedstock processing by multi-cycle cavitation. *Tekhnologii nefii i gaza = Oil and Gas Technologies*. 2015;97(2):9–17 (in Russ.).
17. Skryabov G.Ya. Models of mass transfer and population with saturation mechanism. *Matematicheskoe modelirovanie = Mathematical Models and Computer Simulations*. 2007;19(4):27–36 (in Russ.).
18. Bertalanffy L. Basic concepts in quantitative biology of metabolism. *Helgoländer Wissenschaftliche Meeresuntersuchungen*. 1964;9(1–4):5–37. <https://doi.org/10.1007/BF01610024>
19. Пешнев Б.В., Николаев А.И., Терентьева В.Б., Никишин Д.В. Механохимическая активация нефтяного сырья. *Актуальные проблемы нефтехимии: Сборник тезисов докладов XII Российской конференции*. М.: ИНХС РАН; 2021. С. 153–157. ISBN 978-5-990389144
20. Айнштейн В.Г., Захаров М.К., Носов Г.А. *Процессы и аппараты химической технологии. Общий курс*. М.: БИНОМ. Лаборатория знаний; 2014. 1758 с. ISBN 978-5-9963-2214-5

About the authors:

Boris V. Peshnev, Dr. Sci. (Eng.), Professor, Head of the A.N. Bashkirov Department of Petrochemical Synthesis and Artificial Liquid Fuel Technology, M.V. Lomonosov Institute of Fine Chemical Technologies, MIREA – Russian Technological University (86, Vernadskogo pr., Moscow, 119571, Russia). E-mail: peshnevbv@mail.ru. Scopus Author ID 6507362823, <https://orcid.org/0000-0002-0507-2754>

Elena V. Burlyayeva, Dr. Sci. (Eng.), Professor, Department of Information Systems in Chemical Technology, M.V. Lomonosov Institute of Fine Chemical Technologies, MIREA – Russian Technological University (86, Vernadskogo pr., Moscow, 119571, Russia). E-mail: burlyayeva@mirea.ru. Scopus Author ID 36964878300, RSCI SPIN-code 3566-5894, <https://orcid.org/0000-0003-1371-1410>

Vera B. Terenteva, Cand. Sci. (Eng.), Junior Researcher, 25th State Research Institute of Himmotology, Ministry of Defence of the Russian Federation (10, Molodogvardeyskaya ul., Moscow, 121467, Russia). E-mail: terenteva-vb@mail.ru. RSCI SPIN-code 9086-5440, <https://orcid.org/0000-0003-4624-1507>

Denis V. Nikishin, Postgraduate Student, Head of the Laboratory, A.N. Bashkirov Department of Petrochemical Synthesis and Artificial Liquid Fuel Technology, M.V. Lomonosov Institute of Fine Chemical Technologies, MIREA – Russian Technological University (86, Vernadskogo pr., Moscow, 119571, Russia). E-mail: nikishin@mirea.ru. RSCI SPIN-code 4089-6391, <https://orcid.org/0000-0002-4466-4402>

Alexander I. Nikolaev, Dr. Sci. (Eng.), Professor, A.N. Bashkirov Department of Petrochemical Synthesis and Artificial Liquid Fuel Technology, M.V. Lomonosov Institute of Fine Chemical Technologies, MIREA – Russian Technological University (86, Vernadskogo pr., Moscow, 119571, Russia). E-mail: nikolaev_a@mirea.ru. Scopus Author ID 57197582338, <https://orcid.org/0000-0001-8594-2985>

Konstantin S. Andronov, Master, A.N. Bashkirov Department of Petrochemical Synthesis and Artificial Liquid Fuel Technology, M.V. Lomonosov Institute of Fine Chemical Technologies, MIREA – Russian Technological University (86, Vernadskogo pr., Moscow, 119571, Russia). E-mail: kostya.andronov.88@mail.ru. <https://orcid.org/0000-0001-6214-8607>

Об авторах:

Пешнев Борис Владимирович, д.т.н., профессор, заведующий кафедрой технологии нефтехимического синтеза и искусственного жидкого топлива им. А.Н. Башкирова Института тонких химических технологий им. М.В. Ломоносова ФГБОУ ВО «МИРЭА – Российский технологический университет» (119571, Россия, Москва, пр-т Вернадского, д. 86). E-mail: peshnev@mirea.ru. Scopus Author ID 6507362823, <https://orcid.org/0000-0002-0507-2754>

Бурляева Елена Валерьевна, д.т.н., профессор кафедры информационных систем в химической технологии Института тонких химических технологий им. М.В. Ломоносова ФГБОУ ВО «МИРЭА – Российский технологический университет» (119571, Россия, Москва, пр-т Вернадского, д. 86). E-mail: burlyaeva@mirea.ru. Scopus Author ID 36964878300, SPIN-код РИНЦ 3566-5894, <https://orcid.org/0000-0003-1371-1410>

Терентьева Вера Борисовна, к.т.н., младший научный сотрудник, 25 Государственный научно-исследовательский институт химмотологии Министерства обороны Российской Федерации (121467, Россия, Москва, ул. Молодогвардейская, д. 10). E-mail: terenteva-vb@mail.ru. SPIN-код РИНЦ 9086-5440, <https://orcid.org/0000-0003-4624-1507>

Никишин Денис Васильевич, аспирант, заведующий лабораторией кафедры технологии нефтехимического синтеза и искусственного жидкого топлива им. А.Н. Башкирова Института тонких химических технологий им. М.В. Ломоносова ФГБОУ ВО «МИРЭА – Российский технологический университет» (119571, Россия, Москва, пр-т Вернадского, д. 86). E-mail: nikishin@mirea.ru. SPIN-код РИНЦ 4089-6391, <https://orcid.org/0000-0002-4466-4402>

Николаев Александр Игоревич, д.т.н., доцент, профессор кафедры технологии нефтехимического синтеза и искусственного жидкого топлива им. А.Н. Башкирова Института тонких химических технологий им. М.В. Ломоносова ФГБОУ ВО «МИРЭА – Российский технологический университет» (119571, Россия, Москва, пр-т Вернадского, д. 86). E-mail: nikolaev_a@mirea.ru. Scopus Author ID 57197582338, <https://orcid.org/0000-0001-8594-2985>

Андронов Константин Сергеевич, магистр, кафедра технологии нефтехимического синтеза и искусственного жидкого топлива им. А.Н. Башкирова Института тонких химических технологий им. М.В. Ломоносова ФГБОУ ВО «МИРЭА – Российский технологический университет» (119571, Россия, Москва, пр-т Вернадского, д. 86). E-mail: kostya.andronov.88@mail.ru. <https://orcid.org/0000-0001-6214-8607>

The article was submitted: March 01, 2022; approved after reviewing: June 20, 2022; accepted for publication: November 17, 2022.

*Translated from Russian into English by N. Isaeva
Edited for English language and spelling by Thomas Beavitt*

ISSN 2686-7575 (Online)

<https://doi.org/10.32362/2410-6593-2022-17-6-483-491>

UDC 661.746.54



RESEARCH ARTICLE

Features of triamyl citrate synthesis

Anna D. Shiryayeva, Svetlana V. Moiseeva[✉], Svetlana V. Levanova, Ilya L. Glazko

Samara State Technical University, Samara, 443100 Russia

[✉]Corresponding author, e-mail: sveta_sushkova@mail.ru

Abstract

Objectives. To find an effective way for obtaining triamyl citrate, an environmentally friendly, biodegradable citric acid ester used as a plasticizer for PVC-based polymer compositions.

Methods. The possibilities of heterogeneous catalysis were analyzed using the case study of three commercial samples of macroporous sulfocationites (AmberlystTM 15, AmberlystTM 70, and TULSION[®] 66). Homogeneous catalysis was studied using the example of orthophosphoric acid (H_3PO_4), while self-catalysis was investigated during esterification of citric acid with amyl alcohol (ROH). The syntheses were carried out under identical conditions: $T = 110^\circ C$, the ratio of CA:ROH = 1:5 (mol) amount of catalyst 1 wt % on the reaction mass in a thermostatically controlled reactor of ideal mixing with continuous distillation of the resulting water.

Results. It was found that in all variants (even under self-catalysis conditions), the conversion of citric acid in 180 min reached 94–99%. Triamyl citrate was formed after 9 h with a yield of 90% only when using a homogeneous catalyst (H_3PO_4) and in the presence of a heterogeneous catalyst sample (AmberlystTM 15).

Conclusions. The revealed differences in the reactivity of the studied sulfocationites (AmberlystTM 15, AmberlystTM 70, and TULSION[®] 66) confirm the well-known theoretical positions, according to which the kinetic pseudo-homogeneous model of the esterification process of hydroxy acids in excess of aliphatic alcohols is based on the law of acting masses and depends on the specific surface area of the catalyst, which for AmberlystTM 15 is of the greatest importance as compared to AmberlystTM 70 and TULSION[®] 66 (m^2/g): 53:36:35, respectively.

Keywords: citric acid, amyl alcohol, esterification, heterogeneous catalysts, self-analysis

For citation: Shiryaeva A.D., Moiseeva S.V., Levanova S.V., Glazko I.L. Features of triamyl citrate synthesis. *Tonk. Khim. Tekhnol. = Fine Chem. Technol.* 2022;17(6):483–491 (Russ., Eng.). <https://doi.org/10.32362/2410-6593-2022-17-6-483-491>

НАУЧНАЯ СТАТЬЯ

Особенности синтеза триамилцитрата

А.Д. Ширяева, С.В. Моисеева ✉, **С.В. Леванова, И.Л. Глазко**

Самарский государственный технический университет, Самара, 443100 Россия

✉ Автор для переписки, e-mail: sveta_sushkova@mail.ru

Аннотация

Цели. Поиск эффективного метода получения триамилцитрата – экологически чистого, биоразлагаемого сложного эфира лимонной кислоты, используемого в качестве пластификатора полимерных композиций на основе поливинилхлорида.

Методы. Выявлены возможности гетерогенного катализа на примере трех коммерческих образцов макропористых сульфокатионитов (Амберлист™ 15, Амберлист™ 70 и Тулсион® 66); гомогенного катализа на примере ортофосфорной кислоты (H_3PO_4) и самокатализа при этерификации лимонной кислоты (ЛК) амиловым спиртом (РОН). Синтезы проводили в одинаковых условиях: $T = 110$ °С отношение ЛК:РОН = 1:5 (мольн.) количество катализатора 1 мас. % на реакционную массу в термостатированном реакторе идеального смешения с непрерывным отгоном образующейся воды.

Результаты. Установлено, что во всех вариантах конверсия лимонной кислоты за 180 мин достигает 94–99%. Триамилцитрат с выходом 90% образуется через 9 ч только при использовании гомогенного катализатора (H_3PO_4) и в присутствии образца гетерогенного катализатора – Амберлист™ 15.

Выводы. Выявленные различия в реакционной способности исследованных сульфокатионитов Амберлист™ 15, Амберлист™ 70 и Тулсион® 66 подтверждают известные теоретические положения, в соответствии с которыми кинетическая псевдогомогенная модель процесса этерификации гидроксикислот в избытке алифатических спиртов основывается на законе действующих масс и зависит от удельной поверхности катализатора, которая для Амберлист™ 15 имеет наибольшее значение по сравнению с Амберлист™ 70 и Тулсион® 66 (m^2/g): 53:36:35 соответственно.

Ключевые слова: лимонная кислота, амиловый спирт, этерификация, гетерогенные катализаторы, самокатализ

Для цитирования: Ширяева А.Д., Моисеева С.В., Леванова С.В., Глазко И.Л. Особенности синтеза триамилцитрата. *Тонкие химические технологии.* 2022;17(6):483–491. <https://doi.org/10.32362/2410-6593-2022-17-6-483-491>

INTRODUCTION

Citric acid (CA) is widely used in various sectors of the world economy as a common acidity regulator, antioxidant, and complexing agent. With a current global

annual production volume of 1.8 mln t/year, the annual increase in demand is projected at the level of 4.0–4.5%.

The structure of citric acid consumption in Russia differs from the world by a much smaller share of its use in industries that form the basis of environmentally

friendly synthetic detergents, solvents, plasticizing compositions: 80% of citric acid is used in the food industry, with 10–15% being allocated to the production of detergents, and up to 10% in cosmetics and pharmaceuticals [1].

The dominant portion of citric acid derivatives is comprised of its esters based on higher aliphatic alcohols. These belong to the Hazard Class 4 considered as non-toxic. Products having a flash point of at least 168°C (according to GOST 8728-88¹) have plasticizing properties and provide foaming of polyvinyl chloride (PVC) back foam pastes [2, 3].

To date, the production of higher alkyl citrates in Russia has been limited due to the lack of a raw material base. However, within the framework of the general development of gas chemistry and the increase in the capacity of oxosynthesis processes, it is expected to create a sufficient potential of alcohols C₃–C₅ and higher over the next 20–25 years [4]. The product of esterification of citric acid with amyl alcohol is of the greatest interest.

The technological processes of synthesis of esters are divided into two groups [5–7]:

1) liquid-phase group, i.e., thermal in self-catalysis mode or homogeneous-catalytic, in which the chemical reaction is combined with the process of distilling volatile products;

2) heterogeneous-catalytic group, carried out in liquid or gas phases in flow apparatuses without combining with separation processes.

The processes of the first group are traditional and the most common in the technology of esterification. However, they work satisfactorily only at a high rate of chemical reaction, otherwise the completeness of the transformation and the reactor performance are too low.

It is known that the longer the length of the hydrocarbon radical of the aliphatic alcohol, the higher the molecular weight of the target product and the flash point. This reduces the emission of the plasticizer, improves its operational properties [8]. However, it was found that an increase in the hydrocarbon radical on the CH₂-group in the initial

alcohol reduces the reactivity of the alcohol by an average of 1.3 times and increases the reaction time [9].

Although the use of homogeneous catalysts in industry (*p*-toluene sulfonic acid, orthophosphoric acid, methanesulfonic acid) in esterification reactions offers a good catalytic effect, it is associated with high production costs and negative ecological effects [5]. Therefore, there is a current trend involving the use of heterogeneous catalysts. This eliminates many disadvantages associated with the use of homogeneous catalysts, since their heterogeneous counterparts are easily separated from the reaction mass by decantation or filtration, offer an effective means of reducing or eliminating corrosion problems, as well as suggesting the possibility of switching from a semi-periodic to a continuous process.

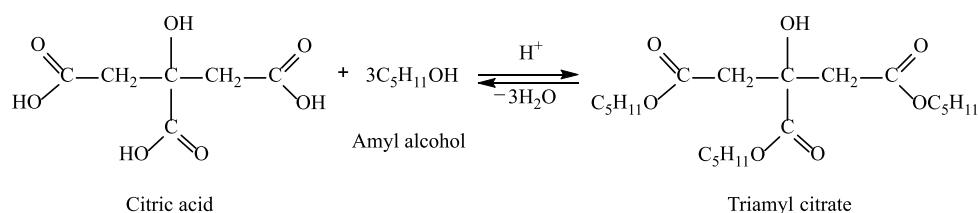
The disadvantages of using heterogeneous catalysts—high temperature, high catalyst consumption, and increased side reactions, lead to tarring of the reaction mass and a decrease in the quality of the target products [10–11].

While the growing interest of domestic producers of citric acid esters is justified by the need to achieve independence from imports, a thorough assessment of the effectiveness of technological solutions and the quality of the target products is required. This position becomes especially significant when expanding the raw material base towards the use of hydroxy acids and high-molecular alcohols of linear and isostructure.

Therefore, as part of this study we conducted comprehensive studies and compared the possibilities of self-catalysis, homogeneous and heterogeneous catalysis during esterification of citric acid with amyl alcohol in order to obtain triamyl citrates with a yield of 85–90%.

EXPERIMENTAL

As initial raw materials, the following substances, which differ in geometric dimensions, were chosen: Citric acid (food grade, monohydrate with a base



Scheme. Esterification of citric acid with amyl alcohol.

¹ GOST 8728-88. Interstate Standard. Plasticizers. Specifications. Moscow: IPK Izd. Standartov; 1988.

substance content of 92.5%) (*Reagent*, Russia); pure grade amyl alcohol with a purity of more than 99% (*Reachim*, Russia); pure grade orthophosphoric acid (homogeneous catalyst) with a purity of 85% (*Reagent*, Russia); three commercial industrial samples of microporous sulfocationites: Amberlyst™ 15 (*Sigma-Aldrich*, Germany), Amberlyst™ 70 (*Sigma-Aldrich*, Germany) and TULSION® 66 (*Thermax*, India).

The characteristics of the catalysts are given in Table 1.

Esterification of citric acid with amyl alcohol was carried out in a thermostated mixing reactor. After dissolving citric acid in amyl alcohol in the reactor, a catalyst was introduced and samples were taken at specified intervals, with the change in the concentration of carboxyl groups in the reaction mass determined by titrimetry. The composition of the reaction mass was determined using gas-liquid chromatography on the Crystal 2000M chromatographic complex (*Chromatec*, Russia) with the

following parameters: capillary column with grafted nonpolar phase OV-101 100 m × 0.2 mm × 0.2 μm; column temperature mode: 120°C (10 min)—15°C/min—260°C; evaporator temperature 300°C; detector temperature 300°C; carrier gas is helium, flow division 1/80. In the analysis, a derivatization method was used to convert polar organic compounds containing carboxyl groups into less volatile ones. Diazomethane was used as a derivatizing agent. The internal standard method was used for the quantitative determination of citric acid esters in the reaction mass. Dicyclohexyl adipate was used as a standard [12].

Based on previous works [2–3, 9, 12], in which data on the effect of temperature, molar ratio of reagents, type, and quantity of homogeneous catalysts were obtained, the following research conditions were selected: temperature 110°C; citric acid:alcohol ratio is 1:5 (mol); amount of catalyst is 1% per reaction mass.

All experiments were carried out in the mode of distillation of the released reaction water with strict observance of the isothermal regime.

Table 1. Characteristics of the catalysts used in the study

Acid	Formula of the substance	Dissociation constant K_a	pK_a	
1. Self-catalysis				
Citric acid	HOOCCH ₂ C(OH)(COOH)CH ₂ COOH	$K_1 = 7.41 \cdot 10^{-4}$ $K_2 = 1.74 \cdot 10^{-5}$ $K_3 = 9.80 \cdot 10^{-6}$	3.13 4.76 5.40	
2. Homogeneous catalysis				
Orthophosphoric acid	H ₃ PO ₄ (85%)	$K_1 = 7.59 \cdot 10^{-3}$ $K_2 = 6.17 \cdot 10^{-8}$ $K_3 = 4.20 \cdot 10^{-13}$	2.12 7.21 12.38	
3. Heterogeneous catalysis				
No.	Indicators	Amberlyst™ 15	Amberlyst™ 70	TULSION® 66
1	Minimum capacity, eq/kg	4.7	2.55	5
2	Shipping weight, g/L	610	770	500
3	Specific surface area, m ² /g	53	36	35
4	Pore diameter, Å	300	220	450–500
5	Recommended max. op. temperature, °C	<120	190	130

RESULTS AND DISCUSSION

Figures 1–5 demonstrate graphs of the evolution of products obtained as a result of research for 180 min.

Table 2 summarizes the results of all experimental studies performed in this work in the range of 180–540 min.

Citric acid was found that to be rapidly esterified by the first carboxyl group with the formation of monoamyl citrates in all variants of catalysis (even under self-catalysis conditions), which corresponds to the literature data [6, 13, 14]. In 180 min, the conversion of citric acid reaches 94–99%. Regardless of the type of catalysis, the content of diamyl citrate for 240 min is 50–60%. Esterification of the third carboxyl group into triamyl citrate is limiting; the yield of triamyl citrate in 84–90% is achieved in 9 h (540 min) only with homogeneous catalysis and in the presence of Amberlyst™ 15 catalyst.

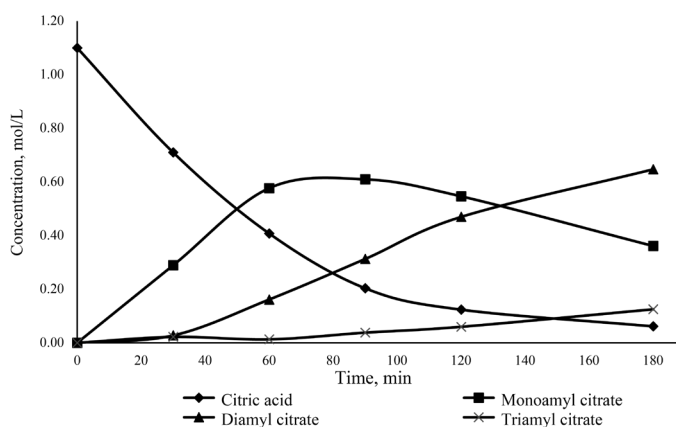


Fig. 1. Esterification of citric acid under conditions of self-catalysis.

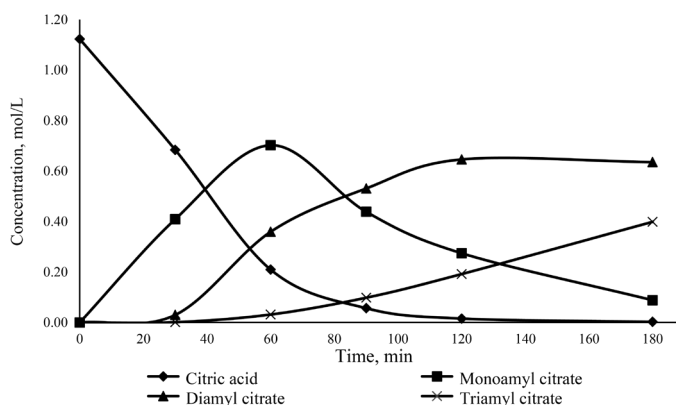


Fig. 2. Esterification of citric acid in the presence of orthophosphoric acid.

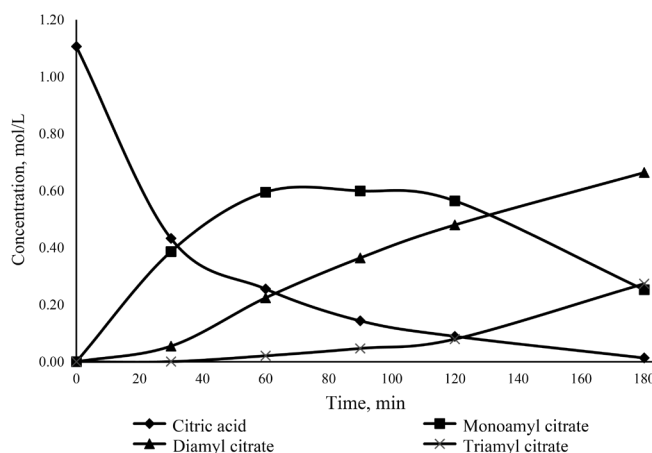


Fig. 3. Esterification of citric acid in the presence of Amberlyst™ 15.

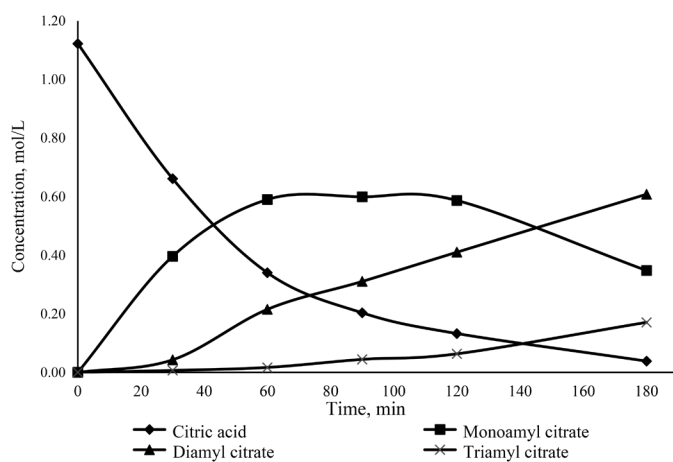


Fig. 4. Esterification of citric acid in the presence of Amberlyst™ 70.

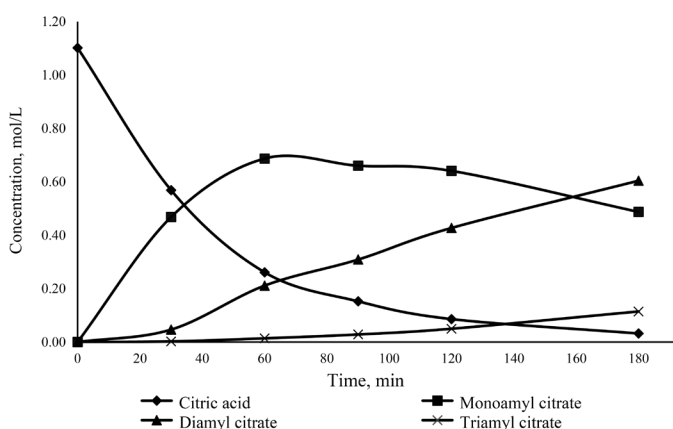


Fig. 5. Esterification of citric acid in the presence of TULSION® 66.

Features of triamyl citrate synthesis

Table 2. Composition of the reaction mass of the esterification reaction of citric acid with amyl alcohol at 110°C, reaction time: 180, 240, and 540 min with the distillation of reaction water

Experiment \ Yield, %	Self-catalysis	Amberlyst™ 15	Amberlyst™ 70	TULSION® 66	H ₃ PO ₄
180 min					
Citric acid (CA)	5.13	1.10	3.31	2.57	0.21
Monoamyl citrate	30.23	20.99	29.85	39.39	7.85
Diamyl citrate	54.17	55.16	52.17	48.82	56.48
Triamyl citrate	10.47	22.75	14.67	9.25	35.44
Conversion by CA, %	94.40	98.80	96.50	97.10	99.78
240 min					
CA	1.52	0.31	0.99	0.85	0
Monoamyl citrate	19.09	8.38	14.53	21.99	2.53
Diamyl citrate	58.32	51.55	55.07	56.18	48.20
Triamyl citrate	21.07	39.76	29.46	20.98	49.26
Conversion by CA, %	98.42	99.66	98.97	99.14	100
540 min					
CA	0	0	0	0	0
Monoamyl citrate	0.80	0	0.68	1.07	0
Diamyl citrate	32.54	10.32	30.63	25.35	15.74
Triamyl citrate	66.66	89.68	68.69	73.58	84.26
Conversion by CA, %	100	100	100	100	100

In Russia, about 300000 t/year of citric acid are obtained from the waste of molasses sugar production [15]. From this amount of citric acid, it is possible to obtain about 150000 t/year of citric

acid esters comprised of trialkyl citrates, of which the esters of citric acid and amyl alcohol have the greatest practical significance as a PVC plasticizer [16].

CONCLUSIONS

The revealed differences in the reactivity of the studied sulfocationites (Amberlyst™ 15, Amberlyst™ 70, TULSION® 66) confirm the well-known theoretical positions, according to which the kinetic pseudo-homogeneous model of the process of esterification of hydroxides by aliphatic alcohols (in excess) is based on the law of acting masses. In this regard, the reaction rate will depend on the specific surface area of the catalyst, which for Amberlyst™ 15 is of the greatest importance compared to Amberlyst™ 70 and TULSION® 66 (m²/g): 53:36:55, respectively.

Based on the obtained results, it can be assumed that the installation of semi-continuous azeotropic esterification of citric acid in excess of alcohol using sulfocationite with a large specific surface area as a catalyst will be the most effective.

Authors' contribution

All authors equally contributed to the research work.

The authors declare no conflicts of interest.

REFERENCES

1. Nikiforova T.A., Novitskaya I.B., Minina T.I. Priority directions of development of food citric acid domestic technology. *Pishchevaya promyshlennost' = Food Industry*. 2010;(5):53–54 (in Russ).
2. Sushkova S.V., Levanova S.V., Glazko I.L., Alexandrov A.Yu. Esterification of citric acid with aliphatic alcohols C₂–C₅. *Tonk. Khim. Technol. = Fine Chem. Technol.* 2017;13(3):28–32. <https://doi.org/10.32362/2410-6593-2017-12-3-28-32>
3. Levanova S.V., Krasnykh E.L., Moiseeva S.V., Safronov S.P., Glazko E.L. Scientific and technological features of synthesis of new ester plasticizers based on renewable raw materials. *Izv. Vyssh. Uchebn. Zaved. Khim. Khim. Tekhnol.* 2021;64(6):69–75 (in Russ.). <https://doi.org/10.6060/ivkkt.20216406.6369>
4. Marochkin D.V., Noskov Yu.G., Kron T.E., Karchevskaya O.G., Korneeva G.A. Products of oxosynthesis in the production of complex lubricating oils. *Nauchno-Tekhnicheskii Vestnik NK Rosneft*. 2016;(4):74–80 (in Russ.).
5. Xu J., Jiang J., Zuo Z., Li J. Synthesis of tributyl citrate using acid ionic liquid as catalyst. *Process Safety and Environmental Protection*. 2010;88(1):28–30. <https://doi.org/10.1016/j.psep.2009.11.002>
6. Kolah A.K., Asthana N.S., Vu D.T., Lira C.T., Miller D.J. Triethyl citrate synthesis by reactive distillation. *Ind. Eng. Chem. Res.* 2008;47(4):1017–1025. <https://doi.org/10.1021/ie070279t>
7. Menshchikova A.A., Filatova E.V., Varlamova E.V., Amirkhanov I.R., Yazmukhamedova I.M., Suchkov Yu.G. Production plasticizers based on succinic acid and alcohols 2-ethylhexanol and cyclohexanol. *Uspekhi v khimii i khimicheskoi tekhnologii = Advances in Chemistry and Chemical Technology*. 2017;31(12/193):66–68 (in Russ.).
8. Rahman M., Brazel C.S. The plasticizer market: an assessment of traditional plasticizers and research trends to meet new challenges. *Prog. Polym. Sci.* 2004;29(12):1223–1248. <https://doi.org/10.1016/j.progpolymsci.2004.10.001>

СПИСОК ЛИТЕРАТУРЫ

1. Никифорова Т.А., Новицкая И.Б., Мина Т.И. Приоритетные направления развития веществ в технологии пищевой лимонной кислоты. *Пищевая промышленность*. 2010;(5):53–54.
2. Сушкова С.В., Леванова С.В., Глазко И.Л., Александров А.Ю. Этерификация лимонной кислоты алифатическими спиртами C₂–C₅. *Тонкие химические технологии*. 2017;12(3):28–32. <https://doi.org/10.32362/2410-6593-2017-12-3-28-32>
3. Леванова С.В., Красных Е.Л., Моисеева С.В., Сафронов С.П., Глазко Е.Л. Научные и технологические особенности синтеза новых сложнэфирных пластификаторов на основе возобновляемого сырья. *Иzv. вузов. Химия и хим. технология*. 2021;64(6):69–75. <https://doi.org/10.6060/ivkkt.20216406.6369>
4. Марочкин Д.В., Носков Ю.Г., Крон Т.Е., Карчевская О.Г., Корнеева Г.А. Продукты оксосинтеза в производстве сложных смазочных масел. *Научно-технический вестник ОАО «НК Роснефть»*. 2016;(4):74–80.
5. Xu J., Jiang J., Zuo Z., Li J. Synthesis of tributyl citrate using acid ionic liquid as catalyst. *Process Safety and Environmental Protection*. 2010;88(1):28–30. <https://doi.org/10.1016/j.psep.2009.11.002>
6. Kolah A.K., Asthana N.S., Vu D.T., Lira C.T., Miller D.J. Triethyl citrate synthesis by reactive distillation. *Ind. Eng. Chem. Res.* 2008;47(4):1017–1025. <https://doi.org/10.1021/ie070279t>
7. Меньщикова А.А., Филатова Е.В., Варламова Е.В., Амирханов И.Р., Язмухамедова И.М., Сучков Ю.Г. Получение пластификаторов на основе янтарной кислоты и спиртов 2-этилгексанола и циклогексанола. *Успехи в химии и хим. технологии*. 2017;31(12/193):66–68.
8. Rahman M., Brazel C.S. The plasticizer market: an assessment of traditional plasticizers and research trends to meet new challenges. *Prog. Polym. Sci.* 2004;29(12):1223–1248. <https://doi.org/10.1016/j.progpolymsci.2004.10.001>

9. Sushkova S.V., Levanova S.V., Glazko I.L., Pavlova K.V. Kinetics of esterification of citric acid in production of trialkyl citrates. *Izv. Vyssh. Uchebn. Zaved. Khim. Tekhnol.* 2017;60(2):74–78 (in Russ). <https://doi.org/10.6060/tcct.2017602.5442>
10. Osorio-Pascuas O.M., Santaella M.A., Rodriguez G., Orjuela A. Esterification kinetics of tributyl citrate production using homogeneous and heterogeneous catalysts. *Ind. Eng. Chem. Res.* 2015;54(50):2534–12542. <https://doi.org/10.1021/acs.iecr.5b03608>
11. Bohórquez W.F., Osorio-Pascuas O.M., Santaella M.A., Orjuela A. Homogeneous and heterogeneous catalytic kinetics in the production of triethyl citrate. *Ind. Eng. Chem. Res.* 2020;59(43):19203–19211. <https://doi.org/10.1021/acs.iecr.0c03690>
12. Mittal A., Nair S., Deshmukh K. The kinetic comparison study of catalytic esterification of butyric acid and ethanol over amberlyst 15 and Indion – 190 resins. *Int. J. Innovative Res. Sci. Eng. Technol.* 2015;4(7):5860–5867.
13. Tsai Y.-T., Lin M.-mu, Lee M.-J. Kinetics of heterogeneous esterification of glutaric acid with methanol over Amberlyst 35. *J. of Taiwan Ins. of Chem. Eng.* 2011;42(2):271–277. <https://doi.org/10.1016/j.jtice.2010.07.010>
14. Schastlivaya S.V., Kondratev D.N., Kozlovskii R.L., Shvets V.F. Development of a heterogeneous-catalytic method for obtaining butyl lactate. *Khimicheskaya promyshlennost' segodnya = Chemical Industry Developments.* 2007;(4):20–25 (in Russ.).
15. Maslova E.V. Analysis and prospects of development of citric acid market. In: *Ekonomika. Obshchestvo. Chelovek (Economy. Society. Human)*. Col. of Sci. Works. V.G. Shukhov Belgorod. gos. tekhnol. univ.; 2014. V. XXII. P. 108–118 (in Russ.).
16. Alhanish A., Ghalia M.A. Developments of biobased plasticizers for compostable polymers in the green packaging applications: A review. *Biotechnol. Prog.* 2021;37(6):e3210. <https://doi.org/10.1002/btpr.3210>
9. Сушкова С.В., Леванова С.В., Глазко И.Л., Павлова К.В. Кинетика этерификации лимонной кислоты в производстве триалкилцитратов. *Иzv. Вузов. Химия и хим. технология.* 2017;60(2):74–78. <https://doi.org/10.6060/tcct.2017602.5442>
10. Osorio-Pascuas O.M., Santaella M.A., Rodriguez G., Orjuela A. Esterification kinetics of tributyl citrate production using homogeneous and heterogeneous catalysts. *Ind. Eng. Chem. Res.* 2015;54(50):2534–12542. <https://doi.org/10.1021/acs.iecr.5b03608>
11. Bohórquez W.F., Osorio-Pascuas O.M., Santaella M.A., Orjuela A. Homogeneous and heterogeneous catalytic kinetics in the production of triethyl citrate. *Ind. Eng. Chem. Res.* 2020;59(43):19203–19211. <https://doi.org/10.1021/acs.iecr.0c03690>
12. Mittal A., Nair S., Deshmukh K. The kinetic comparison study of catalytic esterification of butyric acid and ethanol over amberlyst 15 and Indion – 190 resins. *Int. J. Innovative Res. Sci. Eng. Technol.* 2015;4(7):5860–5867.
13. Tsai Y.-T., Lin M.-mu, Lee M.-J. Kinetics of heterogeneous esterification of glutaric acid with methanol over Amberlyst 35. *J. of Taiwan Ins. of Chem. Eng.* 2011;42(2):271–277. <https://doi.org/10.1016/j.jtice.2010.07.010>
14. Счастливая С.В., Кондратьев Д.Н., Козловский Р.Л., Швец В.Ф. Разработка гетерогенно-каталитического способа получения бутиллактиата. *Химическая промышленность сегодня.* 2007;(4):20–25.
15. Маслова Е.В. Анализ и перспективы развития рынка лимонной кислоты. В сб.: *Экономика. Общество. Человек.* Межвузов. сб. науч. трудов. Белгород. гос. технол. ун-т им. В.Г. Шухова; 2014. Т. XXII. С. 108–118.
16. Alhanish A., Ghalia M.A. Developments of biobased plasticizers for compostable polymers in the green packaging applications: A review. *Biotechnol. Prog.* 2021;37(6):e3210. <https://doi.org/10.1002/btpr.3210>

About the authors:

Anna D. Shiryaeva, Master, Department of Technology of Organic and Petrochemical Synthesis, Samara State Technical University (244, Molodogvardeyskaya ul., Samara, 443100, Russia). E-mail: shiryaeva.100.annet@gmail.com. <https://orcid.org/0000-0003-3495-8412>

Svetlana V. Moiseeva, Cand. Sci. (Chem.), Assistant Professor, Department of Technology of Organic and Petrochemical Synthesis, Samara State Technical University (244, Molodogvardeyskaya ul., Samara, 443100, Russia). E-mail: sveta_sushkova@mail.ru. Scopus Author ID 57163952300, RSCI SPIN-code 9568-0707, <https://orcid.org/0000-0002-9949-3276>

Svetlana V. Levanova, Dr. Sci. (Chem.), Professor, Department of Technology of Organic and Petrochemical Synthesis, Samara State Technical University (244, Molodogvardeyskaya ul., Samara, 443100, Russia). E-mail: kinterm@mail.ru. Scopus Author ID 6701876379, ResearcherID D-6065-2014, SPIN-код РИНЦ 4521-0265, <https://orcid.org/0000-0003-2539-8986>

Ilya L. Glazko, Cand. Sci. (Chem.), Assistant Professor, Department of Technology of Organic and Petrochemical Synthesis, Samara State Technical University (244, Molodogvardeyskaya ul., Samara, 443100, Russia). E-mail: glazko@yandex.ru. Scopus Author ID 6602656909, ResearcherID E-5107-2014, RSCI SPIN-code 7964-8477, <https://orcid.org/0000-0001-5421-8775>

Об авторах:

Ширяева Анна Денисовна, магистр, кафедра «Технология органического и нефтехимического синтеза» ФГБОУ ВО «Самарский государственный технический университет» (443100, Россия, г. Самара, ул. Молодогвардейская, д. 244). E-mail: shiryaeva.100.annet@gmail.com. <https://orcid.org/0000-0003-3495-8412>

Моисеева Светлана Вячеславовна, к.х.н., доцент кафедры «Технология органического и нефтехимического синтеза» ФГБОУ ВО «Самарский государственный технический университет» (443100, Россия, г. Самара, ул. Молодогвардейская, д. 244). E-mail: sveta_sushkova@mail.ru. Scopus Author ID 57163952300, SPIN-код РИНЦ 9568-0707, <https://orcid.org/0000-0002-9949-3276>

Леванова Светлана Васильевна, д.х.н., профессор, профессор кафедры «Технология органического и нефтехимического синтеза» ФГБОУ ВО «Самарский государственный технический университет» (443100, Россия, г. Самара, ул. Молодогвардейская, д. 244). E-mail: kinterm@mail.ru. Scopus Author ID 6701876379, ResearcherID D-6065-2014, SPIN-код РИНЦ 4521-0265, <https://orcid.org/0000-0003-2539-8986>

Глазко Илья Леонидович, к.х.н., доцент кафедры «Технология органического и нефтехимического синтеза» ФГБОУ ВО «Самарский государственный технический университет» (443100, Россия, г. Самара, ул. Молодогвардейская, д. 244). E-mail: glazko@yandex.ru. Scopus Author ID 6602656909, ResearcherID E-5107-2014, SPIN-код РИНЦ 7964-8477, <https://orcid.org/0000-0001-5421-8775>

The article was submitted: September 06, 2022; approved after reviewing: September 28, 2022; accepted for publication: November 24, 2022.

*Translated from Russian into English by N. Isaeva
Edited for English language and spelling by Thomas Beavitt*

BIOCHEMISTRY AND BIOTECHNOLOGY

БИОХИМИЯ И БИОТЕХНОЛОГИЯ

ISSN 2686-7575 (Online)

<https://doi.org/10.32362/2410-6593-2022-17-6-492-503>



UDC 615.014.24:615.015.4

RESEARCH ARTICLE

Investigation of the biological activity of the water-soluble C₆₀/poly-*N*-vinylpyrrolidone complex

Natalia Yu. Loginova¹, Yulia S. Chesovskikh^{1,✉}, Vladimir B. Borodulin^{1,2}

¹V.I. Razumovsky Saratov State Medical University, Ministry of Health of the Russian Federation, Saratov, 410012 Russia

²MIREA – Russian Technological University (M.V. Lomonosov Institute of Fine Chemical Technologies), Moscow, 119571 Russia

✉ Corresponding author, e-mail: Juliachesovskih@gmail.com

Abstract

Objectives. The study aimed to investigate the biological activity of the C₆₀/poly-*N*-vinylpyrrolidone (C₆₀/PVP) complex representing a water-soluble fullerene derivative. *In vitro* and *in vivo* techniques were used to analyze the effect of the C₆₀/PVP complex on the activity of lactate dehydrogenase (LDH) and evaluate changes in the biochemical parameters of blood serum when per os administered to mice.

Methods. In order to determine the activity of a commercial LDH preparation and study the kinetics of this process, the standard Warburg photometric method was used. To assess the effect of polyvinylpyrrolidone (PVP) and the C₆₀/PVP complex on some biochemical parameters *in vivo*, a study was conducted on two-month-old male white mongrel mice weighing 20 ± 3 g. Determination of biochemical parameters of blood serum was carried out using a semi-automatic biochemical analyzer according to standard methods.

Results. The effect of the C₆₀/PVP complex on LDH activity was studied along with changes in the biochemical parameters of mouse blood serum characterizing carbohydrate metabolism. As well as increasing the glucose and pyruvic acid content, the C₆₀/PVP complex was found to reduce lactate content and LDH activity in blood serum along with *in vitro* LDH activity according to the type of mixed inhibition.

Conclusions. The C_{60} /PVP complex and PVP were shown to exhibit biological activity *in vitro* and *in vivo*. The C_{60} /PVP complex, representing a mixed-type LDH, was shown to inhibit LDH activity, as well as contributing to a decrease in lactate concentration and an increase in the concentration of pyruvic acid and glucose in blood serum when administered *per os* to mice. The inhibitory effect of PVP on LDH activity was revealed in both *in vivo* and *in vitro* investigations. *In vivo*, PVP contributes to a decrease in the concentration of lactate in the blood. The less pronounced effect of the C_{60} /PVP complex as compared to PVP alone may be due to the fact that C_{60} molecules are “hidden” in cavities formed in PVP molecules.

Keywords: fullerene, C_{60} , C_{60} /poly-*N*-vinylpyrrolidone, C_{60} /PVP complex, LDH activity, biochemical parameters, biological activity

For citation: Loginova N.Yu., Chesovskikh Yu.S., Borodulin V.B. Investigation of the biological activity of the water-soluble C_{60} /poly-*N*-vinylpyrrolidone complex. *Tonk. Khim. Tekhnol. = Fine Chem. Technol.* 2022;17(6):492–503 (Russ., Eng.). <https://doi.org/10.32362/2410-6593-2022-17-6-492-503>

НАУЧНАЯ СТАТЬЯ

Исследование биологической активности водорастворимого комплекса C_{60} /поли-*N*-винилпирролидон

Н.Ю. Логинова¹, Ю.С. Чесовских^{1,✉}, В.Б. Бородулин^{1,2}

¹Саратовский государственный медицинский университет им. В.И. Разумовского Минздрава России, Саратов, 410012 Россия

²МИРЭА – Российский технологический университет (Институт тонких химических технологий им. М.В. Ломоносова), Москва, 119571 Россия

✉ Автор для переписки, e-mail: Juliachesovskih@gmail.com

Аннотация

Цели. Исследовать биологическую активность водорастворимого производного фуллере́на – комплекса C_{60} /поли-*N*-винилпирролидона (C_{60} /ПВП) – в условиях *in vitro* и *in vivo*; изучить влияние комплекса C_{60} /ПВП на активность лактатдегидрогеназы (ЛДГ) в условиях *in vitro* и *in vivo*; оценить изменения биохимических показателей сыворотки крови при введении мышам C_{60} /ПВП.

Методы. Для определения активности коммерческого препарата ЛДГ и исследования кинетики данного процесса был использован фотометрический метод Варбурга с применением стандартной методики. Для оценки влияния поливинилпирролидона (ПВП) и комплекса C_{60} /ПВП на некоторые биохимические показатели *in vivo* было проведено исследование на двухмесячных самцах белых беспородных мышей весом 20 ± 3 г. Определение биохимических показателей сыворотки крови проводилось с помощью полуавтоматического биохимического анализатора по стандартным методикам.

Результаты. Исследовано влияние комплекса C_{60} /ПВП на активность ЛДГ и проведена оценка изменений биохимических показателей сыворотки крови мышей, характеризующих углеводный обмен. Установлено, что комплекс C_{60} /ПВП увеличивает содержание глюкозы и пировиноградной кислоты, снижает содержание лактата и активность ЛДГ в сыворотке крови по сравнению с контролем, а также снижает активность ЛДГ в условиях *in vitro* по типу смешанного ингибирования.

Выводы. Комплексы C₆₀/ПВП и ПВП проявляют биологическую активность в условиях *in vitro* и *in vivo*. Установлено, что комплекс C₆₀/ПВП является ингибитором АДГ смешанного типа в условиях *in vitro*, угнетает активность АДГ в условиях *in vivo*, а также способствует снижению концентрации лактата и увеличению концентрации пировиноградной кислоты и глюкозы в сыворотке крови при введении мышам C₆₀/ПВП *per os*. При этом также выявлено ингибирующее действие и ПВП на активность АДГ *in vitro* и *in vivo*, причем в условиях *in vivo* ПВП способствует снижению концентрации лактата в крови. Менее выраженное действие комплекса C₆₀/ПВП по сравнению с ПВП может быть связано с тем, что молекулы C₆₀ «скрыты» в полостях, образованных в молекулах ПВП.

Ключевые слова: фуллерен, C₆₀, C₆₀/поли-N-винилпирролидон, комплекс C₆₀/ПВП, активность АДГ, биохимические показатели, биологическая активность

Для цитирования: Логинова Н.Ю., Чесовских Ю.С., Бородулин В.Б. Исследование биологической активности водорастворимого комплекса C₆₀/поли-N-винилпирролидон. *Тонкие химические технологии*. 2022;17(6):492–503. <https://doi.org/10.32362/2410-6593-2022-17-6-492-503>

INTRODUCTION

The influence of C₆₀ fullerene derivatives on biological objects is being actively studied due to their potential for various preparations in medicine and pharmacology. Due to their widespread application in various industries, as well as currently active research for areas of their future application in the medical and pharmaceutical fields in the diagnosis and treatment of diseases, human interaction with such materials has become an integral part of contemporary life. Since the effects of such materials, which are foreign to the organism, can occur directly or following interaction with biomolecules to include significant metabolic changes, an additionally important task involved in contemporary research is the constant assessment of potential risks when interacting with nanomaterials, including identifying and evaluating their potentially toxic properties.

Recent studies on the properties of a number of C₆₀ fullerene derivatives have demonstrated their ability to inhibit HIV-1 protease [1, 2] as a result of their antimicrobial [3] and antioxidant [4] activities. There are also works devoted to the use of fullerenes in the treatment of inflammatory processes [5]. Derivatives of metallofullerenes, in which a metal atom is trapped inside a fullerene cage, are considered especially promising for

radiomedicine applications due their greater stability as compared with currently used chelate complexes.

An analysis of the experimental data given in the literature shows that the biological activity of fullerene is generally determined by its lipophilicity (describing its adhesiveness to proteins and lipids along with various membranotropic properties), electron-withdrawing activity (promoting interaction with free radicals and reactive oxygen species), as well as photoexcitation characteristics (ability to transfer energy from an excited state to a molecule of ordinary oxygen and transform it into singlet oxygen). The ability of fullerene to prevent apoptosis of neurons was revealed in a number of works carried out both *in vivo* and *in vitro* [6, 7]. There are data in the literature on beneficial effects obtained using fullerenes and their derivatives in the treatment of neurodegenerative diseases [8].

Fullerene derivatives have been shown to inhibit the chain reaction of lipid peroxidation [6, 7]. The antioxidant properties of fullerenes are largely due to the system of conjugated double bonds capable of accepting additional electrons, for example, from free radicals. One fullerene molecule can accept up to 34 methyl radicals, capture and inactivate superoxide anion radicals and hydroxyl radicals *in vivo* and *in vitro* [7]. In addition, the use of fullerenes as antioxidants

is due to their ability to localize inside mitochondria and other compartments where free radicals are produced. According to the authors of a number of works, fullerenes are effective neuroprotectors in some forms of sclerosis. Due to evidence of improved cognitive processes under normal and pathological conditions, they are of great interest for the development of therapies for Alzheimer's disease [9, 10].

An analysis of the data available in the literature on the study of the biological activity of C_{60} and of its derivatives in *in vitro* and *in vivo* experiments reveals no serious toxic effects from C_{60} fullerene. The first studies on fullerene toxicity showed [11–13] no side effects in mice when observed over long periods following administration of fullerene at doses of 2.5 g/kg. Data on the effects of aqueous dispersion of C_{60} stabilized by starch [14] also show the absence of chronic toxicity when administered intragastrically to rats, as well as causing no significant differences in hematological and biochemical parameters as compared to the control.

Tests of hydroxylated $C_{60}(OH)_n$ fullerene showed that when it was administered intraperitoneally to mice and rats at a median lethal dose LD_{50} of 0.5–2.4 g/kg [15]. At the same time, the authors of the work noted a decrease in the activity of microsomal enzymes—in particular, P_{450} -dependent monooxygenase—in the presence of the hydroxylated form of C_{60} fullerene (*in vivo*).

Fullerene radically differs from all other biogenic molecules due to its spherical structure. Due to inevitable interactions with molecules having hydrophobic regions (as for example in the case of proteins and lipids) in a physiological hydrophilic environment, the carbon surface of such molecules will be practically inaccessible for recognition by the immune system [16–18].

In other studies, while C_{60} fullerene itself was shown not have acute toxicity, toxic effects have been associated with the organic solvents used to prepare fullerene solutions [19]. A more detailed study on the mechanisms of action and the mechanisms of the response of the organism as a whole to the use of both fullerenes itself and its derivatives is hampered by low solubility in the aquatic environment.

One of the solvents used in medical practice for hydrophobic drugs is polyvinylpyrrolidone (PVP). PVP is non-toxic and included in such medicines as hemodez and enterodez. Medical-grade PVP is obtained by *N*-vinylpyrrolidone-2 polymerization. It is used to prolong the action of some drugs, as well as acting as a binder and stabilizer in the manufacture of tableted forms of drugs, etc.

Previously, biological studies of this complex have already been mentioned in the literature. Fullerenes have been used to protect cells against ultraviolet radiation [20]. Ultraviolet irradiation (320–400 nm) provokes the formation of reactive oxygen species, leading to damage and death of skin cells in humans. A water-soluble C_{60} /poly-*N*-vinylpyrrolidone (C_{60} /PVP) complex was tested as protection against such oxidative stress. In this case, it is the ability of fullerene to penetrate into the deep layers of the human skin epidermis, as well as its resistance to oxidative degradation prevent skin aging without photosensitization and cytotoxicity, that makes it a promising substitute for ascorbic acid.

The potential antiviral effect of C_{60} has been studied in a number of studies. The C_{60} /PVP complex was shown to inhibit the reproduction of influenza A and B RNA-viruses, as well as various DNA-based viruses, in particular, herpes simplex virus (HSV-1) [21, 22]. Here, it was found that morphological changes occur as a result of treating influenza type A virus with the C_{60} /PVP complex. Here, a large number of defective virions and virions with a damaged “brush” were identified along with the presence of lipid membrane disorders. The data suggest that the complex interferes with the assembly process in the viral replication cycle to block the self-tuning of mature viral particles.

Thus, the purpose of this work was to study the biological activity, both under *in vitro* and *in vivo* conditions, of a water-soluble fullerene derivative comprising the C_{60} /PVP complex.

To obtain a water-soluble C_{60} /PVP fullerene derivative, the previously described method of C_{60} fullerene complexation with PVP [23] (Fig. 1) was used.

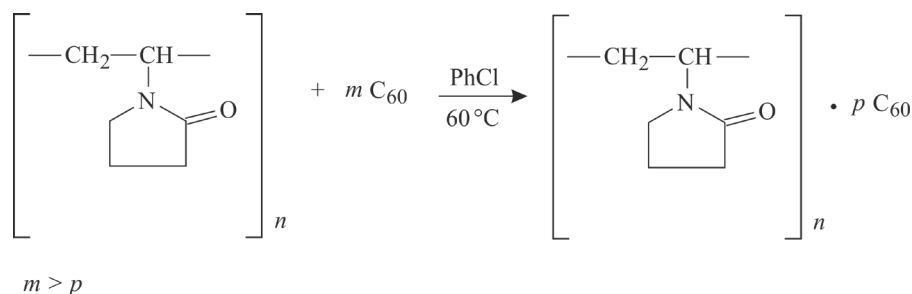


Fig. 1. Scheme of the complexation reaction of fullerene C_{60} with PVP.

This complex is soluble in water and absorbs at 255 and 330 nm. IR spectrum, ν , cm⁻¹: 578, 844, 894, 933, 1077, 1227, 1266, 1375, 1490, 1630–1687, 1703, 2127, 2395, 2575, 2922, 3329, 3493, 3800, 3943.

PVP has good solubility in water and contains cavities in its structure that are close in size to C₆₀ molecules. The cavities are easily filled with fullerene molecules, thus forming a water-soluble complex. The studies were carried out for the C₆₀/PVP complex (the C₆₀ content in the complex is ~1.6%). The effect of the C₆₀/PVP complex on the activity of lactate dehydrogenase (LDH) *in vitro* was studied, as well as changes in the biochemical parameters of blood serum when C₆₀/PVP was administered *per os* to mice.

MATERIALS AND METHODS

Determination of LDH activity in model *in vitro* experiments

To determine the activity of a commercial LDH preparation and study the kinetics of this process, the Warburg photometric method was used using a standard technique. We used solutions of phosphate buffer, sodium pyruvate, coenzyme-bound hydrogen nicotinamide adenine dinucleotide (NAD·H + H⁺), LDH (*Sigma-Aldrich*, USA). The change in LDH activity was determined in the presence of a solution of PVP and an aqueous solution of the C₆₀/PVP complex, which were experimental samples and were compared with a control sample that did not contain PVP and C₆₀/PVP. The spectra were recorded on a Specord UV VIS spectrophotometer (*Analytik Jena*, Germany) in the wavelength range from 220 nm to 400 nm. The maximum absorption of LDH was determined spectrophotometrically: it corresponded to a wavelength of 340 nm. Then, sodium pyruvate (not absorbing at $\lambda = 340$ nm), PVP or C₆₀/PVP solution, and LDH were sequentially added to the determination cuvette. Optical absorption was measured at certain time intervals during the course of the reaction. The activity of LDH was determined by the decrease in the content of NAD·H + H⁺ (maximum absorption at a wavelength of 340 nm) in the reaction mixture as a result of the enzymatic reduction of pyruvate to lactate.

The enzyme activity was expressed in nanomoles of the substrate converted into the reaction product in 1 min per 1 mg of the enzyme at 25°C and optimal pH. It was calculated by formula (1):

$$a = (\Delta A \cdot V) / (\epsilon_{340} \cdot d \cdot V_s) \cdot 10^{-9} \quad (1)$$

where ΔA is the change in the optical absorption of NAD·H + H⁺ for 1 min, rel. un.; V is the final volume in the cell after the addition of the last component, mL; ϵ_{340} is the coefficient of molar absorption of NAD·H + H⁺ equal to 6220 M⁻¹·cm⁻¹; d is the thickness of the investigated liquid layer, cm; V_s is the volume of the enzyme solution taken for the study, mL.

The enzymatic reaction rate was determined by formula (2):

$$v = (C_0 - C_{1/2}) / (\tau - \tau_0) \quad (2)$$

where v is the rate of the enzymatic reaction, mol·L⁻¹·s⁻¹; C_0 is the concentration of NAD·H + H⁺ before the start of the reaction, mol/L; $C_{1/2}$ is half of the total concentration of NAD·H + H⁺, mol/L; τ is the time during which the enzymatic oxidation of 1/2 of NAD·H + H⁺ concentration occurred (s); τ_0 is the reaction start time, s.

The influence of PVP and C₆₀/PVP was also evaluated by analyzing the change in the Michaelis–Menten constant (K_M). To determine K_M , the reaction rate was calculated at various concentrations of the sodium pyruvate substrate.

Determination of biochemical parameters of blood serum

To evaluate the *in vivo* effect of PVP and the C₆₀/PVP complex on some biochemical parameters, whose concentration depends on LDH activity, a study was conducted on mongrel mice. The experimental part of the work was carried out in accordance with the protocols of the Geneva Convention and the principles of good laboratory practice (National Standard of the Russian Federation, GOST R 53434-2009)¹ [24].

The control and experimental groups were formed from two-month-old males weighing 20 ± 3 g. The mice were kept under standard conditions with natural changes in lighting occurring in conformity with the normal vivarium regime. All animals had free access to food and water. The mice of the control group were not exposed to PVP and C₆₀/PVP. The first experimental group received a PVP solution, while the second group received the C₆₀/PVP complex. Each study group of the mice consisted of 15 individuals. The daily dose of

¹ GOST R 53434-2009. National Standard of the Russian Federation. *Principles of good laboratory practice*. Moscow: Standartinform; 2010. 12 p.

² *Prakticheskoe rukovodstvo po biologicheskoi bezopasnosti v laboratornykh usloviyakh (Practical Guide to Biological Safety in the Laboratory)*. Geneva: VOZ; 2007. 188 p. (in Russ.).

administered substances was 0.5 mg/kg. The compounds were administered to the mice as a solution (100 μ L) for 5 days using a probe. Following their decapitation at the end of the experiment, the biochemical blood serum parameters of the animals were analyzed.

Determination of the biochemical parameters of blood serum was carried out using a semi-automatic biochemical analyzer Screenmaster (*Hospitex Diagnostics*, Switzerland) equipped with a thermostat, photometer and microprocessor.

The methods are unified [25].

In the work, the following biochemical parameters were determined: the concentration of glucose, lactate and pyruvic acid (PVA), the activity of LDH.

Determination of glucose concentration was carried out by the glucose oxidase method. The concentration was measured photometrically at a wavelength of 500 nm (480–520 nm).

The determination of the concentration of lactate in the blood serum was based on the conversion of lactate into PVA and hydrogen peroxide by lactate oxidase; the measurement was carried out photometrically at 546 nm (500–550 nm).

The determination of PVA concentration in blood serum was based on the Umbright method. The concentration was determined photometrically at a wavelength of 430 nm.

The determination of LDH activity in blood serum was carried out according to the Warburg method. The activity was measured photometrically at a wavelength of 340 nm.

To determine all the parameters under study, reagent kits from *Diakon DS*, Russia were used.

Statistical processing of results

Statistical data processing was carried out using the Statistica v7.0.61.0 software package (*StatSoft*, USA). The reliability of difference in the considered indicators of the control and experimental groups was judged by the value of Student's criterion t and the significance level p . At $p \leq 0.05$, the difference was considered statistically significant.

RESULTS AND DISCUSSION

The effect of the C_{60} /PVP complex on the course of carbohydrate metabolism in mice was assessed on the basis of data obtained in the course of biochemical analysis of blood serum.

The main indicator of carbohydrate metabolism is glucose, which is present in most organs and tissues. The concentration of glucose in the blood is the result of glycogenolysis, gluconeogenesis and

glycolysis processes. Since it is the main—and for some tissues, the only—source of energy in the cell, maintaining a constant concentration of glucose in the blood is a necessary condition for the normal functioning of the body. Glucose in the body undergoes oxidation with the PVA formation. The latter, depending on the conditions, is oxidized to acetyl-CoA, which enters into the reactions of the Krebs cycle (aerobic conditions), or is reduced to lactate (anaerobic conditions). In turn, as a product of anaerobic glucose metabolism, lactate enters the blood from skeletal muscles, brain and erythrocytes.

The interconversion of PVA to lactate occurs with the participation of the LDH enzyme. LDH is found in all animal and human tissues, especially cardiac and skeletal muscles, erythrocytes, liver and kidneys. Under physiological conditions, the equilibrium of the reaction catalyzed by LDH is shifted towards the formation of lactate. The activity of this enzyme in the blood serum and the relative content of its isoenzymes can be an important biochemical diagnostic test for a number of diseases. LDH activity in the blood serum is a sensitive indicator of hepatocellular damage. A change in activity is usually observed in hepatitis, drug intoxication, cirrhosis, tumors and traumas.

In the course of the studies, the C_{60} /PVP complex was found to double the content of glucose in the blood compared to the control (Table 1). By comparison, PVP does not have a significant effect on changes in blood glucose levels. A reliable decrease in the content of lactate in the blood serum compared to the control group was 55% in the case of the C_{60} /PVP complex and 30% in the case of PVP.

The concentration of PVA in the blood of mice under the influence of PVP is within the normal range, while the introduction of the C_{60} /PVP complex increases it by 27%.

The decrease in lactate content is associated with a decrease in LDH activity under the action of the C_{60} /PVP complex by 7% and PVP by 27% in comparison with the control.

A possible reason for the increase in the level of glucose in the blood under the action of the C_{60} /PVP complex may be a disfunction of glucose entry into the cell. This leads to the activation of compensatory mechanisms, in particular, to the activation of gluconeogenesis, in which lactate can serve as a source for the synthesis of glucose in the cell (as a result, its concentration decreases in the blood). In the process, lactate is converted into PVA (the main a source for the synthesis of glucose) under the action of the LDH enzyme. The content of glucose increased in the blood of experimental animals.

Table 1. Effect of PVP and C₆₀/PVP on the biochemical parameters of blood serum

Biochemical indicator	Control	PVP		C ₆₀ /PVP		
	<i>M</i> ± <i>m</i>	<i>M</i> ± <i>m</i>	<i>p</i>	<i>M</i> ± <i>m</i>	<i>p</i>	<i>p'</i>
Glucose, mmol/L	7.04 ± 1.08	6.82 ± 0.51	>0.05	14.00 ± 0.94	<0.01	<0.001
Lactate, mmol/L	25.30 ± 0.39	17.64 ± 0.46	<0.001	11.32 ± 0.85	<0.001	<0.001
PVA, mmol/L	0.11 ± 0.01	0.11 ± 0.01	>0.05	0.15 ± 0.01	<0.01	<0.01
LDH, IU	2025.25 ± 23.28	1470.00 ± 20.94	<0.001	1892.00 ± 15.60	<0.05	<0.001

Note: *p* is the level of probability of differences in comparison with control; *p'* is level of probability of differences in comparison with PVP. *M* is the average value of molar concentration; *m* is the confidence interval of molar concentration.

The high level of significance of the differences between C₆₀/PVP and PVP (*p* < 0.01) suggests that the effect exerted on metabolic processes in mice in the presence of C₆₀/PVP is due to C₆₀ fullerene.

The effect of PVP on carbohydrate metabolism in mice results in a decrease in lactate levels and LDH activity. The decrease in lactate levels is probably due to a decrease in LDH activity. This is consistent with the data obtained in studies on the effect of PVP and the C₆₀/PVP complex on LDH activity in an *in vitro* experiment.

It was found that the studied compounds are inhibitors of LDH activity. The reaction rate in their presence decreases, and the Michaelis–Menten constant, on the contrary, increases (Table 2 and Fig. 2).

The conducted studies on the effect of the C₆₀/PVP complex on LDH activity in model experiments carried out *in vitro* led to the conclusion that the C₆₀/PVP complex has an inhibitory effect

on LDH activity. In the presence of the C₆₀/PVP complex, there is a decrease in LDH activity by 57.3% compared to the control, which leads to a decrease in the catalyzed reaction. In the presence of PVP in the system under study, LDH activity was reduced by 70.9% as compared to the control.

Lineweaver–Burk (Fig. 4) and Eadie–Hofstee (Fig. 5) plots were constructed to identify the type of inhibition in the presence of the studied compounds.

A decrease in the maximum rate of the reaction catalyzed by LDH in the presence of PVP and C₆₀/PVP combined with an increase in the Michaelis–Menten constant may indicate a reversible non-competitive inhibition of LDH.

Based on the Lineweaver–Burk and Eadie–Hofstee plots, the type of inhibition in the presence of PVP and the C₆₀/PVP complex was determined as a mixed type of inhibition, in which a decrease

Table 2. Influence of the studied compounds on the LDH activity

Compound	Concentration × 10 ⁻² , mg/mL	<i>K_M</i> × 10 ⁻² , M[S]	<i>r_{max}</i> × 10 ⁻⁷ , mol/L·s	Activity × 10 ⁻¹¹ , mol/min	Activity, %
Control	–	0.15 ± 0.01	1.34 ± 0.11	0.96 ± 0.10	100
PVP	2	0.32 ± 0.05	0.90 ± 0.04	0.28 ± 0.04	29.1
C ₆₀ /PVP	2	0.25 ± 0.04	1.14 ± 0.10	0.41 ± 0.01	42.7

Note: *K_M* is the Michaelis–Menten constant; *v_{max}* is the maximum reaction rate; *M*[S] is the substrate molar mass.

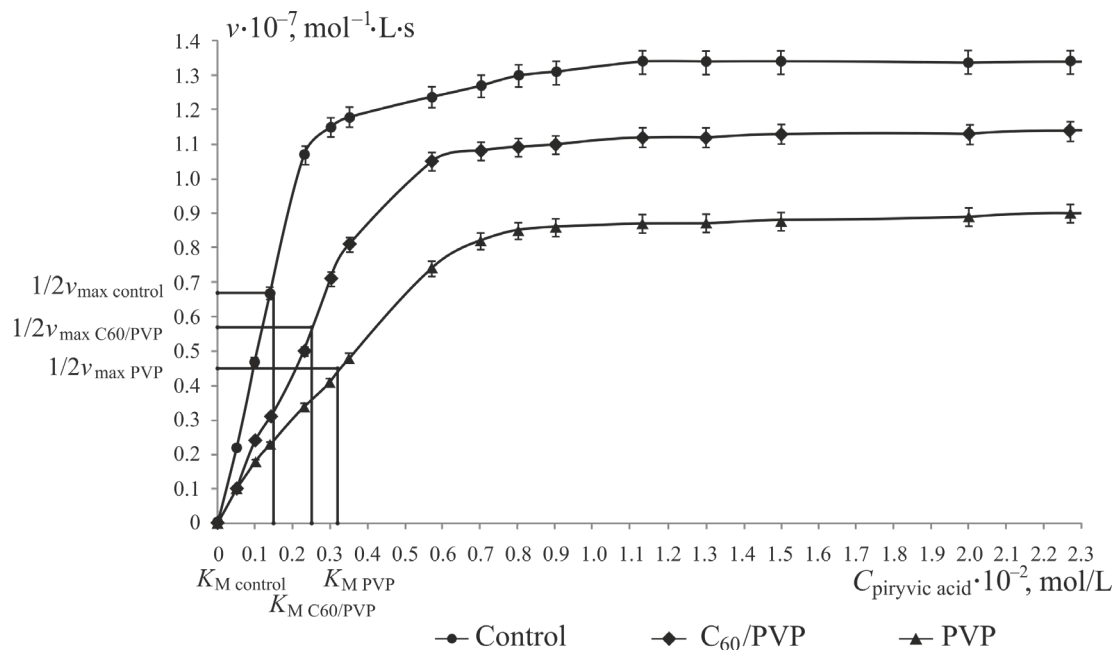


Fig. 2. Graph of the reaction rate (v) versus the substrate concentration (C) in the presence of the compounds under study.

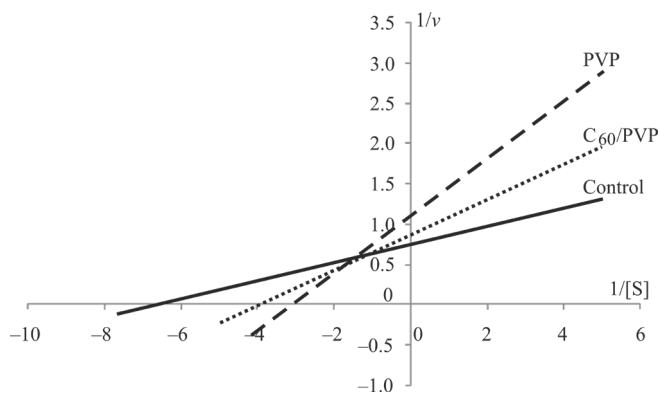


Fig. 3. Lineweaver–Burk graph. S is substrate.

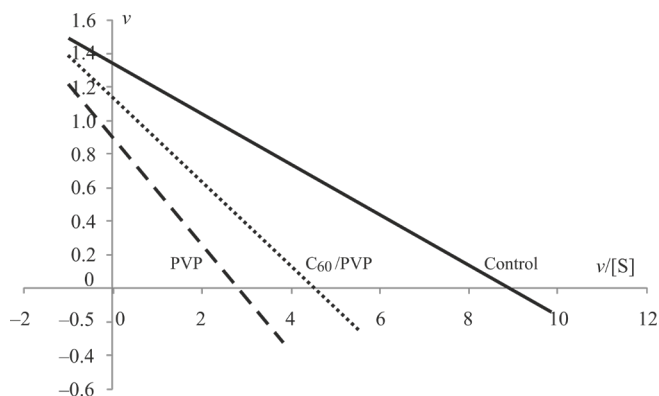


Fig. 4. Eadie–Hofstee graph.

in v_{\max} is combined with a simultaneous increase in K_M values. This means that the enzyme–inhibitor complex retains partial activity, i.e., the ability to form an intermediate triple enzyme–inhibitor–substrate complex, in which the substrate undergoes a delayed catalytic transformation.

CONCLUSIONS

The C_{60} /PVP complex and PVP exhibit biological activity under *in vitro* and *in vivo* conditions. It has been established that the C_{60} /PVP complex acts as a mixed-type LDH

inhibitor under *in vitro* conditions; when C_{60} /PVP is administered to mice *per os* under *in vivo* conditions, it inhibits LDH activity, as well as contributing to a decrease in lactate concentration along with an increase in the concentration of PVA and glucose in the blood serum. An inhibitory effect of PVP on LDH activity *in vitro* was also revealed; moreover, under *in vivo* conditions, PVP was shown to help to reduce the lactate concentration in the blood. The less pronounced effect of the C_{60} /PVP complex compared to PVP may be due to the fact that the C_{60} molecules are “hidden” in the cavities formed in the PVP molecules.

Authors' contributions

N.Yu. Loginova – collecting and processing materials on fullerene derivatives, a water-soluble C₆₀/PVP complex synthesis, and the study of LDH activity under *in vitro* conditions;

Yu.S. Chesovskikh – collecting and processing materials on fullerene derivatives, the biological activity of the C₆₀/PVP complex *in vivo* study;

V.B. Borodulin – scientific consulting at all stages of the work.

The authors of the article guarantee the absence of a conflict of interest.

REFERENCES

- Nielsen G., Roursgaard M., Jensen K., *et al.* *In vivo* Biology and Toxicology of Fullerenes and Their Derivatives. *Basic Clin. Pharmacol. Toxicol.* 2008;103(3):197–208. <https://doi.org/10.1111/j.1742-7843.2008.00266.x>
- Shuster D.I., Wilson S.R., Shinazi R.F. Anti-human immunodeficiency virus activity and cytotoxicity of derivatized buckminsterfullerenes. *Bioorg. Med. Chem. Lett.* 1996;6(11):1253–1256. [https://doi.org/10.1016/0960-894X\(96\)00210-7](https://doi.org/10.1016/0960-894X(96)00210-7)
- Shinazi R.F., Sijbesma R., Sradanov G., *et al.* Synthesis and virucidal activity of a water-soluble, configurationally stable, derivatized C60 fullerene *Antimicrob. Agents Chemother.* 1993;37(8):1707–17110. <https://doi.org/10.1128/AAC.37.8.1707>
- Bakry R., Vallant R., Najam-ul-Haq M., *et al.* Medicinal applications of fullerenes. *Int. J. Nanomedicine.* 2007;2(4):639–649.
- Voroshilov E.A., Degtyarnikov V.P., Shuklina A.A. Prospects for the use of soft dosage forms with the addition of fullerene C₆₀ in the treatment of inflammatory processes. In: *Meditinskaya pomoshch' pri travmakh. Novoe v organizatsii i tekhnologiyakh. Perspektivy importozameshcheniya v Rossii (Medical care for injuries. New in organization and technology. Prospects for import substitution in Russia): Collection of abstracts of the Fifth Anniversary Congress with International Participation.* St. Petersburg; 2020. P. 63–64 (in Russ.).
- Halliwell B. Reactive oxygen species and the central nervous system. *J. Neurochem.* 1992;59(5):1609–1623. <https://doi.org/10.1111/j.1471-4159.1992.tb10990.x>
- Krustic P.J., Wasserman E., Keizer P.N., *et al.* Radical reactions of C₆₀. *Science.* 1991;254(5035):1183–1185. <https://doi.org/10.1126/science.254.5035.1183>
- Aver'yanova M.O., Kurakin G.F., Lopina N.P., Bordina G.E. Prospects for the use of fullerenes and their derivatives as antioxidants. *Modern Science.* 2019;(6–3):11–14 (in Russ.).
- Dugan L.L., *et al.* Fullerene-based antioxidants and neurodegenerative disorders. *Parkinsonism Relat. Disord.* 2001;7(3):243–246. [https://doi.org/10.1016/S1353-8020\(00\)00064-X](https://doi.org/10.1016/S1353-8020(00)00064-X)

СПИСОК ЛИТЕРАТУРЫ

- Nielsen G., Roursgaard M., Jensen K., *et al.* *In vivo* Biology and Toxicology of Fullerenes and Their Derivatives. *Basic Clin. Pharmacol. Toxicol.* 2008;103(3):197–208. <https://doi.org/10.1111/j.1742-7843.2008.00266.x>
- Shuster D.I., Wilson S.R., Shinazi R.F. Anti-human immunodeficiency virus activity and cytotoxicity of derivatized buckminsterfullerenes. *Bioorg. Med. Chem. Lett.* 1996;6(11):1253–1256. [https://doi.org/10.1016/0960-894X\(96\)00210-7](https://doi.org/10.1016/0960-894X(96)00210-7)
- Shinazi R.F., Sijbesma R., Sradanov G., *et al.* Synthesis and virucidal activity of a water-soluble, configurationally stable, derivatized C60 fullerene *Antimicrob. Agents Chemother.* 1993;37(8):1707–17110. <https://doi.org/10.1128/AAC.37.8.1707>
- Bakry R., Vallant R., Najam-ul-Haq M., *et al.* Medicinal applications of fullerenes. *Int. J. Nanomedicine.* 2007;2(4):639–649.
- Ворошилов Е.А., Дегтярников В.П., Шуклина А.А. Перспективы применения мягких лекарственных форм с добавлением фуллерена C₆₀ в терапии воспалительных процессов. В сб.: *Медицинская помощь при травмах. Новое в организации и технологиях. Перспективы импортозамещения в России: Сборник тезисов Пятого юбилейного конгресса с международным участием.* СПб.; 2020. С. 63–64.
- Halliwell B. Reactive oxygen species and the central nervous system. *J. Neurochem.* 1992;59(5):1609–1623. <https://doi.org/10.1111/j.1471-4159.1992.tb10990.x>
- Krustic P.J., Wasserman E., Keizer P.N., *et al.* Radical reactions of C₆₀. *Science.* 1991;254(5035):1183–1185. <https://doi.org/10.1126/science.254.5035.1183>
- Аверьянова М.О., Куракин Г.Ф., Лопина Н.П., Бордина Г.Е. Перспективы применения фуллеренов и их производных как антиоксидантов. *Modern Science.* 2019;(6–3):11–14.
- Dugan L.L., *et al.* Fullerene-based antioxidants and neurodegenerative disorders. *Parkinsonism Relat. Disord.* 2001;7(3):243–246. [https://doi.org/10.1016/S1353-8020\(00\)00064-X](https://doi.org/10.1016/S1353-8020(00)00064-X)

10. Podolski I.Y., Podlubnaya Z.A., Kosenko E.A., Mugantseva E.A., Makarova E.G. Effects of hydrated forms of C₆₀ fullerene on amyloid β -peptide fibrillization *in vitro* and performance of the cognitive task. *J. Nanosci. Nanotechnol.* 2007;7(4–5):1479–1485. <https://doi.org/10.1166/jnn.2007.330>
11. Moussa F., Chretien P., Dubois P., Chuniaud L., Dessante M., Trivin F., Sizaret P.Y., Agafonov V., Ceolin R., Szwarc H., Greugny V., Fabre C., Rassat A. The Influence of C₆₀ Powders on Cultured Human Leukocytes. *Full. Sci. Technol.* 2008;3(3):333–342. <https://doi.org/10.1080/153638X9508543788>
12. Moussa F., Trivin F., Ceolin R., Hadchouel M., Sizaret P.Y., Greugny V., Fabre C., Rassat A., Szwarc H. Early effects of C₆₀ administration in Swiss mice: A preliminary account for *in vivo* C₆₀ toxicity. *Full. Sci. Technol.* 1996;4(1):21–29. <https://doi.org/10.1080/10641229608001534>
13. Baati T., Bourasset F., Gharbi N., Njim L., Abderrabba M., Kerkeni A., Szwarc H., Moussa F. The prolongation of the lifespan of rats by repeated oral administration of [60]fullerene. *Biomaterials.* 2012;33(19):4936–4946. <https://doi.org/10.1016/j.biomaterials.2012.03.036>
14. Hendrickson O., Fedyunina N., Zherdev A., Solopova O., Sveshnikov P. Dzantiev B. Production of monoclonal antibodies against fullerene C₆₀ and development of a fullerene enzyme immunoassay. *Analyst.* 2012;137(1):98–105. <https://doi.org/10.1039/C1AN15745K>
15. Da Ros T., Spalluto G., Prato M. Biological Applications of Fullerene Derivatives: A Brief Overview. *Croatica Chemica Acta.* 2001;74(4):743–755.
16. Belgorodsky B., Fadeev L., Ittah V., Benyamini H., Zelner S., Huppert D., Kotlyar A. B., Gozin M. Formation and characterization of stable human serum albumin-tris-malonic acid [C₆₀]fullerene complex. *Bioconjug. Chem.* 2005;16(5):1058–1062. <https://doi.org/10.1021/bc050103c>
17. Думпис М.А., Николаев Д.Н., Литасова Е.В., Ил'ин В.В., Брусина М.А., Пиотровский П.Б. Biological activity of fullerenes – realities and prospects. *Обзоры по клинической фармакологии и лекарственной терапии (Reviews on Clinical Pharmacology and Drug Therapy).* 2018;16(7):4–20 (in Russ.). <https://doi.org/10.17816/RCF1614-20>
18. Benyamini H., Shulman-Peleg A., Wolfson H.J., Belgorodsky B., Fadeev L., Gozin M. Interaction of C₆₀-fullerene and carboxyfullerene with proteins: docking and binding site alignment. *Bioconjug. Chem.* 2006;17(2):378–386. <https://doi.org/10.1021/bc050299g>
19. Gharbi N., Pressac M., Hadchouel M., Szwarc H., Wilson S.R., Moussa F. [60] Fullerene is a powerful antioxidant *in vivo* with no acute or subacute toxicity. *Nano Lett.* 2005;5(12):2578–2585. <https://doi.org/10.1021/nl051866b>
20. Xiao L., Takada H., Gan X.H., *et al.* The water-soluble fullerene derivative ‘Radical Sponge[®]’ exerts cytoprotective action against UVA irradiation but not visible-light-catalyzed cytotoxicity in human skin keratinocytes. *Bioorg. Med. Chem. Lett.* 2006;16(6):1590–1595. <https://doi.org/10.1016/j.bmcl.2005.12.011>
21. Barzegar A., Naghizadeh E., Zakariazaden M., Azamat J. Molecular dynamics simulation study of the HIV-1 protease inhibit ion using fullerene and new fullerene derivatives of carbon nanostructures. *Mini Rev. Med. Chem.* 2017;17(7):633–647.
10. Podolski I.Y., Podlubnaya Z.A., Kosenko E.A., Mugantseva E.A., Makarova E.G. Effects of hydrated forms of C₆₀ fullerene on amyloid β -peptide fibrillization *in vitro* and performance of the cognitive task. *J. Nanosci. Nanotechnol.* 2007;7(4–5):1479–1485. <https://doi.org/10.1166/jnn.2007.330>
11. Moussa F., Chretien P., Dubois P., Chuniaud L., Dessante M., Trivin F., Sizaret P.Y., Agafonov V., Ceolin R., Szwarc H., Greugny V., Fabre C., Rassat A. The Influence of C₆₀ Powders on Cultured Human Leukocytes. *Full. Sci. Technol.* 2008;3(3):333–342. <https://doi.org/10.1080/153638X9508543788>
12. Moussa F., Trivin F., Ceolin R., Hadchouel M., Sizaret P.Y., Greugny V., Fabre C., Rassat A., Szwarc H. Early effects of C₆₀ administration in Swiss mice: A preliminary account for *in vivo* C₆₀ toxicity. *Full. Sci. Technol.* 1996;4(1):21–29. <https://doi.org/10.1080/10641229608001534>
13. Baati T., Bourasset F., Gharbi N., Njim L., Abderrabba M., Kerkeni A., Szwarc H., Moussa F. The prolongation of the lifespan of rats by repeated oral administration of [60]fullerene. *Biomaterials.* 2012;33(19):4936–4946 <https://doi.org/10.1016/j.biomaterials.2012.03.036>
14. Hendrickson O., Fedyunina N., Zherdev A., Solopova O., Sveshnikov P. Dzantiev B. Production of monoclonal antibodies against fullerene C₆₀ and development of a fullerene enzyme immunoassay. *Analyst.* 2012;137(1):98–105. <https://doi.org/10.1039/C1AN15745K>
15. Da Ros T., Spalluto G., Prato M. Biological Applications of Fullerene Derivatives: A Brief Overview. *Croatica Chemica Acta.* 2001;74(4):743–755.
16. Belgorodsky B., Fadeev L., Ittah V., Benyamini H., Zelner S., Huppert D., Kotlyar A.B., Gozin M. Formation and characterization of stable human serum albumin-tris-malonic acid [C₆₀]fullerene complex. *Bioconjug. Chem.* 2005;16(5):1058–1062. <https://doi.org/10.1021/bc050103c>
17. Думпис М.А., Николаев Д.Н., Литасова Е.В., Ильин В.В., Брусина М.А., Пиотровский П.Б. Биологическая активность фуллеренов – реалии и перспективы. *Обзоры по клинической фармакологии и лекарственной терапии.* 2018;16(7):4–20. <https://doi.org/10.17816/RCF1614-20>
18. Benyamini H., Shulman-Peleg A., Wolfson H.J., Belgorodsky B., Fadeev L., Gozin M. Interaction of C₆₀-fullerene and carboxyfullerene with proteins: docking and binding site alignment. *Bioconjug. Chem.* 2006;17(2):378–386. <https://doi.org/10.1021/bc050299g>
19. Gharbi N., Pressac M., Hadchouel M., Szwarc H., Wilson S.R., Moussa F. [60] Fullerene is a powerful antioxidant *in vivo* with no acute or subacute toxicity. *Nano Lett.* 2005;5(12):2578–2585. <https://doi.org/10.1021/nl051866b>
20. Xiao L., Takada H., Gan X.H., *et al.* The water-soluble fullerene derivative ‘Radical Sponge[®]’ exerts cytoprotective action against UVA irradiation but not visible-light-catalyzed cytotoxicity in human skin keratinocytes. *Bioorg. Med. Chem. Lett.* 2006;16(6):1590–1595. <https://doi.org/10.1016/j.bmcl.2005.12.011>
21. Barzegar A., Naghizadeh E., Zakariazaden M., Azamat J. Molecular dynamics simulation study of the HIV-1 protease inhibit ion using fullerene and new fullerene derivatives of carbon nanostructures. *Mini Rev. Med. Chem.* 2017;17(7):633–647.

22. Martinez Z.S., Castro E., Seong C.-S., Ceron M.R., Echegoyen L., Llano M. Fullerene derivatives strongly inhibit HIV-1 replication by affecting virus maturation without impairing protease activity. *Antimicrob. Agents Chemother.* 2016;60(10):5731–5741. <https://doi.org/10.1128/AAC.00341-16>

23. Gun'kin I.F., Tseluikin V.N., Loginova N.Yu. Synthesis and properties of water-soluble derivatives of fullerene C₆₀. *Russ. J. Appl. Chem.* 2006;79(6):1001–1004. <https://doi.org/10.1134/S1070427206060243>

[Original Russian Text: Gun'kin I.F., Tseluikin V.N., Loginova N.Yu. Synthesis and properties of water-soluble derivatives of fullerene C₆₀. *Zhurnal Prikladnoi Khimii.* 2006;79(6):1011–1013 (in Russ.).]

24. Karkishchenko N.N., Grachev S.V. (Eds.). *Rukovodstvo po laboratornym zivotnym i al'ternativnym modelyam v biomeditsinskikh issledovaniyakh (The Guide to Laboratory Animals and Alternative Models in Biomedical Research)*. Moscow: Profil'-2S; 2010. 358 p. (in Russ.).

25. Karpishchenko A.I. *Meditsinskie laboratornye tekhnologii (Medical Laboratory Technologies)*. St. Petersburg: Intermedika; 1999. 656 p. (in Russ.).

22. Martinez Z.S., Castro E., Seong C.-S., Ceron M.R., Echegoyen L., Llano M. Fullerene derivatives strongly inhibit HIV-1 replication by affecting virus maturation without impairing protease activity. *Antimicrob. Agents Chemother.* 2016;60(10):5731–5741. <https://doi.org/10.1128/AAC.00341-16>

23. Гунькин И.Ф., Целуйкин В.Н., Логинова Н.Ю. Синтез и изучение свойств водорастворимых производных фуллерена C₆₀. *Журн. прикладной химии.* 2006;79(6):1011–1013.

24. Каркищенко Н.Н., Грачев С.В. (ред.). *Руководство по лабораторным животным и альтернативным моделям в биомедицинских исследованиях*. М.: Профиль-2С; 2010. 358 с.

25. Карпищенко А.И. *Медицинские лабораторные технологии*. СПб.: Интермедика; 1999. 656 с.

About the authors:

Natalia Yu. Loginova, Cand. Sci. (Chem.), Senior Lecturer, Department of Biochemistry, V.I. Razumovsky Saratov State Medical University (112, Bolshaya Kazachya ul., Saratov, 410012, Volga Federal District, Saratov oblast, Russia). E-mail: loginova_nu@mail.ru. RSCI SPIN-code 3048-0544, <https://orcid.org/0000-0003-1618-6690>

Yulia S. Chesovskikh, Cand. Sci. (Biol.), Senior Lecturer, Department of Biochemistry, V.I. Razumovsky Saratov State Medical University (112, Bolshaya Kazachya ul., Saratov, 410012, Volga Federal District, Saratov oblast, Russia). E-mail: Juliachesovskih@gmail.com. ResearcherID AAD-8570-2021, Scopus Author ID 56613371400, <https://orcid.org/0000-0002-7732-0796>

Vladimir B. Borodulin, Dr. Sci. (Med.), Professor, Head of the Department of Biochemistry, V.I. Razumovsky Saratov State Medical University (112, Bolshaya Kazachya ul., Saratov, 410012, Volga Federal District, Saratov oblast, Russia); Professor, I.P. Alimarin Department of Analytical Chemistry, M.V. Lomonosov Institute of Fine Chemical Technologies, MIREA – Russian Technological University (86, Vernadskogo pr., Moscow, 119571, Russia). E-mail: borodulinvb@mail.ru. ResearcherID AAE-4632-2021, Scopus Author ID 57206159558, RSCI SPIN-code 7481-1557, <https://orcid.org/0000-0003-1550-313X>

Об авторах:

Логинова Наталья Юрьевна, к.х.н., старший преподаватель кафедры биохимии ФГБОУ ВО «Саратовский государственный медицинский университет им. В.И. Разумовского» Министерства здравоохранения Российской Федерации (410012, Россия, Приволжский федеральный округ, Саратовская область, г. Саратов, ул. Большая Казачья, д. 112). E-mail: loginova_nu@mail.ru. SPIN-код РИНЦ 3048-0544, <https://orcid.org/0000-0003-1618-6690>

Чесовских Юлия Сергеевна, к.б.н., старший преподаватель кафедры биохимии ФГБОУ ВО «Саратовский государственный медицинский университет им. В.И. Разумовского» Министерства здравоохранения Российской Федерации (410012, Россия, Приволжский федеральный округ, Саратовская область, г. Саратов, ул. Большая Казачья, д. 112). E-mail: Juliachesovskih@gmail.com. ResearcherID AAD-8570-2021, Scopus Author ID 56613371400, <https://orcid.org/0000-0002-7732-0796>

Бородулин Владимир Борисович, д.м.н., профессор, заведующий кафедрой биохимии ФГБОУ ВО «Саратовский государственный медицинский университет им. В.И. Разумовского» Министерства здравоохранения Российской Федерации (410012, Россия, Приволжский федеральный округ, Саратовская область, г. Саратов, ул. Большая Казачья, д. 112); профессор кафедры аналитической химии им. И.П. Алимарина Института тонких химических технологий им. М.В. Ломоносова ФГБОУ ВО «МИРЭА – Российский технологический университет» (119571, Россия, Москва, пр-т Вернадского, д. 86). E-mail: borodulinvb@mail.ru. ResearcherID AAE-4632-2021, Scopus Author ID 57206159558, SPIN-код РИНЦ 7481-1557, <https://orcid.org/0000-0003-1550-313X>

The article was submitted: April 04, 2022; approved after reviewing: May 04, 2022; accepted for publication: November 30, 2022.

*Translated from Russian into English by M. Povorin
Edited for English language and spelling by Thomas Beavitt*

**SYNTHESIS AND PROCESSING OF POLYMERS
AND POLYMERIC COMPOSITES**

**СИНТЕЗ И ПЕРЕРАБОТКА ПОЛИМЕРОВ И
КОМПОЗИТОВ НА ИХ ОСНОВЕ**

ISSN 2686-7575 (Online)

<https://doi.org/10.32362/2410-6593-2022-17-6-504-513>

UDC 677.047.625




RESEARCH ARTICLE

Physicochemical fundamentals of processing solutions of thermoplastic poly(ether urethane)s to obtain fibrous-porous polymer composite materials

Grigory M. Kovalenko , Elena S. Bokova, Natalia V. Evsyukova

A.N. Kosygin Russian State University (Technologies. Design. Art), Moscow, 117997 Russia

 Corresponding author, e-mail: gregoryi84@mail.ru

Abstract

Objectives. To study the structure and properties of solutions of thermoplastic poly(ether urethane)s (PEUs) to inform their potential use in the production of fibrous-porous polymer composite materials with a given structure and set of performance properties depending on the field of practical application.

Methods. The composition of PEUs was studied by attenuated total reflection infrared (ATR-IR) spectroscopy using a program for correcting the spectra on an IR Fourier spectrophotometer, as well by differential scanning calorimetry (DSC) using a heat flow calorimeter. The viscosity of PEU solutions was determined on a rotational viscometer.

Results. The chemical composition of PEUs and the nature of the formation of hydrogen bonds were studied. An analysis of the spectra demonstrates the almost complete identity of the PEUs synthesized from the same 4,4'-diphenylmethane diisocyanate. In the studied PEUs of the Vitur and Desmopan® brands, as well as Sanpren, pronounced absorption bands characteristic of urethane groups involved in the formation of hydrogen bonds are visible in the region from 1702 to 1730 cm^{-1} . The temperature transitions and thermal stability of the investigated PEUs were determined by DSC. The influence of the ratio of rigid and flexible blocks, as well as the nature of hydrogen bonds on the melting temperatures of polymers, was shown. Analysis of the DSC curves demonstrated all the studied PEUs to have high melting points ranging from 159 to 215°C.

From the studied temperature dependences of the structural viscosity of thermoplastic PEUs solutions, all solutions were established to have a minimum viscosity anomaly; the value of the logarithm of viscosity depends on the chemical composition and structure of the initial PEUs. It is shown that the viscosity anomaly of PEU solutions can be reduced with increasing temperature.

Conclusions. A comparison of the chemical composition, structure, thermal and rheological characteristics of thermoplastic PEUs with PEU solutions widely used for the production of fibrous-porous materials and coatings of Sanpren LQ-E-6 and Vitur R 0112 grades demonstrates their practicability as production materials and coatings having a predetermined structure and a set of properties depending on the requirements and operating conditions of finished products.

Keywords: poly(ether urethane), polymer solutions, nonwoven substrates, electroforming, phase separation, polymer films

For citation: Kovalenko G.M., Bokova E.S., Evsyukova N.V. Physicochemical fundamentals of processing solutions of thermoplastic poly(ether urethane)s to obtain fibrous-porous polymer composite materials. *Tonk. Khim. Tekhnol. = Fine Chem. Technol.* 2022;17(6):504–513 (Russ., Eng.). <https://doi.org/10.32362/2410-6593-2022-17-6-504-513>

НАУЧНАЯ СТАТЬЯ

Физико-химические основы переработки растворов термопластичных полиэфируретанов для прогнозирования возможности их применения в производстве волокнисто-пористых композиционных материалов

Г.М. Коваленко✉, Е.С. Бокова, Н.В. Евсюкова

Российский государственный университет им. А. Н. Косыгина (Технологии. Дизайн. Искусство), Москва, 119071 Россия

✉ Автор для переписки, e-mail: gregoryi84@mail.ru

Аннотация

Цели. Изучить структуру и свойства растворов термопластичных полиэфируретанов (ПЭУ) для прогнозирования возможности их применения в производстве волокнисто-пористых полимерных композиционных материалов и покрытий с заданной структурой и комплексом эксплуатационных свойств, зависящими от области практического применения.

Методы. Состав ПЭУ изучали методом инфракрасной (ИК) спектроскопии с преобразованием Фурье в сочетании с методом многократного нарушенного полного внутреннего отражения и методом дифференциально-сканирующей калориметрии (ДСК) с использованием калориметра теплового потока. Вязкость растворов ПЭУ определяли на ротационном вискозиметре.

Результаты. Изучен химический состав ПЭУ и характер образования водородных связей. Анализ ИК спектров демонстрирует практически полную идентичность ПЭУ, синтезированных на основе одного и того же 4,4'-дифенилметандиизоцианата. В исследуемых ПЭУ марок Витур и Desmoran®, а также Санпрен, можно увидеть, что в области от 1702 до 1730 см⁻¹ присутствуют явно выраженные полосы

поглощения, характерные для уретановых группировок, задействованных в образовании водородных связей. Методом ДСК определены температурные переходы и термостойкость исследуемых ПЭУ. Показано влияние соотношения жестких и гибких блоков, а также характер водородных связей на температуры плавления полимеров. При анализе кривых ДСК, показано, что все исследуемые ПЭУ обладают высокими температурами плавления, находящимися в диапазоне от 159 до 215 °С. Также исследованы температурные зависимости структурной вязкости растворов термопластичных ПЭУ. Установлено, что все растворы имеют минимальную аномалию вязкости, при этом величина логарифма вязкости зависит от химического состава и структуры исходных ПЭУ. Установлено, что аномалия вязкости растворов ПЭУ может быть снижена при повышении температуры.

Выводы. Исследование химического состава, структуры, термических и реологических характеристик термопластичных ПЭУ с позиции их сравнения и сопоставления с широко применяемыми для производства волокнисто-пористых материалов и покрытий растворами ПЭУ марок Санпрен LQ-E-6 и Витур Р 0112 позволяет прогнозировать возможность их использования для производства материалов и покрытий с заранее заданной структурой и комплексом свойств в зависимости от требований и условий эксплуатации готовых изделий.

Ключевые слова: термопластичные полиэфируретаны, растворы полимеров, полимерные пленки, реологические свойства

Для цитирования: Коваленко Г.М., Бокова Е.С., Евсюкова Н.В. Физико-химические основы переработки растворов термопластичных полиэфируретанов для прогнозирования возможности их применения в производстве волокнисто-пористых композиционных материалов. *Тонкие химические технологии.* 2022;17(6):504–513. <https://doi.org/10.32362/2410-6593-2022-17-6-504-513>

INTRODUCTION

According to classical concepts, poly(ether urethane) (PEU) products, including flexible polymeric materials and coatings based on them, can be obtained from solutions either by fixing the shape by removing the solvent during the drying process or by phase separation in a non-solvent medium. At the same time, the structure of the material and its properties are largely determined by the chemical composition of the initial PEUs, as well as the nature of the structure formation of the solution, depending on the type of solvent used, its thermodynamic

compatibility with the polymer, etc. This constitutes the theoretical basis for obtaining fibrous-porous polymer composite materials having a predictable structure and a set of operational properties.

Approaches have been developed for the targeted modification of PEU solutions in order to create synthetic leather with improved performance properties^{1,2} [1]. Results of a study into the production of nanofibrous medical materials by electrospinning from PEU solutions were presented in [2, 3]. Fibrous-porous composites based on polyurethanes have been obtained for the creation of cell scaffold-type matrices [4]. The structure, as

¹ Bokova E.S. *Physicochemical bases and technology of modification of polymer solutions in the production of fibrous-porous materials*. Dr. Sci. Thesis (Eng.). Moscow: MGUDT. 2007. 467 p. https://new-dissert.ru/_avtoreferats/01003409553.pdf

² Grondkovski M. *Modifikatsiya poliuretanovykh sistem gidrolizatami kollagena dlya sozdaniya iskusstvennykh kozh s uluchshennymi gigenicheskimi svoistvami (Modification of polyurethane systems with collagen hydrolysates to create artificial leathers with improved hygienic properties)*. Cand. Sci. Thesis (Eng.). Moscow: MTILP; 1990. 244 p. (in Russ.).

well as physicomechanical, optical and a number of other indicators of the performance properties of thermoplastic PEUs have been studied in order to create innovative materials by extrusion and 3D printing [3, 5–7]. The creation of protective coatings based on PEUs with a controlled hydrophilic-hydrophobic balance is the subject of research in [8–10]. In this research, known approaches to the processing of PEU solutions and their directed modification are used in relation to thermoplastic PEUs of Russian and foreign production.

EXPERIMENTAL

The following PEU brands were used as objects of study in the work:

– Vitur TM-1413-85 (*NPF Vitur*, Vladimir, Russia)—product of the interaction of 4,4'-diphenylmethane diisocyanate and polyethylene butylene glycol adipate at a ratio of NCO:OH equal to 1:1 obtained by one-stage synthesis; weight average molecular weight (WAMW) is 40000;

– Vitur TM-0533-90 (*NPF Vitur*)—product of the interaction of 4,4'-diphenylmethane diisocyanate and polyoxytetramethylene glycol, at a ratio of NCO:OH groups equal to 1:1, obtained by a one-stage synthesis; WAMW is 40000;

– TPU-2 (*NPF Vitur*)—product obtained in a one-stage method based on polyethylene glycol adipate, diphenylmethane diisocyanate and 1,4-butanediol at a ratio of NCO:OH equal to 1:1; WAMW is 4800;

– Vitur TM-0333-95 (*NPF Vitur*)—product of the interaction of 4,4'-diphenylmethane diisocyanate and polyoxytetramethylene glycol, at a ratio of NCO:OH groups equal to 1:1, obtained by a one-stage synthesis; WAMW is 4400;

– Desmopan® 385 S (*Covestro AG*, Leverkusen, Germany)—product of the interaction of 4,4'-diphenylmethane diisocyanate and polyethylene butylene glycol adipate, obtained by a one-stage synthesis at a ratio of NCO:OH equal to 1:1; WAMW is 5700;

– Desmopan® 9873 (*Covestro AG*, Leverkusen, Germany)—product obtained by a one-stage synthesis based on 4,4'-diphenylmethane diisocyanate and polyoxytetramethylene glycol, at a ratio of NCO:OH groups equal to 1:1; WAMW is 4500.

For the purposes of comparison, we used Sanpren LQ-E-6 PEU (*Sanyo Chemical*, Japan), synthesized in the form of a 30% solution in dimethylformamide and traditionally used to obtain highly porous materials and coatings. PEU was obtained by a two-stage synthesis based on polyethylene glycol adipate and diphenylmethane diisocyanate at a ratio of NCO:OH equal to 4:1; WAMW is 25000.

Based on the recipe features of the synthesis of polyurethanes, the composition and properties of finished products primarily depend on the nature and type of polyesters, diisocyanates and chain extenders used. According to the data given in [11], in the synthesis of polyurethanes, possible variations for obtaining products with different ratios of flexible and rigid blocks (index NCO/OH) include regulating the length of the rigid segment, as well as changing the flexibility of the linear part macromolecules through the use of highly flexible polyethers or polyesters with medium or low flexibility.

In the present work, the PEU composition was studied using the Fourier-transform infrared spectroscopy (FTIR) method in combination with the multiple frustrated total internal reflection on an IFS-113V IR-Fourier spectrophotometer (*Bruker*, Germany), as well as by differential scanning calorimetry (DSC) using a TA 3000 heat flux calorimeter (*Metler*, Switzerland). The viscosity of PEU solutions was determined on a rotational viscometer RN4.1 SE (*Rheotest*, Germany).

RESULTS AND DISCUSSION

The spectral analysis (Fig. 1), which demonstrates the almost complete identity of the PEUs synthesized from the same 4,4'-diphenylmethane diisocyanate, can be used to identify the main absorption bands characteristic of the functional groups that make up the PEUs. Thus, the interval 3328–3331 cm^{-1} corresponds to stretching vibrations of NH groups, while the absorption band in the range 1800–1728 cm^{-1} is characteristic of stretching vibrations of the C=O group. The absorption interval characteristic of the stretching vibrations of the ether group lies in the range from 1300 to 1500 cm^{-1} . The presence of an absorption band in the region of 2800–3200 cm^{-1} is characteristic of stretching vibrations of C–H bonds, while a narrow absorption range of 1450–1460 cm^{-1} is responsible for the phenyl radical in 4,4'-diphenylmethane diisocyanate.

According to [12], the absorption band in the region of 1740 cm^{-1} is characteristic of the urethane group, which is free from the formation of hydrogen bonds (both in the NH and CO groups), while the absorption bands in the range from 1702 to 1730 cm^{-1} correlate with the vibrations of urethane groups included in hydrogen bonds differing in energy. In the studied PEUs of the Vitur and Desmopan® brands, as well as Sanpren, clearly pronounced absorption bands characteristic of urethane groups involved in the formation of hydrogen bonds are clearly visible in the region

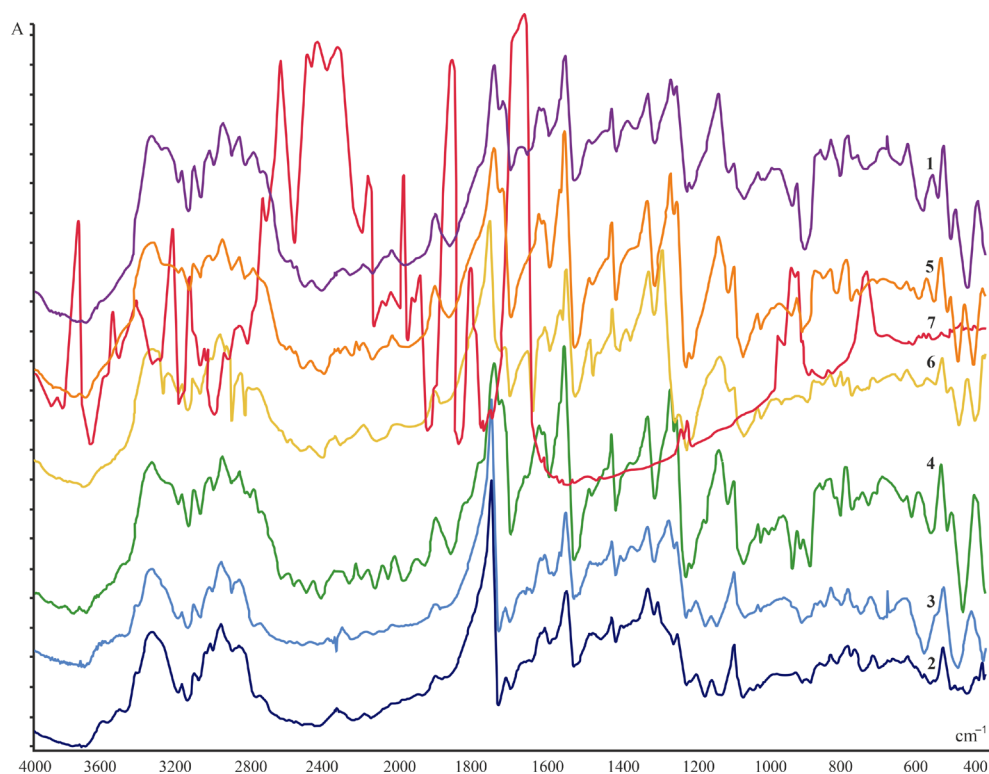


Fig. 1. Infrared spectra of films based on solutions of polyesterurethane brands: (1) Vitur TM-0333-95; (2) Vitur TM-1413-85; (3) Desmopan® 385 S; (4) Desmopan® 9873; (5) TPU-2; (6) Vitur TM-0533-90; (7) Sanpren LQ-E-6.

from 1702 to 1730 cm^{-1} as consistent with the data of [11], in which the object of study was a PEU based on 4,4'-diphenylmethane diisocyanate.

The presence of hydrogen bonds in PEUs predetermines the energy density of cohesion, i.e., the strength of intermolecular interaction, which in turn affects the melting point of PEUs. Thus, it was demonstrated in [11] that the intramolecular approach of the NH group, which is a proton donor, and the CO group, which is an acceptor, occurs more easily if the number of carbon atoms in two neighboring diisocyanate residues is even. On this basis, if n and m are odd, the convergence of the NH and CO groups is insufficient, the PEU has an irregular structure, the intermolecular interaction will be weaker, and, consequently, the melting point will be lower.

In the studied PEUs, the diisocyanate has an even number of carbon atoms, which creates more favorable conditions for the formation of hydrogen bonds and should lead to an increase in the melting point.

Figure 2 shows the temperature transitions of the studied PEUs, determined by the DSC method.

From the analysis of DSC curves, all PEUs under study can be seen to have high melting points ranging from 159 to 215°C. At the same time, as

obtained on the basis of simple oligoesters, there is a single *endo* peak characterizing the melting of the crystalline part polymer on the thermograms of PEU brands Desmopan® 9873, Vitur TM-0333-95, Vitur TM-0533-90 (Fig. 3, curves 1, 4, 6).

In PEUs obtained on the basis of polyesters of the Desmopan® 385 S, TPU-2, Vitur TM-1413-85, and Sanpren LQ-E-6 brands, crystallization is poorer due to the greater rigidity of macromolecules and greater intermolecular interaction; here, since crystallites with different degrees of defectiveness are formed, whose melting occurs in a different temperature range, two *endo* peaks are present on the DSC curves melting (Fig. 2, curves 2, 3, 5, 7).

Such PEU behavior corresponds to the data [13], where, by studying the temperature transitions in PEUs of the Perlon U brand, the authors demonstrated that less perfect (more defective) crystalline formations melt at a lower temperature than less defective ones. Additionally, the presence of two melting ranges in PEUs based on polyesters can be explained by more favorable conditions for the formation of hydrogen bonds, which results in the initial destruction of the associates stabilized by H-bonds followed by the melting of the crystalline part of the polymer.

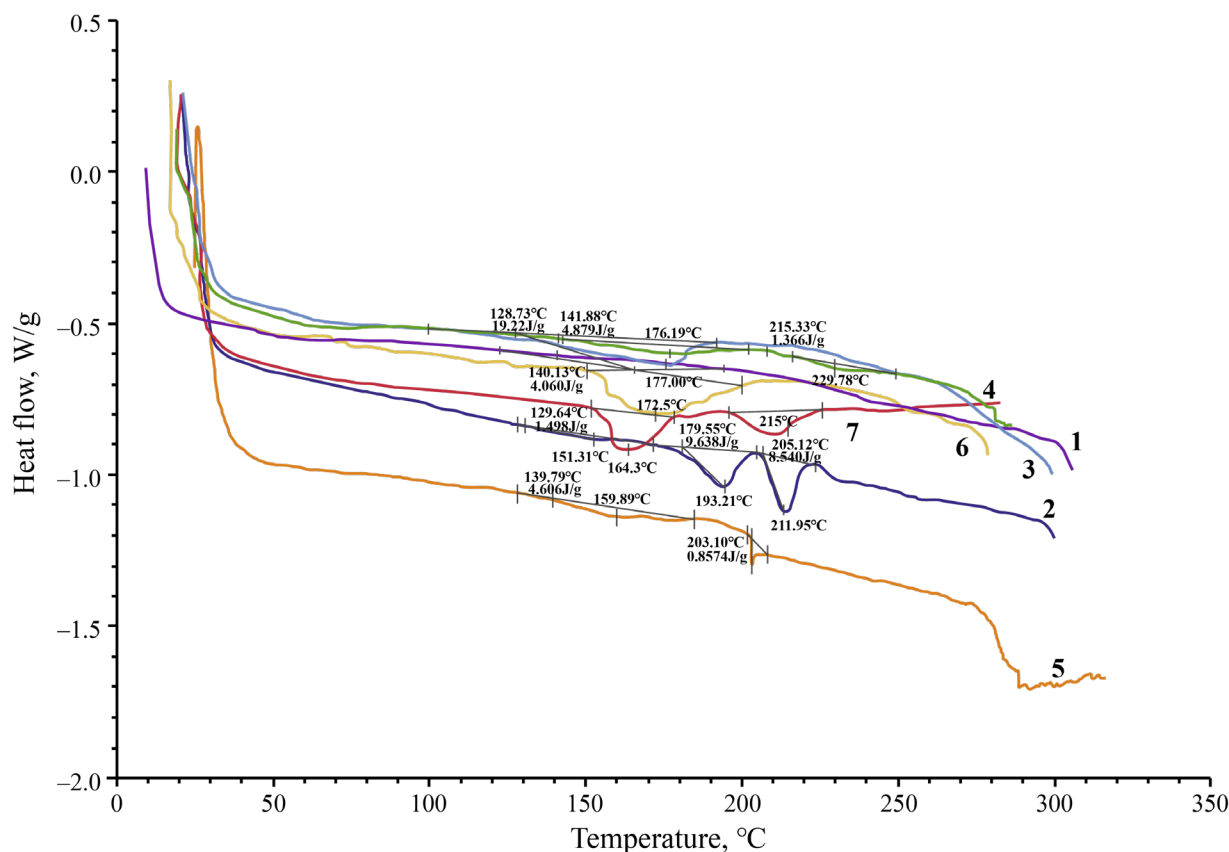


Fig. 2. Differential scanning calorimetry curves of films made of polyesterurethane: (1) Desmopan® 9873; (2) Desmopan® 385 S; (3) TPU-2; (4) Vitur TM-0333-95; (5) Vitur TM-1413-85; (6) Vitur TM-0533-90; (7) Sanpren LQ-E-6.

Based on the classical concepts of the chemical composition of PEUs, as well as numerous experimental studies of the reactions occurring during its synthesis³, linear and spatially cross-linked PEUs include urethane, urea, ether, and ester groups [11], which affect the processes of its processing (dissolution, melting), as well as the structure of the properties of finished products.

PEUs synthesized in the form of concentrated polymer solutions in dimethylformamide (DMF) are traditionally used for the production of fibrous-porous polymer composite materials and coatings. Thermoplastic PEUs used in the present work to solve similar problems related to the possibility of fiber and film formation were converted into a fluid state by dissolving in DMF.

One of the indicators that depends on the chemical composition of the polymer, characterizes its thermodynamic affinity for the solvent,

³ Grondkovski M. *Modifikatsiya poliuretanovykh sistem gidrolizatami kollagena dlya sozdaniya iskusstvennykh kozh s uluchshennymi higienicheskimi svoystvami (Modification of polyurethane systems with collagen hydrolysates to create artificial leathers with improved hygienic properties)*. Cand. Sci. Thesis (Eng.). Moscow: MTILP; 1990. 244 p. (in Russ.).

predetermines the processes of structure formation in solutions and the technological features of their processing into finished products, is structural viscosity.

In this work, the structural viscosity of PEU solutions was determined on a rotational viscometer. The concentration of the studied solutions (C , %) was 15%; the temperatures (T , °C) of the experiment were $20 \pm 2^\circ\text{C}$ and $50 \pm 2^\circ\text{C}$ (Figs. 3 and 4).

From the analysis of the viscosity curves in the range of shear rates under study, most solutions exhibit the behavior of Newtonian fluids without the effect of the viscosity anomaly characteristic of structured polymer systems. At the same time, for PEU grades TPU-2 and Desmopan® 9873 (Fig. 3, curves 4, 5), more hydrogen bonds break at higher shear in the shear rate range from 2 to 3 s^{-1} .

The viscosity values of PEU grades Vitur TM-0533-90, TPU-2, and Sanpren LQ-E-6 (Fig. 3, curves 1, 3, 4) lie in the region of higher values than those of other grades of PEUs. According to the literature data [13], the flexibility of the chain of PEU macromolecules is determined by the properties of the oligoester block. Based on the data on internal rotation in organic molecules [13], it can be argued that internal rotation around the C–O bond is facilitated compared to the C–C bond.

Thus, it can be assumed that PEUs having heterobonds in the form of an ether group in macromolecules will have greater chain flexibility. Therefore, in PEU solutions based on oligoesters (Desmopan® 9873, Vitur TM-0333-95, Vitur TM-0533-90), the hydrodynamic radius of macromolecular coils will be smaller, and, consequently, the structural viscosity will be lower, as confirmed by the data in Figs. 3 and 4.

However, PEU brand Vitur TM-0533-90, synthesized on the basis of a simple oligoester, has viscosity values almost an order of magnitude higher than those of other brands of PEUs, which also contain blocks based on polyethers (Vitur TM-0333-95, Desmopan® 9873).

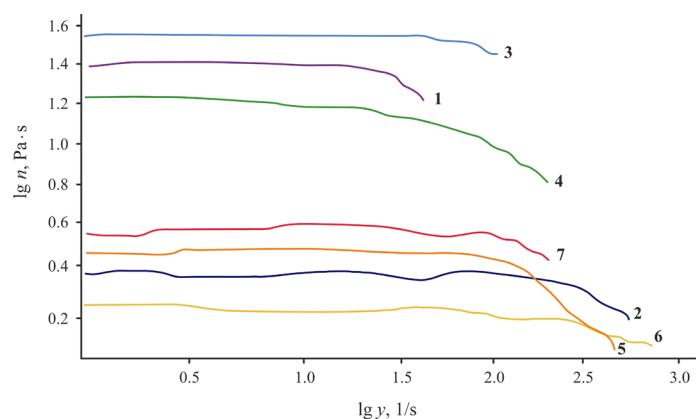


Fig. 3. Viscosity of shear rate dependence for polyesterurethane solutions of the brand: (1) Vitur TM-0533-90; (2) Vitur TM-1413-85; (3) Sanpren LQ-E-6; (4) TPU-2; (5) Desmopan® 9873; (6) Desmopan® 385 S; (7) Vitur TM-0333-95.
 $C_{\text{solution}} = 15\%$; $T = 20 \pm 2^\circ\text{C}$.

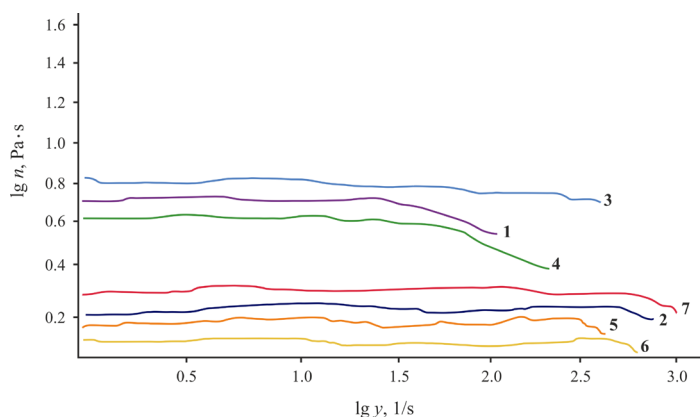


Fig. 4. Viscosity of shear rate dependence for polyesterurethane solutions of the brand: (1) Vitur TM-0533-90; (2) Vitur TM-1413-85; (3) Sanpren LQ-E-6; (4) TPU-2; (5) Desmopan® 9873; (6) Desmopan® 385 S; (7) Vitur TM-0333-95.
 $C_{\text{solution}} = 15\%$; $T = 50 \pm 2^\circ\text{C}$.

Apparently, this is due to the WAMW of Vitur TM-0533-90 (40000), while the WAMW of Vitur TM-0333-95 and Desmopan® 9873 is equal to 4400 and 4500, respectively. Despite the fact that NCO/OH index is 1:1 for all studied grades of PEUs, the higher molecular weight of Vitur TM-0333-90 leads to an increase in viscosity due to the presence of closely spaced polar groups in the polymer chain as compared to low molecular weight grades of PEU Vitur TM-0333-95 and Desmopan® 9873.

Viscosity values for PEU grades Vitur TM-1413-85 and Desmopan® 385 S, synthesized on the basis of oligoesters, are almost an order of magnitude lower than those for PEU grades TPU-2 and Sanpren LQ-E-6, which are also obtained on the basis of adipic acid polyesters. According to [11], polyurethanes with more methyl groups in the oligoester block comprise a more flexible chain, since strongly interacting polar groups will be separated by methyl units, whose rotation is not hindered. Therefore, PEU grades Vitur TM-1413-85 and Desmopan® 385 S, which are synthesized from polyethylene butylene glycol adipate oligoester, have a greater chain flexibility than PEU grades TPU-2 and Sanpren LQ-E-6, which have a more rigid-chain polyethylene glycol adipate. As a result, PEU solutions of the Vitur TM-1413-85 and Desmopan® 385 S brands have a lower viscosity, even though the molecular weight, for example, of TPU-2 PEU is significantly lower than that of Vitur TM-1413-85.

The structural viscosity values can be expected to be inversely related to the temperature of the PEU solution: an increase in temperature leads to a twofold decrease in viscosity, as well as eliminating the effect of its anomaly.

CONCLUSIONS

In this research, Russian and foreign various brands of thermoplastic PEUs in the form of solutions in DMF are studied to investigate the possibility of their use in the production of fibrous-porous composite materials and coatings.

The chemical composition of PEUs and the nature of the formation of hydrogen bonds were studied using FTIR with multiple frustrated total internal reflection. The temperature transitions and thermal stability of the PEUs under study were determined by DSC. The influence of the ratio of rigid and flexible blocks on the melting temperatures of polymers, as well that due to the nature of hydrogen bonds, is demonstrated.

The rheological characteristics of thermoplastic PEU solutions have been studied. It has been established that all solutions have a minimum anomaly in viscosity, while the value of the logarithm of viscosity depends on the chemical composition and structure of the initial PEUs.

The possibility of using thermoplastic PEUs in the production of materials and coatings with a predetermined structure and a set of properties depending on the requirements and operating conditions of finished products has been confirmed by comparing their chemical composition, structure, thermal and rheological characteristics with PEU solutions of Sanpren LQ-E-6 and Vitur R 0112 grades widely used in the production of fibrous-porous materials and coatings.

Authors' contributions

G.M. Kovalenko – setting goals and objectives of the study, conducting experimental research, analyzing the results of the study, and writing the text of the article;

E.S. Bokova – literature analysis, summarizing the results of the study, writing conclusions on the study;

N.V. Evsyukova – literature analysis, experimental data processing, writing the abstract of the study.

The authors declare no conflicts of interest.

REFERENCES

1. Ebabu W., Hossain Md.I., El-Naggar M.E., Kechi A., Hailemariam S.S., Ahmed F.E. Exploration of Functional Polymers for Cleaner Leather Industry. *J. Inorg. Organomet. Polym. Mater.* 2022;32(1):1–14. <https://doi.org/10.1007/s10904-021-02129-4>
2. Luketich S.K., Cosentino F.D., Giuseppe M., Menallo G., Nasello G., Livreri P., Wagner W.R., D'Amore A. Engineering in-plane mechanics of electrospun polyurethane scaffolds for cardiovascular tissue applications. *J. Mech. Behav. Biomed. Mater.* 2022;128:105126. <https://doi.org/10.1016/j.jmbbm.2022.105126>
3. Maleki S., Shamloo A., Kalantarnia F. Tubular TPU/SF nanofibers covered with chitosan-based hydrogels as small-diameter vascular grafts with enhanced mechanical properties. *Sci. Rep.* 2022;12(1):6179. <https://doi.org/10.1038/s41598-022-10264-2>
4. Fathi-Karkan S., Banimohamad-Shotorbani B., Saghati S., Rahbarghazi R., Davaran S. A critical review of fibrous polyurethane-based vascular tissue engineering scaffolds. *J. Biol. Eng.* 2022;16(1):6. <https://doi.org/10.1186/s13036-022-00286-9>
5. Ube T., Nakayama R., Ikeda T. Photoinduced Motions of Thermoplastic Polyurethanes Containing Azobenzene Moieties in Main Chains. *Macromolecules.* 2022;55(2):413–420. <http://doi.org/10.1021/acs.macromol.1c01827>
6. Gumus O.Y., Ilhan R., Canli B.E. Effect of Printing Temperature on Mechanical and Viscoelastic Properties of Ultra-flexible Thermoplastic Polyurethane in Material Extrusion Additive Manufacturing. *J. Mater. Eng. Perform.* 2022;31(5):3679–3687. <http://doi.org/10.1007/s11665-021-06510-9>
7. Yin Z., Yuan F., Zhou D., Li M., Chen X., Liu Y., Xue M., Luo Y., Hong Z., Xie C. Thermal stability, surface wettability and mechanical behavior of highly ordered ZnO-doped thermoplastic polyurethane films with hierarchically porous structures. *J. Appl. Polym. Sci.* 2021;138(38):50989. <https://doi.org/10.1002/app.50989>

СПИСОК ЛІТЕРАТУРИ

1. Ebabu W., Hossain Md.I., El-Naggar M.E., Kechi A., Hailemariam S.S., Ahmed F.E. Exploration of Functional Polymers for Cleaner Leather Industry. *J. Inorg. Organomet. Polym. Mater.* 2022;32(1):1–14. <https://doi.org/10.1007/s10904-021-02129-4>
2. Luketich S.K., Cosentino F.D., Giuseppe M., Menallo G., Nasello G., Livreri P., Wagner W.R., D'Amore A. Engineering in-plane mechanics of electrospun polyurethane scaffolds for cardiovascular tissue applications. *J. Mech. Behav. Biomed. Mater.* 2022;128:105126. <https://doi.org/10.1016/j.jmbbm.2022.105126>
3. Maleki S., Shamloo A., Kalantarnia F. Tubular TPU/SF nanofibers covered with chitosan-based hydrogels as small-diameter vascular grafts with enhanced mechanical properties. *Sci. Rep.* 2022;12(1):6179. <https://doi.org/10.1038/s41598-022-10264-2>
4. Fathi-Karkan S., Banimohamad-Shotorbani B., Saghati S., Rahbarghazi R., Davaran S. A critical review of fibrous polyurethane-based vascular tissue engineering scaffolds. *J. Biol. Eng.* 2022;16(1):6. <https://doi.org/10.1186/s13036-022-00286-9>
5. Ube T., Nakayama R., Ikeda T. Photoinduced Motions of Thermoplastic Polyurethanes Containing Azobenzene Moieties in Main Chains. *Macromolecules.* 2022;55(2):413–420. <http://doi.org/10.1021/acs.macromol.1c01827>
6. Gumus O.Y., Ilhan R., Canli B.E. Effect of Printing Temperature on Mechanical and Viscoelastic Properties of Ultra-flexible Thermoplastic Polyurethane in Material Extrusion Additive Manufacturing. *J. Mater. Eng. Perform.* 2022;31(5):3679–3687. <http://doi.org/10.1007/s11665-021-06510-9>
7. Yin Z., Yuan F., Zhou D., Li M., Chen X., Liu Y., Xue M., Luo Y., Hong Z., Xie C. Thermal stability, surface wettability and mechanical behavior of highly ordered ZnO-doped thermoplastic polyurethane films with hierarchically porous structures. *J. Appl. Polym. Sci.* 2021;138(38):50989. <https://doi.org/10.1002/app.50989>

8. Sarup R., Sharma M., Behl K., Avasthi D.K., Kumar P., Ojha S., Nigam S., Joshi M. Fabrication of superhydrophobic polyurethane sponge coated with oil sorbent derived from textile sludge for oily wastewater remediation. *Environmental Nanotechnology, Monitoring and Management*. 2022;18:100675. <https://doi.org/10.1016/j.enmm.2022.100675>

9. Chen S., Li S., Ye Z., Zhang Y., Gao S., Rong H. Zhang J., Deng L., Deng L., Dong A. Superhydrophobic and superhydrophilic polyurethane sponge for wound healing. *Chem. Eng. J.* 2022;446(19):136985. <https://doi.org/10.1016/j.cej.2022.136985>

10. Ji J., Liu N., Ye T., Li X., Zhai H., Zhao S., Liu Y., Liu G., Wei Y., Feng L. Transparent polyurethane coating with synergistically enhanced antibacterial mechanism composed of low surface free energy and biocide. *Chem. Eng. J.* 2022;445:136716. <https://doi.org/10.1016/j.cej.2022.136716>

11. Zharkov V.V., Strikovskii A.G., Verteletskaya T.E. Description of the association scheme of urethane groups in elastic polyurethanes based on the analysis of the Amide I absorption band contour. *Vysokomolekulyarnye soedineniya. Seriya A.* 1992;34(5):142–147. (in Russ.). URL: http://www.polymsci.ru/static/Archive/1992/VMS_1992_T34_5/VMS_1992_T34_5_142-147.pdf

12. Saunders D.K., Frish K.K. *Khimiya poliuretanov (Chemistry of polyurethanes)*: trans. from Engl. Moscow: Khimiya; 1968. 470 p. (in Russ.).

[Saunders J.H., Frish K.C. *Polyurethanes*. Interscience; 1962. 368 p.]

13. Lipatov Yu.S., Kercha Yu.Yu., Sergeev L.M. *Struktura i svoystva polyurethanov (Polyurethane Structure and Properties)*. Kiev: Naukova Dumka; 1970. 288 p. (in Russ.).

8. Sarup R., Sharma M., Behl K., Avasthi D.K., Kumar P., Ojha S., Nigam S., Joshi M. Fabrication of superhydrophobic polyurethane sponge coated with oil sorbent derived from textile sludge for oily wastewater remediation. *Environmental Nanotechnology, Monitoring and Management*. 2022;18:100675. <https://doi.org/10.1016/j.enmm.2022.100675>

9. Chen S., Li S., Ye Z., Zhang Y., Gao S., Rong H. Zhang J., Deng L., Deng L., Dong A. Superhydrophobic and superhydrophilic polyurethane sponge for wound healing. *Chem. Eng. J.* 2022;446(19):136985. <https://doi.org/10.1016/j.cej.2022.136985>

10. Ji J., Liu N., Ye T., Li X., Zhai H., Zhao S., Liu Y., Liu G., Wei Y., Feng L. Transparent polyurethane coating with synergistically enhanced antibacterial mechanism composed of low surface free energy and biocide. *Chem. Eng. J.* 2022;445:136716. <https://doi.org/10.1016/j.cej.2022.136716>

11. Жарков В.В., Стриковский А.Г., Вертелецкая Т.Е. Описание схемы ассоциации уретановых групп в эластичных полиэфируретанах на основании анализа контура полосы поглощения Амид I. *Высокомолекулярные соединения. Серия А.* 1992;34(5):142–147. URL: http://www.polymsci.ru/static/Archive/1992/VMS_1992_T34_5/VMS_1992_T34_5_142-147.pdf

12. Саундерс Дж.Х., Фриш К.К. *Химия полиуретанов*: пер. с англ. М.: Химия; 1968. 470 с.

13. Липатов Ю.С., Керча Ю.Ю., Сергеев Л.М. *Структура и свойства полиуретанов*. Киев: Наукова Думка; 1970. 288 с.

About the authors:

Grigory M. Kovalenko, Cand. Sci. (Eng.), Associate Professor, Department of Chemistry and Technology of Polymer Materials and Nanocomposites, Institute of Chemical Technology and Industrial Ecology, A.N. Kosygin Russian State University (Technologies. Design. Art) (1, Malaya Kaluzhskaya ul., Moscow, 119071, Russia). E-mail: gregoryi84@mail.ru. Scopus Author ID 54788985600, ResearcherID D-5293-2014, RSCI SPIN-code 4527-6785, <https://orcid.org/0000-0002-7932-5443>

Elena S. Bokova, Dr. Sci. (Eng.), Professor, Department of Chemistry and Technology of Polymer Materials and Nanocomposites, Institute of Chemical Technology and Industrial Ecology, A.N. Kosygin Russian State University (Technologies. Design. Art) (1, Malaya Kaluzhskaya ul., Moscow, 119071, Russia). E-mail: esbokova@yandex.ru. Scopus Author ID 9277812100, RSCI SPIN-code 4025-8186, <https://orcid.org/0000-0001-7769-9639>

Natalia V. Evsyukova, Cand. Sci. (Eng.), Associate Professor, Department of Chemistry and Technology of Polymer Materials and Nanocomposites, Institute of Chemical Technology and Industrial Ecology A.N. Kosygin Russian State University (Technologies. Design. Art) (1, Malaya Kaluzhskaya ul., Moscow, 119071, Russia). E-mail: ev.natali@mail.ru. Scopus Author ID 37046937800, RSCI SPIN-code 2680-5629, <https://orcid.org/0000-0002-3297-5115>

Об авторах:

Коваленко Григорий Михайлович, к.т.н., доцент кафедры химии и технологии полимерных материалов и нанокмпозитов, Институт химических технологий и промышленной экологии ФГБОУ ВО «Российский государственный университет им. А.Н. Косыгина (Технологии. Дизайн. Искусство)» (119071, Россия, Москва, ул. Малая Калужская, д. 1). E-mail: gregoryi84@mail.ru. Scopus Author ID 54788985600, ResearcherID D-5293-2014, SPIN-код РИНЦ 4527-6785, <https://orcid.org/0000-0002-7932-5443>

Бокова Елена Сергеевна, д.т.н., профессор, профессор кафедры химии и технологии полимерных материалов и нанокompозитов, Институт химических технологий и промышленной экологии ФГБОУ ВО «Российский государственный университет им. А.Н. Косыгина (Технологии. Дизайн. Искусство)» (119071, Россия, Москва, ул. Малая Калужская, д. 1). E-mail: esbokova@yandex.ru. Scopus Author ID 9277812100, SPIN-код РИНЦ 4025-8186, <https://orcid.org/0000-0001-7769-9639>

Евсюкова Наталья Викторовна, к.т.н., доцент, доцент кафедры химии и технологии полимерных материалов и нанокompозитов, Институт химических технологий и промышленной экологии ФГБОУ ВО «Российский государственный университет им. А.Н. Косыгина (Технологии. Дизайн. Искусство)» (119071, Россия, Москва, ул. Малая Калужская д. 1). E-mail: ev.natali@mail.ru. Scopus Author ID 37046937800, SPIN-код РИНЦ 2680-5629, <https://orcid.org/0000-0002-3297-5115>

The article was submitted: February 14, 2022; approved after reviewing: June 03, 2022; accepted for publication: November 24, 2022.

Translated from Russian into English by H. Moshkov

Edited for English language and spelling by Thomas Beavitt

**SYNTHESIS AND PROCESSING OF POLYMERS
AND POLYMERIC COMPOSITES**

**СИНТЕЗ И ПЕРЕРАБОТКА ПОЛИМЕРОВ
И КОМПОЗИТОВ НА ИХ ОСНОВЕ**

ISSN 2686-7575 (Online)

<https://doi.org/10.32362/2410-6593-2022-17-6-514-536>



UDC 541.64:532.73:546.264-31

REVIEW ARTICLE

**Modern polymer composite materials for bone surgery:
Problems and prospects**

Pavel A. Povernov¹, Lyudmila S. Shibryaeva^{1,2,✉}, Ludmila R. Lusova², Anatoliy A. Popov^{1,3}

¹*N.M. Emanuel Institute of Biochemical Physics, Russian Academy of Sciences, Moscow, 119334 Russia*

²*MIREA – Russian Technological University (M.V. Lomonosov Institute of Fine Chemical Technologies), Moscow, 119571 Russia*

³*G.V. Plekhanov Russian University of Economics, Moscow, 117997 Russia*

✉ *Corresponding author, e-mail: lyudmila.shibryaeva@yandex.ru*

Abstract

Objectives. To discuss the main problems and prospects of creating modern osteoplastic materials based on polymer compositions used for bone surgery.

Methods. This review summarizes the research works devoted to the creation of materials used for bone implants and issues involved in their practical testing, as well as analyzes and synthesizes data of scientific articles on the following topics: rationale for the use of biodegradable materials in bone surgery; biodegradation and bioreparation bone graft processes; requirements for degradable polymer composite materials (PCMs) for biomedical applications; overview of polymeric materials suitable for use in implant practice; impact of modifications of the PCM on the structure and biological activity of the material in biological media; effect of exhaust and heat treatment on the molecular structure of polyalkanoates.

Results. The most promising biodegradable resorbable materials for reparative bone surgery to date are compared. The requirements for these types of materials are formulated and a rationale for their use is provided that takes into account the advantages over traditional metal and ceramic implants. The features of the kinetics and mechanism of biodegradation of implants in their interaction with the bone biological environment of the body from the moment of implant insertion to complete wound healing are considered. As a result of the analysis, factors that may affect the activity of implant decomposition and methods of adjusting the decomposition rate and mechanical characteristics of the material, such as chemical functionalization, the creation of block copolymers, the inclusion of fibers and mineral fillers in the composite, as well as heat treatment and extraction of the

composite at the manufacturing stage, were identified. Among the main factors, the influence of the structure of the composite material on its biological activity during interaction with biological media was evaluated. Of polymer materials, the main attention is paid to the most common biodegradable polymers widely used in medicine: polyhydroxybutyrate (PHB) of microbiological origin, polylactide (PLA) and other polymers based on polylactic acid, polycaprolactone (PCL). The effect of their modification by such additives as hydroxyapatite (HAP), chitin and chitosan, and beta-tricalcium phosphate (β -TCF) is considered. Materials based on PHB are concluded as the most promising due to their complete biodegradability to non-toxic products (carbon dioxide and water) and good biocompatibility. Nevertheless, existing compositions based on PHB are not without disadvantages, which include fragility, low elasticity, unstable behavior under high-temperature exposure during processing, implant molding, sterilization, etc., which requires improvement both in terms of polymer modification and in terms of composition of compositions.

Conclusions. The review considers approaches to achieving the properties of materials required for perfect implants. The main requirements for implants are optimization of the time of resorption of the osteoplastic matrix, facilitating the resorption of the osteoplastic matrix synchronized in time with the process of bone regeneration. To achieve these requirements, it is necessary to apply technologies that include modification of polymer composite materials by affecting the chemical composition and structure; introduction of fillers; use of chemical functionalization, orientation extraction, heat treatment. The success of using bone materials based on biodegradable polymers is based on an accurate understanding of the mechanism of action of various components of the implant composition and strict compliance with the tightening regulatory requirements of implantation technology.

Keywords: osteoplastic materials, regenerative medicine, tissue engineering, osteogenesis, bone implant material, biodegradable matrices, polyalkanoates, hydroxyapatite, bioactivity of bone implants, molecular structure of implant material

For citation: Povernov P.A., Shibryaeva L.S., Lusova L.R., Popov A.A. Modern polymer composite materials for bone surgery: Problems and prospects. *Tonk. Khim. Tekhnol. = Fine Chem. Technol.* 2022;17(6):514–536 (Russ., Eng.). <https://doi.org/10.32362/2410-6593-2022-17-6-514-536>

ОБЗОРНАЯ СТАТЬЯ

Современные полимерные композиционные материалы для костной хирургии: проблемы и перспективы

П.А. Повернов¹, Л.С. Шибряева^{1,2,✉}, Л.Р. Люсова², А.А. Попов^{1,3}

¹Институт биохимической физики им. Н. М. Эмануэля, Российская академия наук, Москва, 119334 Россия

²МИРЭА – Российский технологический университет (Институт тонких химических технологий им. М.В. Ломоносова), Москва, 119571 Россия

³Российский экономический университет им. Г.В. Плеханова, Москва, 117997 Россия

✉ Автор для переписки, e-mail: lyudmila.shibryaeva@yandex.ru

Аннотация

Цели. Обсуждение основных проблем и перспектив создания современных остеопластических материалов на основе полимерных композиций, используемых для костной хирургии.

Методы. Обзор суммирует научно-исследовательские работы, посвященные созданию материалов, применяемых для костных имплантатов, и их испытанию на практике, анализирует и обобщает данные научных статей по следующим разделам: обоснование использования биоразлагаемых материалов в костной хирургии; закономерности биодеградации и биорепарации костного имплантата; требования, предъявляемые к разлагаемым полимерным композиционным материалам (ПКМ) для биомедицинских применений; обзор полимерных материалов, пригодных для использования в имплантационной практике; влияние модификации ПКМ на структуру и биологическую активность материала в биосредах; влияние вытяжки и термической обработки на молекулярную структуру полиалканоатов.

Результаты. Рассмотрены наиболее перспективные на сегодняшний день биоразлагаемые резорбируемые материалы для репаративной костной хирургии. Сформулированы требования, предъявляемые к данным типам материалов, и дано обоснование их использования с учетом преимуществ по сравнению с традиционными металлическими и керамическими имплантатами. Рассмотрены особенности кинетики и механизма биодеградации имплантатов при их взаимодействии с костными биосредами организма от момента введения имплантата до полного заживления раны. В результате проведенного анализа были установлены факторы, которые могут повлиять на активность разложения имплантата и методы корректировки скорости разложения и механических характеристик материала, такие как химическая функционализация, создание блок-сополимеров, включение в состав композита волокон и минеральных наполнителей, а также термообработка и вытяжка композита на стадии изготовления. Среди основных факторов было оценено влияние структуры композиционного материала на его биологическую активность при взаимодействии с биосредами. Из полимерных материалов основное внимание уделено наиболее распространенным биодеградируемым, широко используемым в медицине полимерам: полигидроксибутирату (ПГБ) микробиологического происхождения, полилактиду и другим полимерам на основе полимолочной кислоты, поликапролактону. Рассмотрены их модификации с такими добавками, как гидроксиапатит, хитин и хитозан и бета-трикальций-фосфат. По итогам работы наиболее перспективными оказались материалы на основе ПГБ благодаря его полной биоразлагаемости на нетоксичные для организма продукты (углекислый газ и вода) и хорошей биосовместимости. Тем не менее, существующие композиции на основе ПГБ имеют недостатки, к которым относятся хрупкость, низкая эластичность, нестабильное поведение при высокотемпературном воздействии при переработке, формовании имплантатов, стерилизации и др. Это требует доработки композиций как в плане модификации полимера, так и по составу.

Выводы. В обзоре рассмотрены подходы к достижению свойств материалов, требуемых для совершенных имплантатов. Основными требованиями, предъявляемыми к имплантатам, являются оптимизация времени резорбции остеопластического матрикса, облегчение рассасывания остеопластического матрикса, синхронизированного по времени с процессом регенерации кости. Для достижения этих требований необходимо применять технологии, которые включают модификацию ПКМ путем воздействия на химический состав и структуру; введение наполнителей; использование химической функционализации, ориентационной вытяжки, термической обработки. Успех использования костных материалов на основе биодеградируемых полимеров основан на точном понимании механизма действия различных компонентов композиции для имплантата и строгом соответствии с ужесточающимися нормативными требованиями технологии имплантации.

Ключевые слова: остеопластические материалы, регенеративная медицина, тканевая инженерия, остеогенез, материал для костных имплантатов, биодеградируемые матриксы, полиалканоаты, гидроксиапатит, биоактивность костных имплантатов, молекулярная структура материала для имплантатов

Для цитирования: Повернов П.А., Шибряева Л.С., Люсова Л.Р., Попов А.А. Современные полимерные композиционные материалы для костной хирургии: проблемы и перспективы. *Тонкие химические технологии*. 2022;17(6):514–536. <https://doi.org/10.32362/2410-6593-2022-17-6-514-536>

INTRODUCTION

Much research attention is currently being paid to areas of medicine involving the development and production of various osteoplastic (bone-substituting) materials [1–7]. These materials are in demand in dentistry, maxillofacial surgery, as well as various areas of bone surgery.

The requirements for the nature and quality of materials intended for the manufacture of implants, as well as technologies for their manufacture, are determined by the application and conditions of functioning of implants and endoprostheses in contact with living tissues.

A common requirement related to the properties of materials for implants is the presence of osteoplastic and osteoconductive properties that support the formation of conductors for the germination of blood vessels with subsequent resorption and replacement with bone tissue. Osteoconductive materials serve as a matrix for the formation of new bone during reparative osteogenesis and have the ability to direct the growth of bone tissue. Implants require hydrophilic properties. Surgical interventions in bone surgery are often associated with pre-infected pathological foci where surgical treatment often is performed due to the development of inflammatory complications. An important problem is the choice of resistant (proof against infections) materials, as well as materials that do not cause thrombosis.

Despite impressive advances achieved in the development of a new generation of osteoplastic materials for bone implant purposes in recent decades, involving work carried out by world-leading research centers conducting experimental and clinical studies of osteoplastic matrices, as well as the devotion of significant material and financial resources to the field of regenerative medicine, a number of unresolved issues remain. These include optimizing the time of resorption of the osteoplastic matrix and the best choice of an effective technology to facilitate the resorption of the osteoplastic matrix synchronized in time with the process of bone regeneration. As a result, the review by D.D. Lykoshin and co-authors [8] shows that autografts still remain the gold standard in clinical practice.

Scientists are searching for materials and compositions having osteoplastic properties, which are at the same time resistant to bacterial influences. Recently, the range of materials with the above properties has been greatly expanded due to the use of synthetic materials, including biopolymers and various other biodegradable compositions. Biopolymer materials are often completely non-immunogenic, can be sterilized by modern medical methods, and are relatively inexpensive to produce. However,

the most valuable advantage consists in their wide range of physicochemical and biochemical properties due to the possibility to regulate of the supramolecular and molecular structure of polymers.

The broadest requirements for materials for implants are realized when using biodegradable compositions. Biodegradable polymer composite materials (PCMs), which are designed to create bioresorbable (gradually dissolving in the body) implants, comprise complex engineering tools from which biologically compatible systems can be constructed. The creation of such a system should be accompanied by the establishment of factors affecting bioresorbability. Thus, there are problems of studying the effect of the initial morphology and structure of PCM used for bioresorbable implants on their properties and qualities. Another important issue is the influence of the technological parameters of the manufacture of PCM on the properties of the implants obtained from them. In order to predict the quality of the implants obtained, it is important to identify the role of the structure of the material in its biological activity relative to the biological environment and body tissues with which the implants made of this material are intended to interact.

When selecting a biodegradable material for bioresorbable implants, as well as in the manufacture of the prosthesis itself, numerous technological problems arise. For example, the use of biodegradable polymer materials is greatly limited by a lack of deformability (elasticity), which is necessary due to most of the bones of the human body being subjected to cyclic loads, gradually leading to an increase in the concentration of stresses in the microstructure of the product and eventually destroying it. It is also important to note that the body's immune response to biopolymer materials in contact with it occurs at various levels, from single molecular interactions to complex perception of volumetric biophysical properties that coordinate reactions at tissue- and system levels.

When creating a PCM implant, the material's osteoinductivity, i.e., the ability to stimulate osteogenesis when it is introduced into the body, leading to the activation of progenitor cells, as well as their proliferation and differentiation into osteogenic cells, becomes an important factor [9]. In this regard, when developing materials for implants, the problem arises of forming a structural organization of the PCM that contributes to the overgrowth of the implant with body cells. This can be achieved by creating a porous morphology (Fig. 1) [9]. At the same time, the formation of a certain porosity is required, i.e., the volume in the material occupied by pores along with the necessary structural characteristics (isolated or combined pores), as well as individual shape and size.

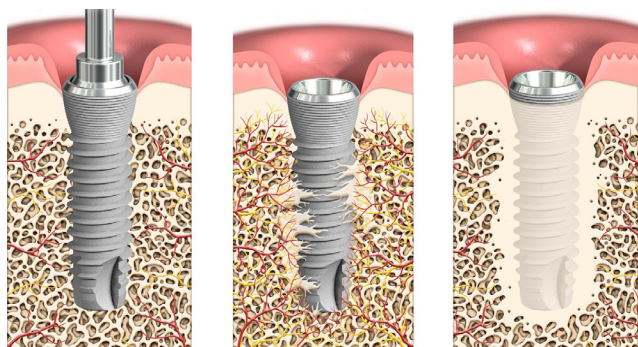


Fig. 1. Overgrowth of bone implants with cells of a living organism – osteogenesis [9].

Another method for achieving osseogenesis involves the use of mineral or organic fillers, drugs with the ability to initiate cell growth and development [10–14]; in any case, the presence of pores enhances this ability due to the sorption of drugs on the inner surface of the pores.

OBJECTIVES OF THE USE OF BIODEGRADABLE MATERIALS IN BONE SURGERY

Biopolymer composites are widely used in dental implantation surgery and dentistry. At the same time, the implantation of biodegradable polymer compositions for the treatment of bone injuries, defects, and fractures is still significantly limited due to the difficulty of achieving the required level of bioresorbability and osteoinductivity of implants made from these materials, as well as due to insufficient research base on the behavior of implants placed in a living organism and arriving there for a long time (Fig. 2) [15].



Fig. 2. Radiography of the distal femoral region of cats, where 70% of polyhydroxybutirate (PHB) and 30% of hydroxyapatite (HA) composite were implanted. The arrow indicates the decrease in the radiotransparent line around the implant over time. (A) Evaluation time in 30 days; (B) evaluation time in 60 days; (C) evaluation time in 90 days [15].

The mechanism of interaction between the implant and the body is based on the processes occurring at the bone–implant interface. The nature of the interaction between living bone cells and macromolecules of the polymer implant material at this boundary is determined by properties such as biocompatibility, corrosion resistance and cytotoxicity (Fig. 3) [15].

As established in [16, 17], such interaction depends on the surface topography, volume composition and morphology of the implant. The implant surface should be able to induce direct contact and functional connection between the implant and the bone tissue on which the load (osseointegration) is applied regardless of the area of location and the bone density, as well as its

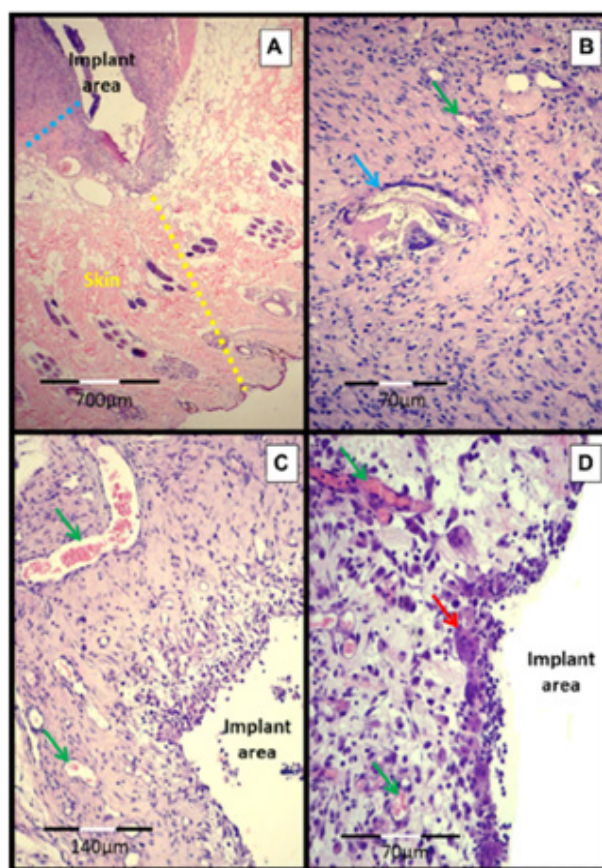


Fig. 3. Orthopedic implant made of a composite containing PHB and HA. Microphotography of the interface of a subcutaneous implant 45 days after an experimental operation to implant a composite of 70% PHB + 30% HA into the subcutaneous tissue of cats. (A) Skin (yellow dotted line), subcutaneous tissue and fibrous capsule or implant (blue dotted line). (B) Fibrous capsule in greater detail, showing the biomaterial (birefringent appearance) towards the giant cell (blue arrow), the green arrow points to the vessel. (C) Fibrous capsule with intensive neovascularization (green arrows) and (D) multinucleated giant cells (red arrow) [15].

quantity [18]. After the implant is installed, the contact area immediately provides the necessary stability due to friction and mechanical blocking forces between the bone trabeculae and the surface of the implant thread, leading to the development of new bone structure that replaces that surrounding the implant [2].

It is important to note that, while contemporary metal composites provide implants with the necessary strength and wear resistance, they have a big disadvantage due to the difference in the gradients of elastic modulus at the border with the bone, leading to tissue injury during the transfer of the occlusal load by the implant [3]. For ceramic products based on ZrO_2 and TiO_2 , studies of such problems caused by the high modulus of elasticity of zirconium dioxide, showed how this can lead to the destruction of bone tissue [4]. As well as overcoming this disadvantage, polymer materials offer a number of additional advantages associated with the bioresorbability and osseointegration of the material.

In the process of osseointegration of a bone replacement product, the interaction between the implant material and bone tissue should support the formation of fibrous tissue around the surface of the PCM leading to its improved structural stability [5]. Achieving such a state in full is often impossible due to the presence of a large number of variable factors affecting this process, among which are included the surface characteristics of the implant, the state of damaged bone tissue, the presence of bacterial infection, and the nature of mechanical loads exerted on the bone–implant system [2].

For a more complete understanding of the requirements for biopolymer materials and the necessary characteristics of these materials, it is necessary to establish the patterns according to which the biodegradation and integration of the material in the body takes place, as well as to understand the features of the osteogenesis process under the conditions of a foreign body introduced into the injured area of the body and its gradual destruction under the action of a biological media (Fig. 3) [8].

PATTERNS OF BIODEGRADATION AND BIOREPARATION OF A BONE IMPLANT

Bone is one of the few tissues whose fracture can heal without the formation of a fibrous scar. A fracture occurs due to exceeding the limits of tensile strength and deformation. The new formation of bone material in the process of fracture healing depends on the size of the gap at the fracture site [19]. The use of polymer materials for implants

depends on the individual characteristics of the body, the type of injury and the mechanism of implantation. At the same time, it is necessary to distinguish between two types of osteogenesis: contact and distant. During contact osteogenesis, bone tissue is formed directly on the surface of the implanted product [13]. With distant osteogenesis, bone tissue regeneration occurs around the implant, i.e., new bone tissue spreads from the surface of the unaffected bone area to the implant [13]. Also involved in these processes are multipotent mesenchymal stromal cells (MMSCs), which are able to differentiate into bone (osteoblasts) or cartilage (chondrocytes) tissue.

Thus, the role of a polymer scaffold is to act a carrier of various growth factors (morphogenetic proteins that stimulate bone mineralization, fibroblast growth factors that enhance osteoblast proliferation, growth peptides that stimulate vascularization of the internal volume of the implant, etc.) at the same time as not triggering rejection by the body [20]. The fundamental characteristic of the implant is the dynamics of its biodegradation and the mechanism of the process. From the time of implantation to the completion of the bone remodeling phase, the strength interaction of the implant and bone at all stages of healing should correspond to one basic principle—the total strength of the bone–implant system at any time should not be lower than the final target bone strength after healing [21]. However, regarding the stability of the bone–implant system, according to studies in dental implantology [13, 18, 22, 23], the total stability changes have a V-shaped profile and may fall to 55–65% of the target in the middle of the healing cycle due to a more intensive decrease in primary stability due to bone resorption in those places where the implant coils exert pressure on the bone trabeculae causing the death of osteocytes. Although secondary stability (the formation of new bone tissue on the surface of the implant) increases over time, its increase fails to compensate for decline in the primary stability in the interval from 15 to 40 days after implantation, resulting in a fall in overall stability.

Although the implant is expected not to completely collapse after three phases until the fracture is completely healed, at the same time, the implant must completely dissolve within 3–6 months after healing in order to exclude a negative reaction of the body to a foreign body. In the case of bone implants, it is important to refer to individual structures of a certain shape, size and strength, on which the features of the biodegradation process of the composition and the possibility of regulating the decomposition rate at the stage of obtaining a polymer material depend, for example, during subsequent 3D printing [21, 24].

Biodegradation of an implant in contact with living cells of the body is a complex multi-stage process involving a number of physical stages and chemical reactions:

- polymer dissolution;
- ionization of ionogenic groups present in polymer macromolecules;
- ionization of ionogenic groups formed during the reactions of destruction and hydrolysis of polymer macromolecules;
- destruction of polymer–polymer complexes;
- hydrolysis of polymer macromolecules;
- dissolution of the products of decomposition reactions in a polymer matrix [25].

The process of biodegradation of PCM in the body can be divided into two mechanisms: degradation of the material in the external diffusion-kinetic region (destruction of the polymer surface); propagation of degradation from the surface into the volume of the polymer matrix. It is important to note that several factors influence the surface and bulk degradation of the polymer. When the external area of the implant is destroyed, the chemical structure of the material, its morphology, the shape and size of the particles of the dispersed phase (filler), the nature of the pores and the degree of porosity of the material, as well as the presence of perforation of the implant play a key role [25, 26].

The penetrating ability of biodegradation is affected by the degree of swelling of the polymer in the biological media with which contact occurs (blood, lymph, synovial fluid). In addition, the relative rate of penetration of the biological medium into the material due to its swelling in comparison with the rate of decay of the surface layer plays a role. In this case, the diffusion parameters of the transfer of the biological medium play a role, due to the structure of the material and its chemical resistance. So, if the swelling rating is high, then the outer layer of the polymer does not have time to degrade, and the penetration of the biological medium into the volume leads to a gradual degradation of the inner layers. In this case, cracking may occur due to the rupture of strained bonds in macromolecules on the polymer surface and the subsequent mechanical destruction of the composite layers, which violates the integrity of the implant and reduces its mechanical characteristics [25, 27], as well as leading to an acceleration of the volumetric destruction of the implant as a whole.

In addition to rectifying unstable strength properties due to high swelling, control of the degree of swelling of the polymer composite plays an important role in the manufacture of bone implantation materials due to the problem of “clogging” the area to be repaired with mechanically destroyed, but not chemically decomposed fragments of the implant

material. Thus, the higher the degree of crystallinity of crystallized polymers in volume, the lower their degree of swelling in water, and hence the lower the degree of penetration of enzymes that promote degradation into the polymer matrix [28].

In most cases, the destruction of the material in the surface layer occurs due to hydrolysis and enzymatic reactions [29]. This stage is non-cellular biodegradation, leading to the formation of microcracks in the material, deformation of the product and the formation of macro-cracks of various shapes and sizes.

The degree of destruction of PCM, which is determined by the composition, chemical nature and structure of the components, is most noticeable in areas with hydrophilic sites of macromolecules due to their more active hydrolysis. Over time, the outer layer becomes looser due to the formation of volumetric microchannels. For example, in [30], the creation of a polyhydroxybutyrate (PHB) composite with polyvinyl alcohol (PVA) having hydrophilic properties made it possible to regulate the moisture permeability of the material by changing the concentration of PVA. At the same time, although such a structure contributes to a more active penetration of the biological medium into the volume of the product, a favorable environment is already created for the splitting of water-soluble fragments of macromolecules outside the implant. Through a network of microchannels, the separated fragments can enter the biological environment, in which their further chemical cleavage into harmless molecules will occur under the action of mainly enzymatic hydrolysis.

It is worth noting that the hydrophilization of polymers, comprising one of the methods of their modification, can be carried out by plasma chemical treatment in an atmosphere of air or pure oxygen [31], in which the oxidation of the surface layer of the polymer material occurs due to the formation of polar groups containing oxygen (hydroxyl, carbonyl, carboxyl, etc.). This effect leads to an increase in the adhesive properties of materials.

In addition, hydrophilization can be carried out by treatment with other chemical processes: sulfonation, chlorosulfation, etching in organic solvents. When treated with a solvent, the surface layer of the polymer is loosened by its swelling, which leads to a weakening of the intermolecular bonds between the polymer chains in the near-surface layer [30].

After sufficient loosening of the outer layer of the implant, the process of cellular destruction begins under the action of monocytic phagocytes. After maturing into macrophages, these cells can concentrate on such a partially degraded surface, transform into epithelioid cell granulomas and coagulate into Langhans giant cells [10].

Langhans giant cells are giant multinucleated cells formed from epithelioid cells during their fusion or during the proliferation of macrophages. These cells can tighten sufficiently large macromolecules into their internal volume, envelop them with a cell membrane and process them at the expense of lysosomes and mitochondria. The beginning of the cellular destruction process and its dynamics are characterized by the size of the detached fragments of macromolecules, the degree of heterogeneity of the implant surface and the size of the protruding loosened fragments. Thus, it is believed that the sufficient size of such fragments for the active inclusion of phagocytic enzymatic hydrolysis is a fragment length of 20–30 μm . The photodestruction of biodegradable polymers (for example, during pretreatment of an implant) can increase the degree of crystallinity of the surface, which will lead to a decrease in the initial rate of enzymatic destruction and a decrease in the length of fragments necessary for its initiation [32]. In another study [33], it was shown that the rate of decomposition of PHB by enzymes is significantly affected by the molecular weight of the polymer and the temperature of destruction. For the human body temperature (37°C) at a molecular weight of 150 kDa in 3 months, the weight loss was 12%, and for high-molecular PHB (300–1000 kDa) only 2%. Consequently, varying the molecular weight of the polymer matrix can also significantly affect the rate of biodegradation.

The products of intracellular decomposition, depending on their composition, can be absorbed by these cells, or excreted into the circulatory system. Since the immune response weakens after some time (5–15 days) with sufficient polymer biocompatibility, the influx of macrophages at the site of the implant localization also decreases, allowing fibroblasts begin to form a tissue capsule. Loose connective tissue is embedded in the microcracks of the implant, followed by the stage of vascularization of the matrix and the germination of nerve-endings.

The germination of connective tissue depends on the morphology of the polymer, its chemical structure, and porosity, as well as the degree of destruction of the surface layer. The cellular stage usually begins quite a long time after the implant is inserted (closer to the reparative phase of fracture healing or the remodeling stage), which can vary greatly depending on the type of polymer [7, 10].

Thus, the sequence of stages of cellular destruction of the implant is reduced to the following:

- localization of macrophages on the implant;
- fusion of macrophages and their transformation into Langhans giant cells;
- activation of the mitochondria of Langhans giant cells in contact with the polymer matrix;

- enveloping of the separated polymer macromolecules and its further processing under the action of hydrolysis and fermentation;

- weakening of the immune response and the beginning of the germination of connective tissue.

Another problem manifesting itself at later stages of bone tissue healing is associated with the manifestation of various secondary processes, among which the most dangerous is excessive calcification of the surface layer of the implant. Since it will certainly come into contact with the bloodstream, the deposition of calcium salts (medium and basic calcium phosphates with different ion ratios) is an integral part of the implant integration process. Increased adsorption of calcium salts causes the formation of microcracks leading to the formation of a loose structure in the outer layer of the implant. The process of dystrophic calcification typically occurs as a response to soft tissue damage, which leads to the formation of significantly mineralized areas that cause blockage of blood vessels and can cause strokes and heart attacks. In this regard, reducing the degree of calcification represents an important problem. Studies demonstrating the effect of dexamethasone on transforming growth factor $\beta 1$ responsible for cell proliferation and differentiation, as well as the ability of dexamethasone to act as an inhibitor of calcification, should be noted [34, 35]. Dystrophic calcification can also be reduced by modifying the polymer surface. This also contributes to the improvement of osseointegration and vascularization of the implant [10–12].

Since the formation of phosphates is an integral stage of degradation of the composite in the body, workarounds are needed to reduce the degree of their adsorption. This can be done by modifying the implant surface, for example, by introducing hydrophilic fillers into the PCM, forming layers on the polymer surface, or by changing the surface charge due to various drugs (heparin, protamine sulfate, etc.).

The authors of [36] developed and investigated experimental porous 3D carriers made of poly-3-hydroxybutyrate, designed for the restoration of bone tissue defects. The ability of the developed 3D carriers to support adhesion, proliferation and directed differentiation of cells in the osteoblastic direction was studied using the example of MMSC culture isolated from bone marrow and adipose tissue. Based on the results, the differentiation of MMSCs into osteoblasts was confirmed and measured. An increase in the expression of genes for osteocalcin, which is the most informative marker of bone formation, was revealed. Its release and entry into the blood occurs during osteosynthesis from osteoblasts.

REQUIREMENTS FOR DEGRADABLE PCMs FOR BIOMEDICAL APPLICATIONS

To create bone implants, it is necessary to develop a biodegradable material with the necessary deformation properties, strength, capable of withstanding high-temperature exposure during 3D modeling of the implant [37], as well as ensuring its sterilization. At the same time, the achievement of an optimal biological reaction between the implant and the cells developing on its surface is realized if the implant has a micro- and macroporous structure [38].

A pore surface from 40 μm to 1 mm is the main factor ensuring cell germination [39, 40]. Under conditions of porosity, especially internal continuous porous areas in the polymer material, the cells of the body can easily attach to the inner surface of the pores and germinate through the entire implant, with the formation of blood vessels [41, 42].

In addition, the material should minimize the possible negative reaction of body tissues to foreign inclusion, not support or prevent the growth of bacteria on its surface, and avoid triggering an allergic or immune response of the host body. In terms of its mechanical characteristics, with the exception of various individual features of the damaged area of bone tissue and the localization of injury, the material should have high shear and tensile strength.

To provide parameters for the biodegradation process of an individually tunable bone repair material depending on the patient's age, presence or absence of infectious infection, tissue conditions near the affected area, and type and size of the lesion, fine-tuning of the decomposition conditions is necessary to vary the dynamics of material strength, mass, volume and size, taking into account the kinetics of bone tissue healing.

Thus, the role of the PCM structure for biomedical use in bone surgery should be considered from the perspective of three aspects:

- morphological aspect (structure of amorphous and crystalline regions): the size and shape of the polymer matrix crystallites, the amount of free volume in the composite for cell proliferation and differentiation into osteoblasts;
- pore formation (the ability of a material to form pores of a certain structure): porosity parameters include pore size and shape, the presence of isolated or combined pores and connections between them;
- reactivity (parameters of biodegradation of the material): chemical destruction, mechanical destruction of the composite due to overstressed bonds in macromolecules and the formation of microcracks, the formation of macrocracks due to the rupture of layers of the material by germinating cells.

By setting the optimal ratios between these aspects, it is possible to create a biodegradable polymer composite suitable for bone implantation. The condition for this adjustment is such a ratio between their contributions that the rate of implant biodegradation and the associated loss of strength does not exceed the rate of increase in the strength of newly formed bone material.

OVERVIEW OF POLYMER MATERIALS SUITABLE FOR USE IN IMPLANTATION

To date, various synthetic and natural polymer materials, as well as mineral-based materials, have been created and used for bone and dental implants. Among the mineral materials that have been widely used, it should be noted hydroxyapatite (HA), beta-tricalcium phosphate (β -TCP) and ceramics, including organic (collagen) and natural biopolymers (polysaccharides) variants.

Among the mineral components, HA is the most promising due to its excellent biocompatibility, as well as ability stimulate osteogenesis and form a matrix for the formation of new bone tissue. Nanocrystalline HA is able to more actively adsorb proteins necessary for the vital activity of cells [43], while according to [44] its ability to stimulate reparative osteogenesis is even higher than that of polycrystalline HA.

In [45], a method for the synthesis of nanoscale HA was developed along with a proposed method for its purification and methods for the formation of porous calcium-phosphate composites based on HA and collagen. The methods described in the article make it possible to produce tissue-engineered structures offering an adjustable architecture for solving various biomedical tasks.

Materials based on β -TCP are also thought to be quite promising [46] due to their high degree of degradation, excellent biocompatibility and the ability of this substance to create a matrix for the germination of osteoblasts in the process of reparative osteogenesis. However, due to the excessively rapid degradation of the material leading to a significant drop in its compressive strength, it cannot provide a basis for the formation of new bone tissue [47].

Calcium-phosphate ceramic materials are characterized by heterogeneity of the particle sizes of the material and pores [48], in connection with which work is underway to find more promising bone implantation materials.

Collagen is a filamentous protein that is the main component of connective tissue. Approximately 30–35% of all proteins in the human body and most mammals are made up of collagen, including most

of the joints, tendons, skin, walls of blood vessels, as well as forming part of nail-, tooth- and bone tissue. Collagen obtained from cattle tissues is generally appropriate and cost-effective.

Among polysaccharides, chitin-, chitosan-, alginate-, and starch-based materials have been widely used.

In modern medical science, technologies for the development of materials based on various polyolefins are considered, the possibilities for their use in replacement implantation surgery are studied. Despite the creation of polypropylene-based synthetic materials characterized by a high degree of biocompatibility [49], their use is associated with a number of disadvantages, such as the occurrence of postoperative complications due to rejection of the material by the body. For example, in [50], the inflammatory reaction of the body to the implantation of a polypropylene product was studied, during which it was found that 6 months after implantation, a tightly formed connective tissue formed around the material, while the leukocyte-lymphocyte inflammatory reaction to a foreign body remained throughout the entire period. At the same time, significantly fewer cells involved in phagocytosis were formed around the material than during the decomposition of biopolymer materials.

Compared with polyolefins, materials based on biopolymers obtained by chemical synthesis in living organisms—plants or microbial systems [6]—have a number of advantages. Such polymers have a more complex and well-defined structure compared to synthetic polymers and are characterized by high biodegradability and renewability.

One of the most promising biopolymers is a polymer based on lactic acid—polylactide (PLA). PLA is obtained from natural raw materials: rice, potatoes, corn, etc. Due to the bioabsorbability of PLA, it can be used as stents for implantation into the body without the need for repeated surgical intervention due to their complete biodegradation in a relatively short time [7, 8]. At the same time, the hemocompatibility of this polymer is comparable with the indicators of other materials used as stents such as stainless steel.

Composite frameworks based on PLA can be carriers for morphogenetic proteins that stimulate the formation of bone tissue [51].

In the study [52], PLA was compared with other biopolymers (polycaprolactone, chitosan, PHB). Histological data showed that, in addition to offering good supporting functions for connective and bone tissue, PLA does not cause pronounced inflammatory infiltration by lymphocytes, neutrophils and Langhans giant cells. The metabolites of the breakdown of PLA have no negative effect on the

body or on the dynamics of osteogenesis as a whole. Based on the results of the work, the materials from the PLA are recognized as promising for use in veterinary bone surgery.

In addition to pure PLA, copolymers of PLA and polyglycolic acid (PLA-PGA) are more often used. Such copolymers are used as surgical decomposable screws, fingers, pins, and whole plates for the restoration and remodeling of bone defects, as well as the formation of cartilage tissue. Such copolymers are not cytotoxic, and the rate of their decomposition can be regulated by changing the ratio of components.

Another naturally degradable polymer of microbiological origin is poly-3-hydroxybutyrate (PHB, P-3-HB). Despite the presence of significant disadvantages of this material limiting its use in its pure form, which include thermal instability and high brittleness, a large number of studies are being conducted on the use of PHB in composite materials together with the introduction of a range of various fillers of both natural origin (including mineral) and synthetic [53–55] (including modifiers and plasticizers).

Studies on the regeneration of bone defects of various rat bones using PHB have shown that implantation of an element made of pure PHB or filled with mineral components of PHB does not worsen the conditions of bone tissue regeneration and does not cause an inflammatory reaction. In addition, the material usually has a high resorption capacity and promotes the propagation of the regeneration front towards the damaged area from the periphery to the center of the regenerate.

THE EFFECT OF PCM MODIFICATION ON THE STRUCTURE AND BIOLOGICAL ACTIVITY OF THE MATERIAL IN BIOLOGICAL MEDIA

The biodegradable capacity of polymers to be absorbed by microorganisms depends on a number of parameters and structural characteristics. The most important are the chemical nature of the polymer, the branching of the macromolecule (the presence and nature of side groups), as well as the molecular weight, supramolecular structure, structure of the crystalline regions, and the conformation of the chain in the amorphous region [7, 10]. Natural and synthetic polymers containing bonds that are easily hydrolyzed have a high biodegradability. The presence of substituents in a polymer chain often contributes to increased biodegradation. The latter also depends on the degree of chain substitution, the length

of its sections between functional groups, and the flexibility of macromolecules.

Thus, biodegradable polymers should:

1) be heterochain and contain bonds available for biodegradation: $R=CH_2$; $R=CH-R_1$; $R-CH_2-OH$; $R-CH(OH)-R$; $R-CO-H$; $R-CO-R_1$, etc.;

2) contain fragments that include no more than 5 groups of CH_2 in a row;

3) have volumetric substituents in the composition: the larger the volume of the substituent, the faster the polymer is destroyed;

4) include natural products in the macromolecular chain—starch, cellulose, lactose, urea, which can be used as fillers, and then microorganisms absorb them.

Polymers having an amorphous supramolecular structure are invariably less resistant to biodegradation than crystalline ones. This is due to the fact that the compact arrangement of structural fragments of semi-crystalline and crystalline polymers limits their swelling in water and prevents the penetration of enzymes into the polymer matrix, making it difficult for enzymes to act not only on the main carbon chain of the polymer, but also on the biodegradable parts of the chain.

An important factor determining the resistance of a polymer to biodegradation is the size of its molecules. While monomers or oligomers can be affected by microorganisms and serve as carbon sources for them, polymers with a large molecular weight are more resistant to the action of microorganisms.

Biodegradation of most technical polymers is usually initiated by non-biological processes (thermal, photo-oxidative, mechanical degradation, etc.). The mentioned degradation processes lead to a decrease in the molecular weight of the polymer. In this case, low-molecular bioassimilable fragments arise, having hydroxyl, carbonyl, or carboxyl groups at the ends of the chain. The resistance of polymer materials to the action of microorganisms also depends on the plasticizers, fillers, stabilizers, and other technological additives included in their composition, as well as on the extent to which these substances can be a source of carbon and nitrogen for microorganisms. It is known that inorganic components (silicates, sulfates, phosphates, carbonates) do not support the growth of fungi.

When creating biodegradable materials, the process of modifying synthetic polymers and composites using natural polymers has become widespread. An important place in the research is occupied by the problem of giving the properties of biodegradation to well-mastered multi-tonnage industrial polymers: polyethylene, polypropylene, polyvinyl chloride, polystyrene, polyethylene terephthalate, polyurethane. For this purpose, three modification directions are being actively developed [56]:

– admission of synthetic polymers of molecules containing functional groups, such as complex ether, amide, anhydride, urethane, etc. into the structure, with the presence of such groups promoting accelerated photodegradation of the polymer to provide the ability to sorption of water, hydrolysis, which results in the formation of water-soluble products;

– preparation of compositions of multi-tonnage polymers with biodegradable natural additives capable of initiating the decomposition of the main polymer to a certain extent;

– directed synthesis of biodegradable plastics based on industrially mastered synthetic products, in which it is possible to change the properties of the material by regulating the hydrophilic and hydrophobic properties of its surface.

The idea of creating a composition of various synthetic polymers with starch appeared in the 1970s. Thus, in the article [57] G.J. Griffin described the process of developing composites with starch based on low-density polyethylene to create biodegradable film materials for packaging. The addition of starch allowed the material to decompose without exposure to ultraviolet radiation and water. Soil microorganisms contribute to the swelling and hydrolysis of starch, the formation of dextrin and glucose molecules, an increase in the surface area of the composite material and further peroxide destruction of the polymer. The formed low molecular weight fragments are subsequently assimilated by soil microorganisms.

An important scientific direction in the creation of a new class of biodegradable materials is the creation of modifiers composed of hyperbranched polyether polyol-based surfactants. The works of V.I. Gomzyak *et al.* are devoted to the synthesis of such surfactants [58]. Surfactants based on super-branched biodegradable polyether polyols are widely used as modifiers of polymer materials. Their activity depends on the degree of branching [59]. Polyether polyols are also used as a basis for the production of biodegradable block copolyesters [60]. To date, such compounds are used in medicine for the manufacture of containers for the targeted delivery of medicinal substances, which opens up wide possibilities for regulating the issuance of medicinal contents in a living body.

The study of the role of modifying additives introduced into materials based on PHB, PLA, and other polymers had demonstrated their significant effect on the biological activity of PCM in biological media [61–65]. These additives also have a great impact on the biocompatibility, strength and proliferation of cells for the scaffold material: a temporary mechanical structure that mimics the extracellular matrix of bone tissue, serving to create an optimal

environment for the repair of damaged bone. In order for healing to occur at a high rate and without complications, the scaffold should not be rejected by mesenchymal stem cells. For successful completion of all stages of healing, a high level of adhesion between the implant and organic tissues is required; in some situations, this can be achieved by introducing stem cells at the site of the scaffold [61].

An effective scaffold should provide adequate physical support similar to real bone in order to stimulate bone regeneration while ensuring a continuous supply of nutrients and metabolites of tissues formed on the skeleton. The paper [63] demonstrates the effect of well-delaminated organo-modified montmorillonite clay on the PHB matrix. This increased modulus of elasticity of the system as a result of this modification can be traced by the results of transmission electron microscopy and X-ray diffraction analysis. To understand the influence of temperature on the mechanical properties of the frame, the modulus of elasticity was studied both at room temperature, at which the implant itself is installed in the body, and at 37°C, which corresponds to the physiological temperature of a human body. It was found that at room temperature, the modulus of elasticity increases by an amount from 40 to 90% at filler concentrations from 3 to 5%. At the temperature of the human body, the same characteristic was 25–50% higher than the initial indicators. This filler was also shown to significantly affect the surface roughness. The rougher topography of the implant promotes attachment and proliferation of osteoblast cells to the surface. Studies have shown that a significant degree of proliferation over a large surface area was observed already on the fourth day after cell culture. Osteoblasts were attached by branching microfilaments and the formation of lamellipodia and microarrays at the interface of the bone–implant phases. When studying the rate of proliferation of body tissue by cell division (proliferation) on human osteoblast cells when they were stained with a fluorescent dye, positive results were obtained after 7 days of incubation. The thermal stability of nanohybrid materials was improved by using a nanocomposite with a clay content of 5%. The structure of the PCM with a low clay content (up to 1–2%) was heterophase; here, while the stratified state prevailed, an increase in clay concentration to 3–5% was noted along with the increased prevalence of intercalated state with small individual fragments by which means stratification was detected. Thus, the inclusion of nanoclay and similar fillers based on montmorillonite can be used to increase the rigidity of the composite material and its thermal stability without affecting the biocompatibility of the material in comparison with that of pure PHB (Fig. 4).

Concerning the decomposability of PHB-based materials in the body and the body's response to the introduced foreign object, studies into suture materials and threads are relevant [64, 65]. Materials from PHB and from the copolymer of PHB with hydroxyvalerate (PHB-co-3HV) following intramuscular implantation to experimental animals did not cause any acute diseases, vascular reaction at the implantation site or any side effects, such as purulent inflammation, necrosis, calcification of the fibrous capsule or the formation of a malignant tumor for a long period (up to 1 year) [64]. The tested monofilament sutures made of PHB and PHB-co-3HV demonstrated the necessary strength for the healing of muscle-fascial wounds [64].

In the article [65], the degradation of a monofilament filament made of PHB-co-3HV was investigated both in a lipase solution and during implantation into the tergal muscles of a rat. The results showed that the monofilament thread gradually lost its tensile strength, which was accompanied by a decrease in molecular weight. Implantation to a rat did not show noticeable body responses during degradation *in vivo*. Reactions to the foreign body were much weaker than those of chrome catgut, which is one of the most commonly used medical suture products.

It was found that the introduction of chitin/chitosan as a rigid filler into the PHB matrix improves mechanical properties [66]. However, the high cost and complexity of manufacturing such a composition is a limiting factor in their use. Since chitosan is susceptible to carbonation at high temperature in a mixture of melts, it is necessary to use a solution or other technology [66]. Compared with pure chitosan films, the mixture of PHB (30%)–chitosan (70%) showed higher tensile strength and elongation at break by 40% and 60%, respectively. In addition, these properties, combined with the porous structure of PHB–chitosan films, increase the likelihood of using these composites in tissue engineering.

When studying a mixture of PHB–chitin prepared by casting from a solution, the authors [67] established the formation of an intermolecular hydrogen bond between the carbonyl groups of PHB and the amino groups of chitin. At the same time, the crystallization process was accelerated due to heterogeneous nucleation on chitin particles, which contributed to the rapid growth of PHB crystals. However, decreased crystallinity at higher chitin concentrations can be explained by a concomitant decrease in the mobility of PHB chains due to intermolecular hydrogen bonds between PHB and chitin.

In the study [25], the structure and properties of biodegradable compositions based on PLA, chitosan and ethyl cellulose obtained in a Brabender

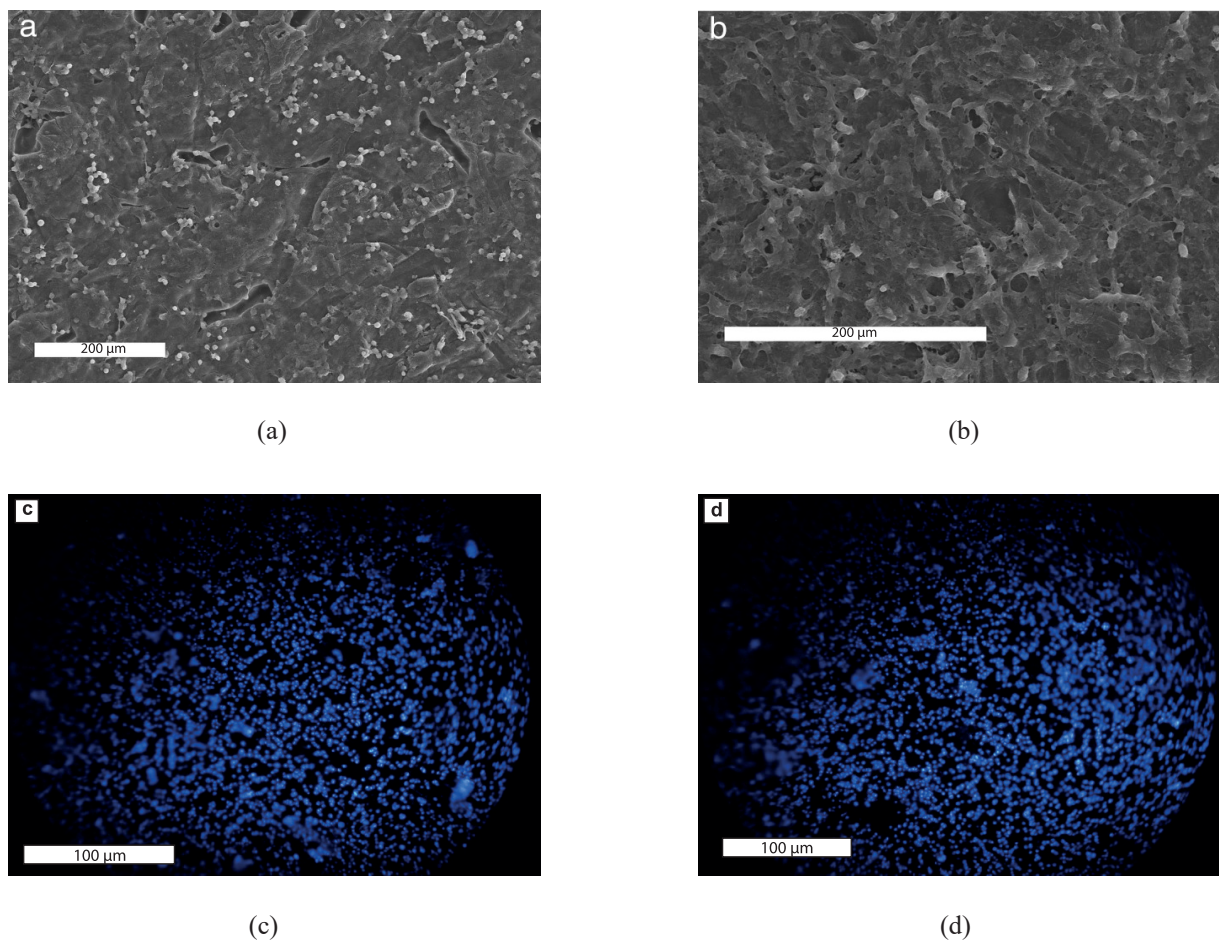


Fig. 4. SEM (300×) visualization of human osteoblast cells after 7 days of cultivation: (a) on pure PHB; (b) on PHB/5, wt % clay. Staining of 4',6-diamidino-2-phenylindole cells of human osteoblasts after 7 days of cultivation: (c) on pure PHB, (d) on PHB/5 wt % clay [63].

type mixer were studied. It was shown that the addition of low molecular weight polyethylene glycol leads to an increase in the elongation of rigid PLA–ethyl–cellulose compositions. At the same time, the compositions have a sufficient level of biodegradability as estimated by weight loss under conditions of exposure in the soil.

In [68], a polymer PHB–chitosan composition for prolonged transport of biologically active substances was developed and studied. It was shown that the ratio of components allows varying the sorption capacity of the drug carrier (rifampicin), as well as the profile of its release. During the decomposition of the biopolymer matrix, voluminal microcracks are formed, contributing to the gradual release of the drug enclosed inside into the biological environment. Such gradual release of the substance can be used in other ways, for example, by including growth factors in the composition that promote proliferation (vascular endothelial growth factor) and bone formation (morphogenetic proteins).

In [69], the thermal properties of a porous PLA were studied. Porophores based on ammonium carbonate in a solution of acetone and supercritical CO₂ were used to prepare the porous composition. It has been shown that pore formation leads to the destruction of the crystalline regions of the PLA, reducing the melting heat of the crystallites. Changes in the crystal structure of the matrix also occur under the action of polymer plasticization caused by exposure to high temperature with the influence of pore-forming gaseous reagents. The internal pressure of gases significantly disrupts the pore structure; by varying the kinetics of the formation of crystal structures when the polymer is cooled [69], it is possible to change the strength and elastic properties.

In the three-block copolymer PHB–PLA–polycaprolactone, a decrease in the probability of formation of large crystallites was identified as due to a decrease in the length of oligomeric segments and a restriction of the mobility of the chain of PHB blocks [709]. These factors, which lead to an

increase in the flexibility of the material, have a positive effect on its biocompatibility.

EFFECT OF EXTRACTION AND HEAT TREATMENT ON THE MOLECULAR STRUCTURE OF POLYALKANOATES

Crystallization and the size of crystallites have a great influence on the mechanical and thermal properties of polymers. The exceptional stereochemical regularity and low density of nucleation in polyalkanoates, for example, in PHB, contributes to interspherulitic cracking. In addition, secondary crystallization of PHB during heat treatment occurs in such a way that amorphous intercrystalline regions are enriched with pass-through chains in an extremely straightened conformation, which reduces segmental mobility, leads to a change in the thickness of lamellae in the crystallite structure, causing embrittlement of the polymer, and, consequently, deteriorates the mechanical characteristics of PHB [71].

The improvement of the deformation properties of the material typically occurs along with a decrease in its strength [72–74]. However, since both of these parameters are important in the case of manufacturing bone replacement products, it is important to implement methods that increase flexibility without significantly reducing strength. In this regard, the combination of extraction, which changes the orientation of molecular chains along the direction of extraction, thermal annealing at elevated temperatures and re-aging at room temperature can eliminate secondary crystallization, improving the overall impact strength [23].

Mixing of PHB with chitosan changes the structure of the crystalline regions of PHB during heat treatment. High-temperature annealing of composites consists in alternating melting and crystallization cycles in a non-isothermal mode. It was shown in [68] that the interaction of the components leads to a more ordered structure of chitosan and a higher stability of PHB crystallites, since chitosan prevents the recrystallization of PHB during annealing. In addition, intermolecular hydrogen bonds formed in the composition were found to represent a factor affecting the structure of PHB crystallites; the scope of this effect, however, depends on the localization of bonds in the amorphous regions of the composite.

There are results of experimental studies on the production of films from ultrahigh molecular weight PHB (UMW PHB) by uniaxial broaching with annealing at 160°C, according to which the strength characteristics of such materials were

significantly improved. Thus, in [75], this method allowed to increase the elongation at break by 10–60% and the tensile strength by 30% to 100 MPa. The results of other studies show that the addition of UMW PHB in small concentrations also gives a significant improvement in the mechanical characteristics of the resulting mixture due to the effect of nucleation. At the same time, the extraction and simultaneous annealing of the fiber makes it possible to combine two immiscible components, such as PHB–UMW PHB [76], or PHB–ethylene-methylacrylate-glycidyl-methacrylate copolymer [76].

The work of J.C.C. Yeo [53] reports key areas of research associated with increasing the strength of biodegradable polymers on the example of PHB (Fig. 5).

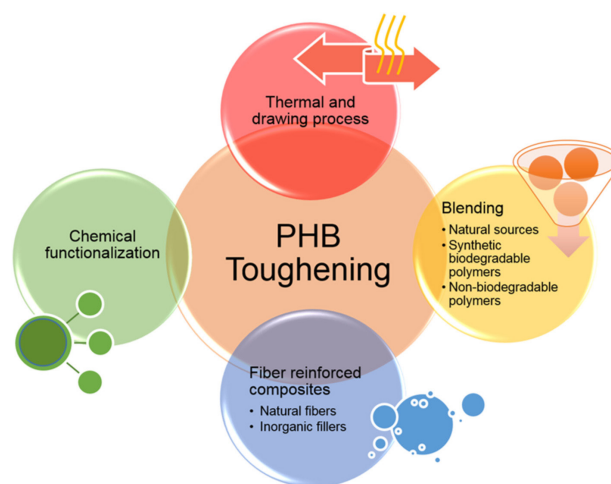


Fig. 5. Possible ways for hardening of PHB [53].

CONCLUSIONS

The development of a biodegradable composite material with excellent mechanical properties opens up new possibilities for the use of polymer materials in bone implantation surgery.

The present review has considered approaches to achieving this goal and identified requirements for a finished medical device, including optimization of the time of resorption of the osteoplastic matrix, facilitating its resorption, synchronization of the resorption time with the process of regeneration of bone material. Achieving these requirements is possible by introducing fillers, mixing with materials from natural sources, including synthetic biodegradable and non-biodegradable polymers, as well as the introduction of natural fibers or rigid fillers to form reinforced composites, modification by chemical functionalization, orientation extraction and heat treatment.

To date, due to their characteristics of biological compatibility and complete biodegradability into fragments that are non-toxic to the body, a number of polyalkanoates represent the most promising materials for further study. In future, the collective efforts of research groups working on materials of the polyalkanoate class are likely to significantly increase their popularity and distribution in the industry. It is to be anticipated that the success of using new bone materials based on biodegradable polymers will be due to a more accurate understanding of the mechanism of action of various components and strict compliance with regulatory requirements.

Authors' contributions

- P.A. Povernov** – literary review on the topic of the study, writing the text of the article;
L.S. Shibryaeva – the research idea, drawing up the outline of the study, assistance in writing the text;
L.R. Lyusova – consulting on the selection of materials for bone implants based on plastics and elastomers;
A.A. Popov – consulting on the creation of composite materials for medical purposes.

The authors declare no conflicts of interest.

REFERENCES

1. Bauer S., Schmuki P., von der Mark K., Park J. Engineering biocompatible implant surfaces. Part I: Materials and surfaces. *Prog. Mater. Sci.* 2016;58(3):261–326. <https://doi.org/10.1016/j.pmatsci.2012.09.001>
2. Schwitalla A., Müller W.D. PEEK dental implants: A review of the literature. *J. Oral Implantol.* 2013;39(6):743–749. <https://doi.org/10.1563/AAID-JOI-D-11-00002>
3. Özkurt Z., Kazazoğlu E. Clinical success of zirconia in dental applications. *J. Prosthodont.* 2010;19(1):64–68. <https://doi.org/10.1111/j.1532-849X.2009.00513.x>
4. Li Y., Brånemark R. Osseointegrated prostheses for rehabilitation following amputation. *Unfallchirurg.* 2017;120(4):285–292. <https://doi.org/10.1007/s00113-017-0331-4>
5. Verma M.L., Kumar S., Jeslin J., Dubey N.K. Microbial Production of Biopolymers with Potential Biotechnological Applications. In: *Biopolymer-Based Formulations*. Elsevier; 2020. P. 105–137. <https://doi.org/10.1016/B978-0-12-816897-4.00005-9>
6. Rebelo R., Vila N., Rana S., Figueiro R. Poly Lactic Acid Fibre Based Biodegradable Stents and Their Functionalization Techniques. In: Figueiro R., Rana S. (Eds.). *Natural Fibres: Advances in Science and Technology Towards Industrial Applications*. RILEM Bookseries. Dordrecht: Springer. 2017;12:331–342. https://doi.org/10.1007/978-94-017-7515-1_25
7. Rebelo R., Fernandes M., Figueiro R. Biopolymers in medical implants: A brief review. *Procedia Eng.* 2017;200:236–243. <https://doi.org/10.1016/j.proeng.2017.07.034>

СПИСОК ЛИТЕРАТУРЫ

1. Bauer S., Schmuki P., von der Mark K., Park J. Engineering biocompatible implant surfaces. Part I: Materials and surfaces. *Prog. Mater. Sci.* 2016;58(3):261–326. <https://doi.org/10.1016/j.pmatsci.2012.09.001>
2. Schwitalla A., Müller W.D. PEEK dental implants: A review of the literature. *J. Oral Implantol.* 2013;39(6):743–749. <https://doi.org/10.1563/AAID-JOI-D-11-00002>
3. Özkurt Z., Kazazoğlu E. Clinical success of zirconia in dental applications. *J. Prosthodont.* 2010;19(1):64–68. <https://doi.org/10.1111/j.1532-849X.2009.00513.x>
4. Li Y., Brånemark R. Osseointegrated prostheses for rehabilitation following amputation. *Unfallchirurg.* 2017;120(4):285–292. <https://doi.org/10.1007/s00113-017-0331-4>
5. Verma M.L., Kumar S., Jeslin J., Dubey N.K. Microbial Production of Biopolymers with Potential Biotechnological Applications. In: *Biopolymer-Based Formulations*. Elsevier; 2020. P. 105–137. <https://doi.org/10.1016/B978-0-12-816897-4.00005-9>
6. Rebelo R., Vila N., Rana S., Figueiro R. Poly Lactic Acid Fibre Based Biodegradable Stents and Their Functionalization Techniques. In: Figueiro R., Rana S. (Eds.). *Natural Fibres: Advances in Science and Technology Towards Industrial Applications*. RILEM Bookseries. Dordrecht: Springer. 2017;12:331–342. https://doi.org/10.1007/978-94-017-7515-1_25
7. Rebelo R., Fernandes M., Figueiro R. Biopolymers in medical implants: A brief review. *Procedia Eng.* 2017;200:236–243. <https://doi.org/10.1016/j.proeng.2017.07.034>

8. Lykoshin D.D., Zaitsev V.V., Kostromina M.A., Esipov R.S. New-generation osteoplastic materials based on biological and synthetic matrices. *Tonk. Khim. Tekhnol. = Fine Chem. Technol.* 2021;16(1):36–54 (in Russ.). <https://doi.org/10.32362/2410-6593-2021-16-1-36-54>
9. Albrektsson T., Chrcanovic B., Östman P.-O., Sennerby L. Initial and long-term crestal bone responses to modern dental implants. *Periodontol. 2000.* 2017;73(1):41–50. <https://doi.org/10.1111/prd.12176>
10. Alghamdi H.S. Methods to Improve Osseointegration of Dental Implants in Low Quality (Type-IV) Bone: An Overview. *J. Funct. Biomater.* 2018;9(1):7. <https://doi.org/10.3390/jfb9010007>
11. Li J., Lu X.L., Zheng Y.F. Effect of surface modified hydroxyapatite on the tensile property improvement of HA/PLA composite. *Appl. Surf. Sci.* 2008;255(2):494–497. <https://doi.org/10.1016/j.apsusc.2008.06.067>
12. Wang J., et al. Fabrication and characterization of composites composed of a bioresorbable polyester matrix and surface modified calcium carbonate whisker for bone regeneration. *Polym. Adv. Technol.* 2017;28(12):1892–1901. <https://doi.org/10.1002/pat.4078>
13. Poroytsky S.V., Mikhalychenko D.V., Yarigina E.N., Khvostov S.N., Zhidovinov A.V. On the osseointegration of dental implants and methods of its stimulation. *J. VolgSMU.* 2015;3(55):6–9 (in Russ.).
14. Mirsaeva F.Z., Ubaidullaev M.B., Vyatkina A.B., Fatkullina S.Sh. *Dental'naya implantologiya (Dental implantology): textbook.* Ufa: BGMU; 2015. 124 p. (in Russ). URL: <http://library.bashgmu.ru/elibdoc/elib624.pdf>
15. Alves E.G.L., de Faria Rezende C.M., Serakides R., et al. Orthopedic implant of a polyhydroxybutyrate (PHB) and hydroxyapatite composite in cats. *J. Feline Med. Surg.* 2011;13(8):546–552. <http://doi.org/10.1016/j.jfms.2011.03.002>
16. Barysh A.E., Dedukh N.V. Bone morphology around ceramic-coated implants with different surface topography. *Ortopediya, travmatologiya i protezirovanie = Orthopedics, Traumatology and Prosthetics.* 2009;(1):38–44 (in Russ.).
17. Popkov A.V. Biocompatible implants in traumatology and orthopaedics (A review of literature). *Genii ortopedii = Orthopaedic Genius.* 2014;(3):94–99 (in Russ.).
18. Popkov A.V. *Bioaktivnye implantaty v travmatologii i ortopedii (Bioactive implants in traumatology and orthopaedics).* Irkutsk: Elizarov Center; 2012. 434 p. (in Russ). ISBN 978-5-98277-155-1
19. Mansourvar M.I., Maizatul A., Herawan T., Gopal R.R., Abdul K.S., Nasaruddin F.H. Automated Bone Age Assessment: Motivation, Taxonomies, and Challenges. *Comput. Math. Methods Med.* 2013;2013:391626. <https://doi.org/10.1155/2013/391626>
20. Narayanan R., Seshadri S.K., Kwon T.Y., Kim K.H. Calcium phosphate-based coatings on titanium and its alloys. *J. Biomed. Mater. Res. B. Appl. Mater.* 2008;85B(1):279–299. <https://doi.org/10.1002/jbm.b.30932>
21. Kurusu R.S., Demarquette N.R., Gauthier C., Chenal J.M. Effect of ageing and annealing on the mechanical behaviour and biodegradability of a poly(3-hydroxybutyrate) and poly(ethylene-co-methyl-acrylate-co-glycidyl-methacrylate)blend. *Polym. Int.* 2014;63(6):1085–1093. <https://doi.org/10.1002/pi.4616>
22. Sun J., Wang J., Yeo J.C.C., Yuan D., Li H., Stubbs L.P., He C. Lignin epoxy composites: preparation, morphology, and mechanical properties. *Macromol. Mater. Eng.* 2016;301(3):328–336. <https://doi.org/10.1002/mame.201500310>
8. Лыкошин Д.Д., Зайцев В.В., Костромина М.А., Есипов Р.С. Остеопластические материалы нового поколения на основе биологических и синтетических матриц. *Тонкие химические технологии.* 2021;16(1):36–54. <https://doi.org/10.32362/2410-6593-2021-16-1-36-54>
9. Albrektsson T., Chrcanovic B., Östman P.-O., Sennerby L. Initial and long-term crestal bone responses to modern dental implants. *Periodontol. 2000.* 2017;73(1):41–50. <https://doi.org/10.1111/prd.12176>
10. Alghamdi H.S. Methods to Improve Osseointegration of Dental Implants in Low Quality (Type-IV) Bone: An Overview. *J. Funct. Biomater.* 2018;9(1):7. <https://doi.org/10.3390/jfb9010007>
11. Li J., Lu X.L., Zheng Y.F. Effect of surface modified hydroxyapatite on the tensile property improvement of HA/PLA composite. *Appl. Surf. Sci.* 2008;255(2):494–497. <https://doi.org/10.1016/j.apsusc.2008.06.067>
12. Wang J., et al. Fabrication and characterization of composites composed of a bioresorbable polyester matrix and surface modified calcium carbonate whisker for bone regeneration. *Polym. Adv. Technol.* 2017;28(12):1892–1901. <https://doi.org/10.1002/pat.4078>
13. Поройский С.В., Михальченко Д.В., Ярыгина Е.Н., Хвостов С.Н., Жидовинов А.В. К вопросу об остеоинтеграции дентальных имплантов и способах ее стимуляции. *Вестник ВолгГМУ.* 2015;3(33):6–9.
14. Мирсаева Ф.З., Убайдуллаев М.Б., Вяткина А.Б., Фаткуллина С.Ш. *Дентальная имплантология: уч. пособие.* Уфа: Изд-во ГБОУ ВПО БГМУ Минздрава России; 2015. 124 с. URL: <http://library.bashgmu.ru/elibdoc/elib624.pdf>
15. Alves E.G.L., de Faria Rezende C.M., Serakides R., et al. Orthopedic implant of a polyhydroxybutyrate (PHB) and hydroxyapatite composite in cats. *J. Feline Med. Surg.* 2011;13(8):546–552. <http://doi.org/10.1016/j.jfms.2011.03.002>
16. Барыш А.Е., Дедух Н.В. Морфология кости вокруг имплантатов с керамическим покрытием и различной топографией поверхности. *Ортопедия, травматология и протезирование.* 2009;(1):38–44.
17. Попков А.В. Биосовместимые имплантаты в травматологии и ортопедии (Обзор литературы). *Гений ортопедии.* 2014;(3):94–99.
18. Попков А.В. *Биоактивные имплантаты в травматологии и ортопедии.* Иркутск: РИЦ ВТО им. Г.А. Илизарова; 2012. 434 с. ISBN 978-5-98277-155-1
19. Mansourvar M.I., Maizatul A., Herawan T., Gopal R.R., Abdul K.S., Nasaruddin F.H. Automated Bone Age Assessment: Motivation, Taxonomies, and Challenges. *Comput. Math. Methods Med.* 2013;2013:391626. <https://doi.org/10.1155/2013/391626>
20. Narayanan R., Seshadri S.K., Kwon T.Y., Kim K.H. Calcium phosphate-based coatings on titanium and its alloys. *J. Biomed. Mater. Res. B. Appl. Mater.* 2008;85B(1):279–299. <https://doi.org/10.1002/jbm.b.30932>
21. Kurusu R.S., Demarquette N.R., Gauthier C., Chenal J.M. Effect of ageing and annealing on the mechanical behaviour and biodegradability of a poly(3-hydroxybutyrate) and poly(ethylene-co-methyl-acrylate-co-glycidyl-methacrylate)blend. *Polym. Int.* 2014;63(6):1085–1093. <https://doi.org/10.1002/pi.4616>
22. Sun J., Wang J., Yeo J.C.C., Yuan D., Li H., Stubbs L.P., He C. Lignin epoxy composites: preparation, morphology, and mechanical properties. *Macromol. Mater. Eng.* 2016;301(3):328–336. <https://doi.org/10.1002/mame.201500310>

23. Schenk R.K., Buser D. Osseointegration: a reality. *Periodontology* 2000. 1998;17(1):22–35. <https://doi.org/10.1111/j.1600-0757.1998.tb00120.x>
24. Freier T., Kunze C., Nischan C., et al. *In vitro* and *in vivo* degradation studies for development of a biodegradable patch based on poly(3-hydroxybutyrate). *Biomaterials*. 2002;23(13):2649–2657. [https://doi.org/10.1016/S0142-9612\(01\)00405-7](https://doi.org/10.1016/S0142-9612(01)00405-7)
25. Rogovina S., Aleksanyan K., Grachev A., Gorenberg A. Investigation of Structure and Properties of Biodegradable Compositions of Polylactide with Ethyl Cellulose and Chitosan Plasticized by Poly(Ethylene Glycol). *Science Journal of Volgograd State University. Technology and innovations*. 2014;6(15):73–85. <https://doi.org/10.15688/jvolsu10.2014.6.7>
26. Shibryaeva L.S., Shatalova O.V., Krivandin A.V., et al. Specific structural features of crystalline regions in biodegradable composites of poly-3-hydroxybutyrate with chitosan. *Russ. J. Appl. Chem.* 2017;90(9):1443–1453. <https://doi.org/10.1134/S1070427217090117>
27. Tertyshnaya Yu.V., Shibryaeva L.S. Degradation of poly(3-hydroxybutyrate) and its blends during treatment with UV light and water. *Polymer Science. Series B*. 2013;55(3–4):164–168. <https://doi.org/10.1134/S1560090413030068>
[Original Russian Text: Tertyshnaya Yu.V., Shibryaeva L.S. Degradation of poly(3-hydroxybutyrate) and its blends during treatment with UV light and water. *Vysokomolekulyarnye Soedineniya. Ser. B*. 2013;55(3):363–368. (in Russ.). <https://doi.org/10.7868/S0507547513030124>]
28. Bogatova I.B. Obtaining biosynthetic polymer packaging materials is a solution to the problem of polymer waste. *Vestnik Volzhskogo universiteta im. V.N. Tatishcheva = Vestnik of V.N. Tatischev Volzhsky University*. 2015;23(1):95–100 (in Russ.).
29. Muraev A.A., Ivanov S.Yu., Artifeksova A.A., Ryabova V.M., Volodina E.V., Polyakova I.N. Biological properties study of a new osteoplastic nondemineralized collagen-based material containing vascular endothelial growth factor in bone defect replacement. *Sovremennye tekhnologii v meditsine = Modern Technologies in Medicine*. 2012;(1):21–26 (in Russ). <http://www.stm-journal.ru/ru/numbers/2012/1/847/pdf>
30. Iordanskii A.L., Ol'khov A.A., Pankova Yu.N., Bonartsev A.P., Bonartseva G.A., Popov V.O. Hydrophilicity impact upon physical properties of the environmentally friendly poly(3-hydroxybutyrate) blends: modification via blending. *Macromolecular Symposia. Special Issue: Fillers, Filled Polymers and Polymer Blends*. 2006;233(1):108–116. <https://doi.org/10.1002/masy.200690005>
31. Lique-Agudo V., Hierro-Oliva M., Gallardo-Moreno M., Gonzalez-Martin Ml. Effect of plasma treatment on the surface properties of polylactic acid films. *Polymer Testing*. 2021;96:107097. <https://doi.org/10.1016/j.polymertesting.2021.107097>
32. Sadi R.K., Fehine G.J.M., Demarquette N.R. Photodegradation of poly(3-hydroxybutyrate). *Polym. Degrad. Stab.* 2010;95(12):2318–2327. <https://doi.org/10.1016/j.polymdegradstab.2010.09.003>
33. Artsis M.I., Bonartsev A.P., Iordanskii A.L., et al. Biodegradation and Medical Application of Microbial Poly(3-hydroxybutyrate). *Mol. Cryst. Liq. Cryst.* 2012;555(1):232–262. <https://doi.org/10.1080/15421406.2012.635549>
34. Zhu B., Bailey S.R., Mauli A.C. Calcification of primary human osteoblast cultures under flow conditions using polycaprolactone scaffolds for intravascular applications. *J. Tissue Eng. Regen. Med.* 2012;6(9):687–695. <https://doi.org/10.1002/term.472>
35. Yu H., Wooley P.H., Yang S.Y. Biocompatibility of Poly-ε-caprolactone-hydroxyapatite composite on mouse bone marrow-derived osteoblasts and endothelial cells. *J. Orthop. Surg. Res.* 2009;4:5. <https://doi.org/10.1186/1749-799X-4-5>
23. Schenk R.K., Buser D. Osseointegration: a reality. *Periodontology* 2000. 1998;17(1):22–35. <https://doi.org/10.1111/j.1600-0757.1998.tb00120.x>
24. Freier T., Kunze C., Nischan C., et al. *In vitro* and *in vivo* degradation studies for development of a biodegradable patch based on poly(3-hydroxybutyrate). *Biomaterials*. 2002;23(13):2649–2657. [https://doi.org/10.1016/S0142-9612\(01\)00405-7](https://doi.org/10.1016/S0142-9612(01)00405-7)
25. Rogovina S., Aleksanyan K., Grachev A., Gorenberg A. Investigation of Structure and Properties of Biodegradable Compositions of Polylactide with Ethyl Cellulose and Chitosan Plasticized by Poly(Ethylene Glycol). *Science Journal of Volgograd State University. Technology and innovations*. 2014;6(15):73–85. <https://doi.org/10.15688/jvolsu10.2014.6.7>
26. Shibryaeva L.S., Shatalova O.V., Krivandin A.V., et al. Specific structural features of crystalline regions in biodegradable composites of poly-3-hydroxybutyrate with chitosan. *Russ. J. Appl. Chem.* 2017;90(9):1443–1453. <https://doi.org/10.1134/S1070427217090117>
27. Тertyшная Ю.В., Шибряева Л.С. Деструкция поли-3-гидроксibuтирата и смесей на его основе под действием ультрафиолета и воды. *Высокомолекулярные соединения. Серия Б*. 2013;55(3):363–368. <https://doi.org/10.7868/S0507547513030124>
28. Богатова И.Б. Получение биосинтетических полимерных упаковочных материалов – решение проблемы полимерного мусора. *Вестник Волжского университета имени В.Н. Татищева*. 2015;23(1):95–100.
29. Мураев А.А., Иванов С.Ю., Артифексова А.А., Рябова В.М., Володина Е.В., Полякова И.Н. Изучение биологических свойств нового остеопластического материала на основе недеминерализованного коллагена, содержащего фактор роста эндотелия сосудов при замещении костных дефектов. *Современные технологии в медицине*. 2012;(1):21–26.
30. Iordanskii A.L., Ol'khov A.A., Pankova Yu.N., Bonartsev A.P., Bonartseva G.A., Popov V.O. Hydrophilicity impact upon physical properties of the environmentally friendly poly(3-hydroxybutyrate) blends: modification via blending. *Macromolecular Symposia. Special Issue: Fillers, Filled Polymers and Polymer Blends*. 2006;233(1):108–116. <https://doi.org/10.1002/masy.200690005>
31. Lique-Agudo V., Hierro-Oliva M., Gallardo-Moreno M., Gonzalez-Martin Ml. Effect of plasma treatment on the surface properties of polylactic acid films. *Polymer Testing*. 2021;96:107097. <https://doi.org/10.1016/j.polymertesting.2021.107097>
32. Sadi R.K., Fehine G.J.M., Demarquette N.R. Photodegradation of poly(3-hydroxybutyrate). *Polym. Degrad. Stab.* 2010;95(12):2318–2327. <https://doi.org/10.1016/j.polymdegradstab.2010.09.003>
33. Artsis M.I., Bonartsev A.P., Iordanskii A.L., et al. Biodegradation and Medical Application of Microbial Poly(3-hydroxybutyrate). *Mol. Cryst. Liq. Cryst.* 2012;555(1):232–262. <https://doi.org/10.1080/15421406.2012.635549>
34. Zhu B., Bailey S.R., Mauli A.C. Calcification of primary human osteoblast cultures under flow conditions using polycaprolactone scaffolds for intravascular applications. *J. Tissue Eng. Regen. Med.* 2012;6(9):687–695. <https://doi.org/10.1002/term.472>
35. Yu H., Wooley P.H., Yang S.Y. Biocompatibility of Poly-ε-caprolactone-hydroxyapatite composite on mouse bone marrow-derived osteoblasts and endothelial cells. *J. Orthop. Surg. Res.* 2009;4:5. <https://doi.org/10.1186/1749-799X-4-5>

35. Yu H., Wooley P.H., Yang S.Y. Biocompatibility of Poly- ϵ -caprolactone-hydroxyapatite composite on mouse bone marrow-derived osteoblasts and endothelial cells. *J. Orthop. Surg. Res.* 2009;4:5. <https://doi.org/10.1186/1749-799X-4-5>
36. Shumilova A.A., Nikolaeva E.D. Differentiation of MMSCs into osteoblasts on porous 3d-carriers from poly-3-hydroxybutyrate. *Zhurnal Sibirskogo federal'nogo universiteta. Seriya: Biologiya = Journal of the Siberian Federal University. Biology.* 2016;9(1):53–62 (in Russ.).
37. Ji S., Guvendiren M. Recent Advances in Bioink Design for 3D Bioprinting of Tissues and Organs. *Front. Bioeng. Biotechnol.* 2017;5:23. <https://doi.org/10.3389/fbioe.2017.00023>
38. Gurkan U.A., El Assal R., Yildiz S.E., Sung Y., Trachtenberg A.J., Kuo W.P., Demirci U. Engineering Anisotropic Biomimetic Fibrocartilage Microenvironment by Bioprinting Mesenchymal Stem Cells in Nanoliter Gel Droplets. *Mol. Pharmaceutics.* 2014;11(7):2151–2159. <https://doi.org/10.1021/mp400573g>
39. Povernov P.A., Shibryaeva L.S. Scientific approaches to the development of materials based on compositions of poly-3-hydroxybutyrate and polylactide for bone implants. *Innovatsii v sozdanii materialov i metodov dlya sovremennoi meditsiny (Innovations in the Creation of Materials and Methods for Modern Medicine): Proceedings of the regional conference.* 2020;173–179 (in Russ.).
40. Puppi D., Mota C., Gazzari M. Additive manufacturing of wet-spun polymeric scaffolds for bone tissue engineering. *Biomed. Microdevices.* 2012;14(6):1115–1127. <https://doi.org/10.1007/s10544-012-9677-0>
41. Zhang H., Mao X., Zhao D. Three dimensional printed polylactic acid-hydroxyapatite composite scaffolds for prefabricating vascularized tissue engineered bone: An *in vivo* bioreactor model. *Sci. Rep.* 2017;7(1):15255. <https://doi.org/10.1038/s41598-017-14923-7>
42. Cui H., Zhu W., Holmes B., Zhang L.G. Biologically Inspired Smart Release System Based on 3D Bioprinted Perfused Scaffold for Vascularized Tissue Regeneration. *Adv. Sci.* 2016;3(8):1600058. <https://doi.org/10.1002/adv.201600058>
43. Иванов С.Ю., Мухаметшин Р.Ф., Мураев А.А., Бонартцев А.П., Рябова В.М. Синтетические материалы, используемые в стоматологии для замещения дефектов костной ткани. *Современные проблемы науки и образования.* 2013;(1):60.
44. Крутько В.К., Кулак А.И., Лесникович Л.А., Трофимова И.В., Мусская О.Н., Жавнерко Г.К., Парибок И.В. Влияние способа дегидратации геля гидроксипатита на физико-химические свойства нанокристаллического ксерогеля. *Журн. общей химии.* 2007;77(3):366–373.
45. Горшенёв В.Н., Зиангирова М.Ю., Колесов В.В., Краснопольская Л.М., Просвирин А.А., Телешев А.Т. Новые аддитивные технологии формирования сложных костных структур для медико-биологических применений. *Радиоэлектроника. Наносистемы. Информационные технологии (РЭНСИТ).* 2019;11(3):369–390. <https://doi.org/10.17725/rensit.2019.11.369>
46. Chappard D., Guillaume B., Mallet R., Pascaretti-Grizon F., Baslé M.F., Libouban H. Sinus lift augmentation and beta-TCP: a microCT and histologic analysis on human bone biopsies. *Micron.* 2010;41(4):321–326. <https://doi.org/10.1016/j.micron.2009.12.005>
47. Shigeishi H., Takechi M., Nishimura M., Takamoto M., Minami M., Ohta K., Kamata N. Clinical evaluation of novel interconnected porous hydroxyapatite ceramics (IP-CHA) in a maxillary sinus floor augmentation procedure. *Dent. Mater. J.* 2012;31(1):54–60. <https://doi.org/10.4012/dmj.2011-089>
48. Ebrahimi M., Pripatnanont P., Monmaturapoj N., Suttapreyasri S. Fabrication and characterization of novel nano hydroxyapatite/ β -tricalcium phosphate scaffolds in three different composition ratios. *J. Biomed. Mater. Res. A.* 2012;100(9):2260–2268. <https://doi.org/10.1002/jbm.a.34160>

46. Chappard D., Guillaume B., Mallet R., Pascaretti-Grizon F., Baslé M.F., Libouban H. Sinus lift augmentation and beta-TCP: a microCT and histologic analysis on human bone biopsies. *Micron*. 2010;41(4):321–326. <https://doi.org/10.1016/j.micron.2009.12.005>
47. Shigeishi H., Takechi M., Nishimura M., Takamoto M., Minami M., Ohta K., Kamata N. Clinical evaluation of novel interconnected porous hydroxyapatite ceramics (IP-CHA) in a maxillary sinus floor augmentation procedure. *Dent. Mater. J.* 2012;31(1):54–60. <https://doi.org/10.4012/dmj.2011-089>
48. Ebrahimi M., Pripatnanont P., Monmaturapoj N., Suttapreyasri S. Fabrication and characterization of novel nano hydroxyapatite/ β -tricalcium phosphate scaffolds in three different composition ratios. *J. Biomed. Mater. Res. A*. 2012;100(9):2260–2268. <https://doi.org/10.1002/jbm.a.34160>
49. Sukovatykh B.S., Polevoy Yu.Yu., Netyaga A.A., Blinkov Yu.Yu., Zhukovskiy V.A. Comparative experimental-morphological research of light and light strengthened endoprosthesis for hernioplasty. *Novosti Khirurgii*. 2018;26(4):402–411 (in Russ.).
50. Eisenakh I.A., Bakarev M.A., Lapiy G.A., Moses V.G., Moses K.B. Study of tissue inflammatory response to implantation of a biodegradable polymer compared to polypropylene in an animals experiment. *Meditsina v Kuzbasse = Medicine in Kuzbass*. 2020;19(3):13–20 (in Russ.). <https://doi.org/10.24411/2687-0053-2020-10022>
51. Chang P., Liu B., Liu C., Chou H., Ho M., Liu H. Bone tissue engineering with novel rhBMP2-PLLA composite scaffolds. *J. Biomed. Mater. Res. A*. 2007;81(4):771–780. <https://doi.org/10.1002/jbm.a.31031>
52. Ol'hov A.A., Muraev A.A., Volkov A.V., Ivashkevich S.G., Kim E.V., Pozdnyakov M.S., Staroverova O.V., Iordanskij A.L., Gorshenev V.N. Structure and properties of bioresorbed materials based on polylactide for regenerative medicine. *Vse Materialy. Entsiklopedicheskii Spravochnik = All materials. Encyclopaedic Reference Manual*. 2021;(1):7–15 (in Russ.).
53. Yeo J.C.C., Muiruri J.K., Thitsartam W., Li Z., He C. Recent advances in the development of biodegradable PHB-based toughening materials: Approaches, advantages and applications. *Mate. Sci. Eng.: C*. 2018;92:1092–1116. <https://doi.org/10.1016/j.msec.2017.11.006>
54. Sadat-Shojai M., Khorasani M.-T., Jamshidi A. A new strategy for fabrication of bone scaffolds using electrospun nano-HAp/PHB fibers and protein hydrogels. *Chem. Eng. J.* 2016;289:38–47. <https://doi.org/10.1016/j.cej.2015.12.079>
55. Gumel A.M., Aris M.H., Annuar M.S.M. Modification of Polyhydroxyalkanoates (PHAs). In: *Polyhydroxyalkanoate (PHA) Based Blends. Composites and Nanocomposites*. (Eds.) Ipsita R., Visakh P.M. 2016. P. 141–182. <https://doi.org/10.1039/9781782622314-00141>
56. Крутько Э.Т., Прокопчук Н.Р., Глоба А.И. *Технология биоразлагаемых полимерных материалов*. Минск: БГТУ; 2014.105 p. ISBN 978-985-530-354-2.
57. Griffin G.J.L. Starch polymer blends. *Polymer Degradation and Stability*. 1994;45(2):241–247. [https://doi.org/10.1016/0141-3910\(94\)90141-4](https://doi.org/10.1016/0141-3910(94)90141-4)
58. Гомзяк В.И., Пучков А.А., Артамонова Н.Е., Поляков Д.К., Симакова Г.А., Грицкова И.А., Чвалун С.Н. Физико-химические свойства нового биодеструктурируемого гиперразветвленного полиэфирполиола на основе 2,2-бис(метиллол пропио-новой кислоты). *Тонкие химические технологии*. 2018;13(4):67–73. <https://doi.org/10.32362/2410-6593-2018-13-4-67-73>
59. Гомзяк В.И., Артамонова Н.Е., Ковтун И.Д., Камышинский Р.А., Грицкова И.А., Чвалун С.Н. Гетерофазная полимеризация стирола в присутствии полиэфирполиола boltorn. *Высокомолекулярные соединения. Серия Б*. 2020;62(1):26–34. <https://doi.org/10.31857/S2308113919050048>
60. Седуш Н.Г., Кадина Ю.А., Разуваева Е.В., Пучков А.А., Широкова Е.М., Гомзяк В.И., Калинин К.Т., Кулебякина А.И., Чвалун С.Н. Наносомальные лекарственные формы на основе биоразлагаемых сополимеров лактида с различной молекулярной структурой и архитектурой. *Российские нанотехнологии*. 2021;16(4):462–481. <https://doi.org/10.1134/S1992722321040117>
61. Гомзяк В.И., Седуш Н.Г., Пучков А.А., Поляков Д.К., Чвалун С.Н. Линейные и разветвленные полимеры лактида для систем направленной доставки лекарственных средств. *Высокомолекулярные соединения. Серия Б*. 2021;63(3):190–206. <https://doi.org/10.31857/S2308113921030062>

59. Gomzyak V.I., Kamyshtinsky R.A., Chvalun S.N., Artamonova N.E., Kovtun I.D. Gritskova I.A. Heterophase polymerization of styrene in the presence of boltorn polyester polyol. *Polym. Sci. Ser. B.* 2020;62(1):22–29. <https://doi.org/10.1134/S156009041905004X>
- [Original Russian Text: Gomzyak V.I., Artamonova N.E., Kovtun I.D. Kamyshtinsky R.A., Gritskova I.A. Chvalun S.N. Heterophase polymerization of styrene in the presence of boltorn polyester polyol. *Vysokomolekulyarnye Soedineniya. Ser. B.* 2020;62(1):26–34. (in Russ.). <https://doi.org/10.31857/S2308113919050048>]
60. Sedush, N.G., Kadina, Y.A., Razuvaeva, E.V. *et al.* Nanoformulations of Drugs Based on Biodegradable Lactide Copolymers with Various Molecular Structures and Architectures. *Nanotechnol. Russia.* 2021;16(4):421–438. <https://doi.org/10.1134/S2635167621040121>
- [Original Russian Text: Sedush N.G., Kadina Yu.A., Razuvaeva E.V., Puchkov A.A., Shirokova E.M., Gomzyak V.I., Kalinin K.T., Kulebyakina A.I., Chvalun S.N. Nanoformulations of Drugs Based on Biodegradable Lactide Copolymers with Various Molecular Structures and Architectures. *Rossiiskie nanotekhnologii.* 2021;16(4):462–481 (in Russ.). <https://doi.org/10.1134/S1992722321040117>]
61. Gomzyak V.I., Sedush N.G., Puchkov A.A., Polyakov D.K., Chvalun S.N. Linear and branched lactide polymers for targeted drug delivery systems. *Polym. Sci. Ser. B.* 2021;63(3):257–271. <https://doi.org/10.1134/S1560090421030064>
- [Original Russian Text: Gomzyak V.I., Sedush N.G., Puchkov A.A., Polyakov D.K., Chvalun S.N. Linear and branched lactide polymers for targeted drug delivery systems. *Vysokomolekulyarnye Soedineniya. Ser. B.* 2021;63(3):190–206. (in Russ.). <https://doi.org/10.31857/S2308113921030062>]
62. Becker S.T., Douglas T., Acil Y., Seitz H., Sivananthan S., Wiltfang J., Warnke P.H. Biocompatibility of individually designed scaffolds with human periosteum for use in tissue engineering. *J. Mater. Sci.: Mater. Med.* 2010;21(4):1255–1262. <https://doi.org/10.1007/s10856-009-3878-y>
63. Panayotidou E., Kroustalli A., Baklavariadis A., Zuburtikudis I., Achilias D.S., Deligianni D. Biopolyester-based nanocomposites: structural, thermo-mechanical and biocompatibility characteristics of poly(3-hydroxybutyrate)/montmorillonite clay nanohybrids. *J. Appl. Polym. Sci.* 2015;132(11):41628. <https://doi.org/10.1002/app.41628>
64. Volova T., Shishatskaya E., Sevastianov V., Efremov S., Mogilnaya O. Results of biomedical investigations of PHB and PHB/PHV fibers. *Biochem. Eng. J.* 2003;16(2):125–133. [https://doi.org/10.1016/s1369-703x\(03\)00038-x](https://doi.org/10.1016/s1369-703x(03)00038-x)
65. Chen X., Yang X., Pan J., Wang L., Xu K. Degradation Behaviors of Bioabsorbable P3/4HB Monofilament Suture, *in Vitro* and *in Vivo*. *J. Biomed. Mater. Res. B.: Appl. Biomater.* 2010;92B:447–455. <https://doi.org/10.1002/jbm.b.31534>
66. Cao W., Wang A., Jing D., Gong Y., Zhao N., Zhang X. Novel biodegradable films and scaffolds of chitosan blended with poly(3-hydroxybutyrate). *J. Biomater. Sci. Polym. Ed.* 2005;16(11):1379–1394. <https://doi.org/10.1163/156856205774472308>
67. Raghunatha K., Sato H., Takahashi I. Intermolecular hydrogen bondings in the poly(3-hydroxybutyrate) and chitin blends: their effects on the crystallization behavior and crystal structure of poly(3-hydroxybutyrate). *Polymer.* 2015;75:141–150. <https://doi.org/10.1016/j.polymer.2015.08.011>
68. Иванцова Е.Л., Иорданский А.Л., Косенко Р.Ю., Роговина С.З., Грачев А.В., Прут Э.В. Новая биоразлагаемая композиция поли(3-гидроксибутират)хитозан для пролонгированного транспорта биологически активных веществ. *Хим.-фарм. журн.* 2011;45(1):39–44.
69. Shibryaeva L.S., Gorshenev V.N., Krashennikov V.G. Thermal properties of porous polylactide. *Polym. Sci. Ser. A.* 2019;61(2):162–174. <https://doi.org/10.1134/S0965545X19020123>
70. Wu L., Chen S., Li Z., Xu K., Chen G.-Q. Synthesis, characterization and biocompatibility of novel biodegradable poly(((R)-3-hydroxybutyrate)-*block*-(D,L-lactide)-*block*-(ϵ -caprolactone)) triblock copolymers. *Polym. Int.* 2008;57(7):939–949. <https://doi.org/10.1002/pi.2431>
71. Di Lorenzo M.L., Righetti M.C. Evolution of crystal and amorphous fractions of poly[(R)-3-hydroxybutyrate] upon storage. *J. Therm. Anal. Calorim.* 2013;112(3):1439–1446. <https://doi.org/10.1007/s10973-012-2734-3>
72. Sun Y., Yang L., Lu X., He C. Biodegradable and renewable poly(lactide)–lignin composites: synthesis, interface and toughening mechanism. *J. Mater. Chem. A.* 2015;3(7):3699–3709 <https://doi.org/10.1039/C4TA05991C>
73. Muiruri J.K., Liu S., Teo W.S., Kong J., He C. Highly biodegradable and tough polylactic acid-cellulose nanocrystal composite. *ACS Sustainable Chem. Eng.* 2017;5(5):3929–3937. <https://doi.org/10.1021/acssuschemeng.6b03123>
74. Crétois R., Chernal J.-M., Sheibat-Othman N., Monnier A., Martin C., Astruz O., Kurusu R., Demarquette N.R. Physical explanations about the improvement of polyhydroxybutyrate ductility: hidden effect of plasticizer on physical ageing. *Polymer.* 2016;102:176–182. <https://doi.org/10.1016/j.polymer.2016.09.017>
75. Kabe T., Tsuge T., Kasuya K., Takemura A., Hikima T., Takata M., Iwata T. Physical and Structural Effects of Adding Ultrahigh-Molecular-Weight Poly[(R)-3-hydroxybutyrate] to Wild-Type Poly[(R)-3-hydroxybutyrate]. *Macromolecules.* 2012;45(4):1858–1865. <https://doi.org/10.1021/ma202285c>

[Original Russian Text: Ivantsova E.L., Iordanskii A.L., Kosenko R.Y., *et al.* Poly(3-hydroxybutyrate)-chitosan: a new biodegradable composition for prolonged delivery of biologically active substances. *Khimiko-Farmatsevticheskii Zhurnal*. 2011;45(1):39–44.]

69. Shibryaeva L.S., Gorshenev V.N., Krashennikov V.G. Thermal properties of porous polylactide. *Polym. Sci. Ser. A*. 2019;61(2):162–174. <https://doi.org/10.1134/S0965545X19020123>

70. Wu L., Chen S., Li Z., Xu K., Chen G.-Q. Synthesis, characterization and biocompatibility of novel biodegradable poly[(R)-3-hydroxybutyrate]-*block*-(D,L-lactide)-*block*-(ϵ -caprolactone) triblock copolymers. *Polym. Int.* 2008;57(7):939–949. <https://doi.org/10.1002/pi.2431>

71. Di Lorenzo M.L., Righetti M.C. Evolution of crystal and amorphous fractions of poly[(R)-3-hydroxybutyrate] upon storage. *J. Therm. Anal. Calorim.* 2013;112(3):1439–1446. <https://doi.org/10.1007/s10973-012-2734-3>

72. Sun Y., Yang L., Lu X., He C. Biodegradable and renewable poly(lactide)–lignin composites: synthesis, interface and toughening mechanism. *J. Mater. Chem. A*. 2015;3(7):3699–3709. <https://doi.org/10.1039/C4TA05991C>

73. Muiruri J.K., Liu S., Teo W.S., Kong J., He C. Highly biodegradable and tough polylactic acid-cellulose nanocrystal composite. *ACS Sustainable Chem. Eng.* 2017;5(5):3929–3937. <https://doi.org/10.1021/acssuschemeng.6b03123>

74. Crétois R., Chernal J.-M., Sheibat-Othman N., Monnier A., Martin C., Astruz O., Kurusu R., Demarquette N.R. Physical explanations about the improvement of polyhydroxybutyrate ductility: hidden effect of plasticizer on physical ageing. *Polymer*. 2016;102:176–182. <https://doi.org/10.1016/j.polymer.2016.09.017>

75. Kabe T., Tsuge T., Kasuya K., Takemura A., Hikima T., Takata M., Iwata T. Physical and Structural Effects of Adding Ultrahigh-Molecular-Weight Poly[(R)-3-hydroxybutyrate] to Wild-Type Poly[(R)-3-hydroxybutyrate]. *Macromolecules*. 2012;45(4):1858–1865. <https://doi.org/10.1021/ma202285c>

76. Kabe T., Hongo C., Tanaka T., Hikima T., Takata M., Iwata T. High tensile strength fiber of poly[(R)-3-hydroxybutyrate-*co*-(R)-3-hydroxyhexanoate] processed by two-step drawing with intermediate annealing. *J. Appl. Polym. Sci.* 2015;132(2):41258. <https://doi.org/10.1002/app.41258>

76. Kabe T., Hongo C., Tanaka T., Hikima T., Takata M., Iwata T. High tensile strength fiber of poly[(R)-3-hydroxybutyrate-*co*-(R)-3-hydroxyhexanoate] processed by two-step drawing with intermediate annealing. *J. Appl. Polym. Sci.* 2015;132(2):41258. <https://doi.org/10.1002/app.41258>

About the authors:

Pavel A. Povernov, Postgraduate Student, Junior Researcher, Laboratory of Physico-Chemistry of Compositions of Synthetic and Natural Polymers, N.M. Emanuel Institute of Biochemical Physics, Russian Academy of Sciences (4, Kosygina ul., Moscow, 119334, Russia). E-mail: pav3444@yandex.ru. Scopus Author ID 57210264564, ResearcherID ABC-5732-2021, RSCI SPIN-code 1408-2867, <https://orcid.org/0000-0003-3017-4397>

Lyudmila S. Shibryaeva, Dr. Sci. (Chem.), Professor, Leading Researcher, Laboratory of Physico-Chemistry of Compositions of Synthetic and Natural Polymers, N.M. Emanuel Institute of Biochemical Physics, Russian Academy of Sciences (4, Kosygina ul., Moscow, 119334, Russia); Professor, F.F. Koshelev Department of Chemistry and Technology of Processing of Elastomers, M.V. Lomonosov Institute of Fine Chemical Technologies, MIREA – Russian Technological University (86, Vernadskogo pr., Moscow, 119571, Russia). E-mail: lyudmila.shibryaeva@yandex.ru. Scopus Author ID 7003539026, ResearcherID A-7634-2014, RSCI SPIN-code 3664-7997, <https://orcid.org/0000-0001-6805-4492>

Ludmila R. Lusova, Dr. Sci. (Eng.), Professor, Head of the F.F. Koshelev Department of Chemistry and Technology of Processing of Elastomers, M.V. Lomonosov Institute of Fine Chemical Technologies, MIREA – Russian Technological University (86, Vernadskogo pr., Moscow, 119571, Russia). E-mail: luslr@mail.ru. Scopus Author ID 6508196636, ResearcherID ABC-7835-2021, RSCI SPIN-code 6390-2313, <https://orcid.org/0000-0001-9515-6347>

Anatoliy A. Popov, Dr. Sci. (Chem.), Professor, Head of the Laboratory of Physico-Chemistry of Compositions of Synthetic and Natural Polymers, Deputy Director for Scientific and Educational Work, N.M. Emanuel Institute of Biochemical Physics, Russian Academy of Sciences (4, Kosygina ul., Moscow, 119334, Russia). E-mail: popov@sky.chph.ras.ru. Scopus Author ID 7402986626, ResearcherID I-9835-2014, SPIN-код РИНЦ 5556-7816, <https://orcid.org/0000-0002-8006-6215>

Об авторах:

Повернов Павел Алексеевич, аспирант, младший научный сотрудник лаборатории Физико-химии композиций природных и синтетических полимеров, ФГБУН Институт биохимической физики им. Н.М. Эмануэля Российской академии наук (199334, Россия, Москва, ул. Косыгина, д.4). E-mail: pav3444@yandex.ru. Scopus Author ID 57210264564, ResearcherID ABC-5732-2021, SPIN-код РИНЦ 1408-2867, <https://orcid.org/0000-0003-3017-4397>

Шибряева Людмила Сергеевна, д.х.н., профессор, ведущий научный сотрудник лаборатории Физико-химии композиций природных и синтетических полимеров, ФГБУН Институт биохимической физики им. Н.М. Эмануэля Российской академии наук (199334, Россия, Москва, ул. Косыгина, д. 4); профессор кафедры Химии и технологии переработки эластомеров им. Ф.Ф. Кошелева Института тонких химических технологий им. М.В. Ломоносова ФГБОУ ВО «МИРЭА – Российский технологический университет» (119571, Россия, Москва, пр-т Вернадского, д. 86). E-mail: lyudmila.shibryaeva@yandex.ru. Scopus Author ID 7003539026, ResearcherID A-7634-2014, SPIN-код РИНЦ 3664-7997, <https://orcid.org/0000-0001-6805-4492>

Люсова Людмила Ромульдовна, д.т.н., профессор, заведующий кафедрой Химии и технологии переработки эластомеров им. Ф.Ф. Кошелева Института тонких химических технологий им. М.В. Ломоносова ФГБОУ ВО «МИРЭА – Российский технологический университет» (119571, Россия, Москва, пр-т Вернадского, д. 86). E-mail: luslr@mail.ru. Scopus Author ID 6508196636, ResearcherID ABC-7835-2021, SPIN-код РИНЦ 6390-2313, <https://orcid.org/0000-0001-9515-6347>

Попов Анатолий Анатольевич, д.х.н., профессор, заведующий лабораторией Физико-химии композиций природных и синтетических полимеров, заместитель директора по научно-образовательной работе ФГБУН Институт биохимической физики им. Н.М. Эмануэля Российской академии наук (199334, Россия, Москва, ул. Косыгина, д. 4). E-mail: popov@sky.chph.ras.ru. Scopus Author ID 7402986626, ResearcherID I-9835-2014, SPIN-код РИНЦ 5556-7816, <https://orcid.org/0000-0002-8006-6215>

The article was submitted: January 25, 2022; approved after reviewing: April 28, 2022; accepted for publication: November 28, 2022.

Translated from Russian into English by N. Isaeva

Edited for English language and spelling by Thomas Beavitt

MIREA – Russian Technological University
78, Vernadskogo pr., Moscow, 119454, Russian Federation.
Publication date *December 30, 2022.*
Not for sale

МИРЭА – Российский технологический университет
119454, РФ, Москва, пр-т Вернадского, д. 78.
Дата опубликования *30.12.2022.*
Не для продажи

